UNIVERSITY OF OULU

FACULTY OF INFORMATION TECHNOLOGY AND ELECTRICAL ENGINEERING

Marjut Salovaara

LOW-FREQUENCY OSCILLATIONS OF THE CARDIOVASCULAR SYSTEM IN DIABETICS DURING TEMPERATURE EXPOSURE

Master's Thesis
Degree Programme in Biomedical Engineering
June 2022

Salovaara M. (2022) Low-frequency oscillations of the cardiovascular system in diabetics during temperature exposure. The University of Oulu, Degree Programme in Biomedical Engineering. Master's Thesis, 90 p.

ABSTRACT

Diabetes is a metabolic disorder characterized by elevated blood glucose levels. The disease, therefore, reflects an imbalance in blood glucose and is a result of the body's inability to produce enough or to use the produced insulin efficiently. The impairments in temperature regulation during exposure to thermal stress have been linked to diabetes in recent years. During extreme heat events, diabetics have been reported to be particularly vulnerable, leading to high rates of hospitalizations and deaths. As climate change leads to higher global average temperatures, this area of research has attracted special interest.

This thesis was carried out as part of a research group at the Centre for Environmental and Respiratory Health Research (CERH), where an experimental study was conducted to investigate how advanced type 2 diabetes affects the neurological, cardiovascular, and metabolic responses in cold and warm environments. The aim of this thesis is to study cardiovascular system responses such as low-frequency oscillations of blood pressure, heart rate, and tissue blood flow during heat exposure.

The thesis's first part focuses on the cardiovascular system and its function, and how it is changing in diabetes. Also, human thermoregulation is discussed, and a general overview of the studied cardiovascular signals is presented. The second part describes the methods used to analyze the signals. All the signal processing is done in the Matlab environment. The third part of the thesis presents the results.

The results of this thesis showed that, in general, all calculated mean parameters were lower in diabetics. Also, the change in the intervention was generally dampened in diabetics, which suggests that the thermoregulatory response is different between diabetic and control groups. Overall, the results suggest that there is a difference between diabetics and controls in the parameters of studied signals, and the difference is reflected in the time-domain parameters as well as in the amplitude and power parameters of the frequency-domain.

Keywords: diabetes, heart rate variability, blood pressure, laser Doppler flowmetry, thermoregulation

Salovaara M. (2022) Sydän- ja verenkiertojärjestelmän matalataajuinen värähtely diabeetikoilla lämpötila-altistuksen aikana. Oulun yliopisto, Lääketieteen tekniikan tutkinto-ohjelma. Diplomityö, 90 s.

TIIVISTELMÄ

Diabetes on aineenvaihduntasairaus, jolle on ominaista kohonnut veren glukoosipitoisuus. Sairaus kuvastaa siis veren glukoosipitoisuuden epätasapainoa ja se johtuu siitä, että elimistö ei pysty tuottamaan riittävästi tai käyttämään tuottamaansa insuliinia tehokkaasti. Lämpötilan säätelyn heikkeneminen lämpöstressille altistumisen aikana on viime vuosina yhdistetty diabetekseen. Äärimmäisten helleilmiöiden aikana diabeetikoiden on raportoitu olevan erityisen alttiita, mikä johtaa suuriin sairaalahoito- ja kuolemantapauksiin. Koska ilmastonmuutos johtaa maailmanlaajuisesti korkeampiin keskilämpötiloihin, tämä tutkimusalue on herättänyt erityistä kiinnostusta.

Tämä diplomityö tehtiin osana Ympäristöterveyden ja keuhkosairauksien tutkimuskeskuksen (CERH) tutkimusryhmää, jossa tehtiin kokeellinen tutkimus, jossa selvitettiin, miten pitkälle edennyt tyypin 2 diabetes vaikuttaa neurologisiin, kardiovaskulaarisiin ja metabolisiin vasteisiin kylmässä ja lämpimässä ympäristössä. Tämän diplomityön tavoitteena on tutkia sydän- ja verenkiertoelimistön vasteita kuten verenpaineen, sykkeen ja kudosverenkierron matalataajuista värähtelyä lämpöaltistuksessa.

Diplomityön ensimmäisessä osassa keskitytään sydän- ja verisuonijärjestelmään ja sen toimintaan sekä siihen, miten se muuttuu diabeteksessa. Lisäksi käsitellään ihmisen lämmönsäätelyä ja esitetään yleiskatsaus tutkituista sydän- ja verisuonisignaaleista. Toisessa osassa kuvataan signaalien analysointiin käytetyt menetelmät. Kaikki signaalinkäsittely tehdään Matlab-ympäristössä. Työn kolmannessa osassa esitellään tulokset.

Tämän diplomityön tulokset osoittivat, että yleisesti ottaen kaikki lasketut keskimääräiset parametrit olivat alhaisempia diabetesta sairastavilla. Myös lämpötila-altistuksen muutokset olivat yleisesti ottaen vaimeampia diabetesta sairastavilla, mikä viittaa siihen, että lämmönsäätelyvaste on erilainen diabetesta sairastavilla ja kontrolliryhmän välillä. Kaiken kaikkiaan tulokset viittaavat siihen, että diabetesta sairastavien ja kontrolliryhmän välillä on eroja tutkittujen signaalien parametreissa, ja ero näkyy aika-alueparametreissa sekä taajuusalueen amplitudi- ja tehoparametreissa.

Avainsanat: diabetes, sydämen sykevaihtelu, verenpaine, laser-Doppler-virtausmittaus, lämmönsäätely

TABLE OF CONTENTS

FOREWORD

This work was conducted as part of the research group at the Centre for Environmental and Respiratory Health Research (CERH) at the University of Oulu, where an experimental study was conducted to investigate how advanced type 2 diabetes (T2DM) combined with hypertension affects the neurological, cardiovascular, and metabolic response in cold and warm environments.

I would like to thank my supervisors, Professor of Biomedical Engineering Physiological Signal Analysis Team Center for Machine Vision and Signal Analysis Tapio Seppänen and Associate Professor at the Center for Environmental and Respiratory Health Research and Institute of Health Sciences at the University of Oulu Tiina Ikäheimo for their good advice during the planning, measurement, analysis and writing phases of this work. Thank you to all the people in the research group for the guidance and insight on the execution of the experimental study and for providing a great place to work during my internship and thesis.

Oulu, 22.6.2022

Marjut Salovaara

LIST OF ABBREVIATIONS AND SYMBOLS

Abbreviations

ANS	The Autonomic Nervous System
BMI	Body Mass Index
BP	Blood pressure
BPM	Beats per Minute
CNS	The Central Nervous System
CVC	Cutaneous Vascular Conductance
CVD	Cardiovascular Disease
DBP	Diastolic Blood Pressure
ECG	Electrocardiogram
EEG	Electroencephalogram
FT	Fourier Transform
HbA1c	Glycated hemoglobin (glycohemoglobin, hemoglobin A1c). Measured primarily to determine the three-month average blood sugar level and can be used as a diagnostic test for diabetes mellitus and as an assessment test for glycemic control in people with diabetes.
HF	High Frequency
HR	Heart Rate
HRV	Heart rate variability
LF	Low Frequency
LDF	Laser-Doppler Flowmetry
MAD	Median Absolute Deviations
MAP	Mean Arterial Pressure
PNS	Peripheral Nervous System
PSNS	The Parasympathetic Nervous System

RR	Time interval between two R-waves in electrocardiograph
RSA	Respiratory Sinus Arrhythmia
SA node	Sinoatrial node
SBP	Systolic Blood Pressure
SoNS	The Somatic Nervous System
SNS	The Sympathetic Nervous System
T1DM	type 1 diabetes
T2DM	type 2 diabetes
WT	Wavelet Transform

Symbols

μ	mean
σ	standard deviation
$\sum$	summation
ψ	wavelet function
s	scale
t	time
π	pi
e	exponential
N	number of data points

1. INTRODUCTION

Diabetes mellitus, commonly known as diabetes, is a metabolic disorder characterized by elevated blood glucose levels. Diabetes is therefore an imbalance in blood glucose in a person's body and is a result of the body's inability to produce enough insulin or to use the insulin it does produce efficiently. [1, 2] It can be classified into four categories: type 1 diabetes (T1DM), type 2 diabetes (T2DM), gestational diabetes due to pregnancy, and other types of diabetes (due to monogenic diabetes syndromes, diseases of the exocrine pancreas or drug-induced diabetes) [3]. Type 1 and type 2 diabetes are the most common forms of the disease, accounting for around 10 % and 90 % of cases respectively. Type 1 diabetes is the result of immune-mediated destruction of islet β-cells and is characterized by the cessation of insulin production by the endocrine pancreas. Therefore, the management of type 1 diabetes always requires the administration of exogenous insulin. Type 2 diabetes typically involves a combination of insulin resistance and relative (rather than absolute) insulin deficiency, and it is most often diagnosed in adults. Type 2 diabetes is usually associated with several comorbidities such as metabolic syndrome, obesity, hypertension, dyslipidemia, and other cardiovascular diseases. In general, type 2 diabetes is related to general health and lifestyle, as well as changes associated with normal aging. Unlike type 1 diabetes, type 2 diabetes can be treated in a variety of ways, including lifestyle changes, non-insulin drugs, and the administration of exogenous insulin. [4]

Diabetes is a global public health problem. In 2014 there were about 422 million people with diabetes worldwide, most of them living in low- and middle-income countries, and each year 1,5 million deaths are directly derived from diabetes [1]. The number of cases and the prevalence of diabetes have increased over the past few decades and the prevalence is estimated to increase to 693 million diabetics worldwide by the year 2045 (age 18-99 years) [5]. In 2010 health expenditure for diabetes in the European region was estimated at US$ 105,5 billion, and by the year 2030, the health expenditure is expected to reach US$ 124,6 billion, according to the International Diabetes Federation [6]. Much of the burden of diabetes is due to disabling and common complications of the disease, which are typically related to glycemic control levels (i.e., HbA1c). People with type 2 diabetes are a particularly vulnerable population because they tend to have relatively poor general health combined with multiple comorbidities [4].

The impairments in temperature regulation during exposure to thermal stress have been linked to diabetes in recent years. During extreme heat events, type 1 and type 2 diabetics have been reported to be particularly vulnerable, leading to disproportionately high rates of hospitalization and death. It has been suggested that diabetics are more susceptible to cold stress, but several studies in the field have also suggested that cold exposure could have potential therapeutic effects for type 2 diabetics. However, both high and low ambient temperatures have been associated with increased diabetes mortality. As climate change leads to higher global average temperatures and increases the frequency of heatwaves, this area of research has attracted special interest. When climate change is linked to the increasing prevalence of diabetes, it has become a double threat, increasing the burden of the disease. [4, 7]

Thermal stress can challenge human homeostasis, especially the cardiovascular system and glycemic control. Cardiovascular regulation plays a crucial role in temperature regulation during heat and cold stress when blood must redistribute towards the periphery (i.e., vasodilatation) and towards the core (i.e., vasoconstriction)

to maintain a stable core temperature and thus temperature balance. However, vulnerable individuals with potentially impaired cardiovascular capacity, such as many people with type 1 and type 2 diabetes, may not be able to respond appropriately. [4]

Hemodynamic and physiological parameters such as blood pressure (BP), heart rate (HR), and tissue blood flow can provide information on the health status of an individual. These parameters can change with changes in ambient temperature and can therefore provide valuable information on the physiological regulation of the individual, the pathophysiological state of diseases and their progression. This thesis was carried out as part of a research group at the Centre for Environmental and Respiratory Health Research (CERH) at the University of Oulu, where an experimental study was conducted to investigate how advanced type 2 diabetes combined with hypertension affects the neurological, cardiovascular, and metabolic responses in cold and warm environments. The objective of this thesis is to explore the low-frequency oscillatory characteristics of the cardiovascular system based on tissue blood flow, heart rate, and blood pressure parameters in diabetic and healthy subjects in response to acute exposures to heat and cold. The above parameters will be analyzed and studied before, during, and after temperature exposure to see how these parameters evolve and potentially change. The main goal of this thesis is to explore if these parameters change in T2DM patients compared to the control group during the thermal challenge and whether these differences are reflected in the amplitude and/or power of low-frequency oscillations between the groups. In addition, the parameters will be analyzed in the time-domain to examine responses between individuals, and between diabetic patients and healthy controls. The thesis will focus on the processing and analysis of the measured data using Matlab.

The Centre for Environmental and Respiratory Health Research (CERH) is a multidisciplinary research group at the Faculty of Medicine at the University of Oulu. CERH's strategy is related to education, awareness, and research on global environmental health impacts. Research activities will make use of registry, population-based, clinical, and experimental studies. CERH also provides training in public health, epidemiology, and environmental health for medical students and Ph.D. students. [8]

2. BACKGROUND

The human body is made up of trillions of cells. They form organs and organ systems that work together to carry out vital functions. Many functions and tasks are overlapping and interdependent, so cooperation requires communication between cells and mechanisms to regulate vital functions. Interactions and functions of the cardiovascular and nervous systems play a key role in this regulation. [9, 10 p. 10-11]

The body is constantly maintaining its internal state through various physiological and biochemical reactions. This steady-state of internal conditions maintained by living beings is called homeostasis. Maintaining homeostasis requires constant monitoring of the internal conditions of the human body. Each physiological condition, from body temperature to blood pressure and the levels of certain nutrients, has a specific set point, which is a physiological value around which the normal range of variation fluctuates. The normal range is a restricted set of values that is optimal for a healthy and stable condition. The control centers in the brain and other parts of the body monitor and react to deviations from homeostasis using negative feedback, which is the mechanism that reverses the deviation from the set point. Therefore, negative feedback keeps the body's parameters within the normal range. The maintenance of homeostasis by negative feedback continues throughout the body at all times. [9, 10 p. 17-18]

2.1. Cardiovascular System

The cardiovascular system is one of the organ systems of the human body, and its function is to circulate blood throughout the human body to provide nutrition, building materials, and oxygen while removing carbon dioxide and other metabolic waste from the cells. In addition to this vital function, it works alongside the nervous system to mediate communication between cells and transport hormones and other neurotransmitters to target organs, and without a functioning cardiovascular system, human thermoregulation would not be possible. The cardiovascular system consists of three components: blood, heart, and blood vessels. These form a continuous connection consisting of a pump (the heart), a high-pressure distribution circuit, exchange blood vessels, and a low-pressure collection and return circuit [9, 10 p.128-129, 15 p. 303-323].

2.1.1. Heart and Blood vessels

The heart is a vital organ, and its function is to pump blood into circulation. The heart is a four-chamber organ, where the two atriums collect the blood, and the two ventricles pump out the blood to the lungs i.e., the pulmonary circulation, and the rest of the body i.e., the systemic circulation. The pumping action of the heart is largely autonomic, which means that the heart functions fairly independently under the control of its own regulatory system. Figure 1 shows the anatomy of the heart and the main blood vessels connecting to it. The resting or the filling phase of the ventricle is called diastole, and the contracting or pumping phase is called systole. [9, 16 p. 14-28.]

The heart muscle, myocardium, is formed out of special cardiac muscle cells, which resemble skeletal muscle but are multinucleated and the individual cells or fibers are interconnected in a latticework fashion, thus the stimulation or the depolarization of

one cell spreads the action potential through the myocardium to all cells and makes the heart function as a unit [10 p. 90, 15 p. 303-323].

In the junction of the superior vena cava and the right atrium are specialized pacemaker cells that form the sinoatrial (SA) node, which controls the heart rate or cardiac rhythm. Impulses from the autonomous and central nervous systems control the SA node firing, leading to the delivery of acetylcholine or adrenaline neurotransmitters. The former causes a decrease in heart rate upon vagal stimulation and the latter causes an increase in heart rate upon sympathetic stimulation. The SA node is a natural pacemaker that triggers its own series of action potentials, which propagate along with a specialized conduction system in the rest of the heart, causing a specific pattern of excitation and contraction. The average resting heart rate is about 70 beats per minute (bpm). Heart rate is lower during sleep and higher during exercise when it can reach as high as 200 bpm. In most people, a resting heart rate lower than 50 bpm can indicate a disorder called bradycardia. A high resting heart rate, on the other hand, can be due to illness, disease, or cardiac abnormalities, and is called tachycardia. Arrhythmias are any disorders of the regular rhythmic activity of the heart, which can be caused by irregular firing patterns of the SA node or by excessive and abnormal pacing activity in other parts of the heart. [9, 16 p. 14-28.]

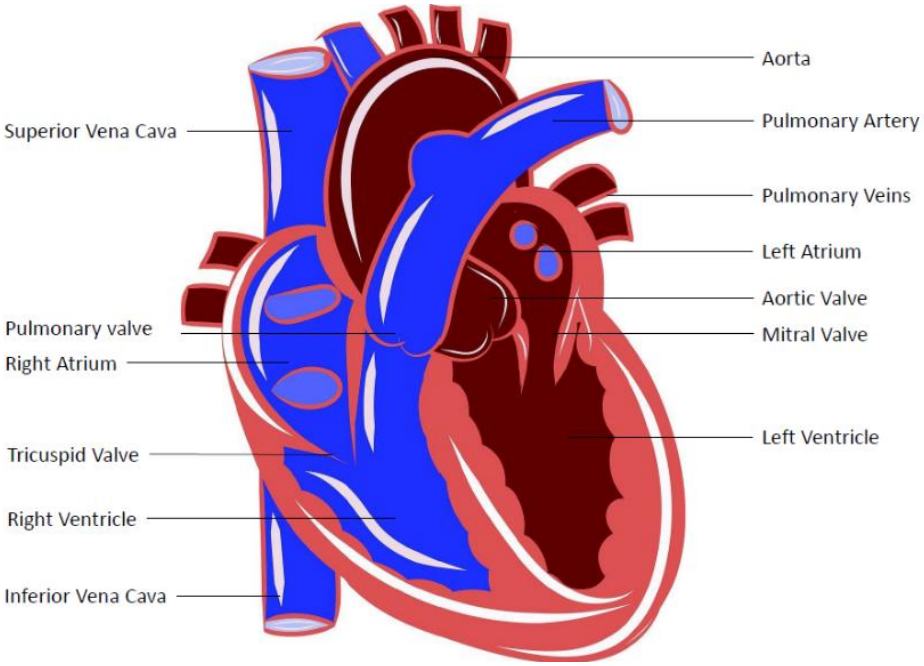

Figure 1. The heart [17].

The right atrium receives the blood from the systemic circulation through the inferior and superior vena cava. During the atrial contraction, blood is passed to the right ventricle through the tricuspid valve. During ventricular systole, the blood is pumped out to the pulmonary circulation, through the pulmonary valve, and into the lungs for oxygenation. The left atrium receives the oxygenated blood from the pulmonary circulation, and it is further passed on to the left ventricle during atrial contraction via the mitral valve. The left ventricle pumps the blood to the systemic circulation during ventricular systole, and it is the strongest among the chambers

because it has to pump the blood through the aortic valve and the aorta against the pressure of the systemic circulation. [16 p. 14-28.]

Blood vessels provide a transportation system for the blood throughout the whole body and the physical site where gases, nutrients, and other substances can change with cells. Figure 2 illustrates the human circulatory system and shows the main blood vessels. The arteries compose the high-pressure tubing that propels oxygen-rich blood away from the heart into the tissues. The arteries have thick walls and therefore no gaseous exchange happens between arterial blood and surrounding tissues. From the heart, the blood is pumped into the highly muscular but elastic aorta and from there distributed into the body through an intricate and efficient network of arteries and smaller arterial branches called arterioles. The walls of arterioles constitute circular layers of smooth muscle that either constrict or relax regulating blood flow to the periphery. They can dramatically change their internal diameter to rapidly react to changing conditions and therefore adjust blood flow through the vascular circuit, the arterioles are thus sometimes referred to as "resistance vessels". The arterioles form and branch to smaller and less muscular vessels called metarterioles and these end in a mesh of microscopically small blood vessels called capillaries. The capillary wall usually consists of a single layer of rolled-up endothelial cells and some capillaries are so small in diameter that only one red blood cell is able to pass through at a time. The capillary diameter is controlled by a precapillary sphincter, a ring of smooth muscle at the origin of the vessel. This sphincter provides an important local means of blood flow regulation by contracting and relaxing within specific tissue to meet the metabolic requirements. Vascular continuity continues into the venous system, where capillaries feed the deoxygenated blood into the small venules and veins. The blood flow velocity here again raises as the venous system cross-sectional area is smaller than capillaries. The small veins in the lower body (abdomen, pelvis, and lower extremities) eventually empty into the inferior vena cava, the body's largest vein. From the upper body (head, neck, shoulder regions, thorax, and part of the abdominal wall) blood flows into the superior vena cava. Both inferior and superior vena cava empties into the right atrium of the heart and flows through the right ventricle into the pulmonary artery to the lungs where the gas exchange takes place in the alveolar-capillary network. The oxygenated blood returns through the pulmonary veins into the left atrium to begin the passage once again throughout the body. [9, 15 p. 303-323]

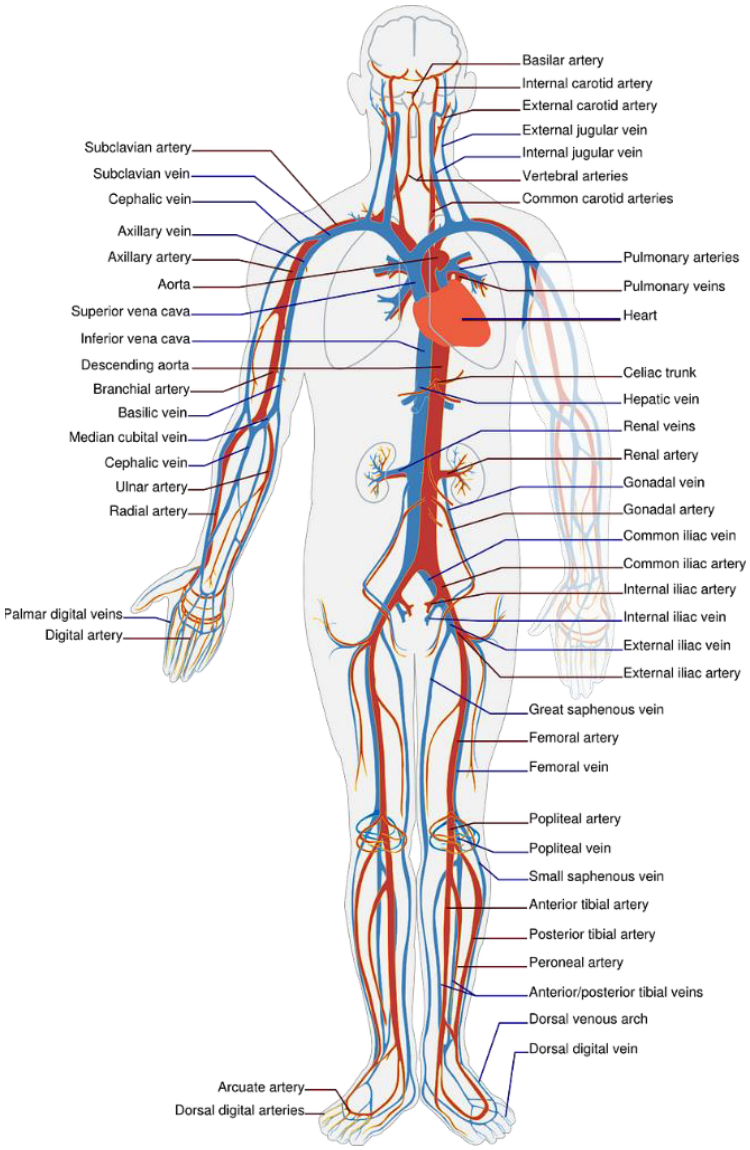

Figure 2. Human circulation system [18].

2.1.2. Blood Pressure

Blood flow is initiated by the contraction of the heart's ventricles. The contraction of the left ventricle ejects blood through the aorta into the major arteries, creating pressure within the arterial system, causing a pressure wave to travel down to the distal branches of the arterial tree. Arterial blood pressure reflects the combined effect of the arterial blood flow per minute (i.e., the cardiac output) and resistance to that flow in the peripheral vasculature. Blood pressure is controlled by the relationship between circulating fluid volume and peripheral vascular resistance. Circulating fluid volume is regulated by blood fluid volume and cardiac contractile force. Blood fluid volume is influenced by the balance of sodium storage and excretion (reflecting salt sensitivity and sodium intake). Cardiac contractility is regulated by both sympathetic nervous activity and cardiac function. Peripheral vascular resistance is regulated by vascular

tone, which is influenced by both vascular remodeling and vasoactive substances such as the renin-angiotensin system. [9, 15 p.306-310, 18]

The highest pressure produced by the heart averages 120 mmHg in normotensive people at rest during left ventricular contraction (systole). This systolic blood pressure is an estimate of the work of the heart and the force with which blood is exerted to the artery walls during ventricular systole. During the relaxation phase of the heart, the natural elasticity of the arteries maintains a constant pressure head. This ensures a steady flow of blood to the periphery until the next blood burst. During the relaxation phase of the cardiac cycle (diastole), arterial blood pressure falls to 60-80 mmHg. This diastolic blood pressure indicates peripheral resistance, i.e., the ease with which blood flows from the arteries into the capillaries. When peripheral resistance is high, the pressure in the arteries after systole does not disappear rapidly. Instead, it remains elevated for most of the cardiac cycle. [15 p. 306-310]

2.1.3. Cardiovascular system and diabetes

With a large proportion of people with type 2 diabetes being older adults, the effect of type 2 diabetes can be confounded by the typical age-related decline in cardiovascular function. It has been reported that people with type 2 diabetes had higher resting heart rates (as a percentage of maximum heart rate) and reduced stroke volume and cardiac output per minute compared with healthy young controls but were no different from the age-matched control group. On the other hand, other studies have reported that although the decline in cardiovascular function with aging is similar to that in people with type 2 diabetes, their absolute functional levels are lower, suggesting that aging and type 2 diabetes have synergistic negative effects. It is also known that people with type 2 diabetes have reduced exercise capacity compared to healthy individuals. Although the mechanism(s) underlying this functional impairment is not clear, it is thought to be related to a dampening of cardiac output growth during exercise due to left ventricular diastolic dysfunction. [4]

During intense heat exposure/exercise, people with type 2 diabetes may also have difficulty regulating blood flow. For example, type 2 diabetes is associated with impaired sympathetic neural control of blood pressure, manifested by greater orthostatic intolerance compared to age-matched controls. In addition, type 2 diabetics have a reduced baroreflex sensitivity, which is closely related to the level of insulin resistance. Thus, it would be expected that individuals with type 2 diabetes would be less able to maintain blood pressure and cardiovascular stability during extreme heat exposure and/or exercise. [4]

T2DM is associated with macrovascular changes, such as arterial stiffness in large elastic arteries. In addition, vascular endothelial dysfunction has been reported in patients with T2DM. These macrovascular events are usually accompanied by significant and progressive microvascular events due to functional and structural changes. The microvasculature can be characterized as a network of arteries, capillaries, and veins with diameters of less than 150 μm and is responsible for regulating tissue perfusion for optimal gas exchange and removal of metabolic waste products. Functional changes in the microcirculation in T2DM include altered microvascular blood flow, vascular resistance, and vascular permeability characteristics. One of the major causes of vascular abnormalities in diabetes is hyperglycemia, which affects among other things impaired vascular permeability, vascular tone, and automatic regulation of blood flow. In people with T2DM, the

media cross-sectional area of small blood vessels is increased, suggesting hypertrophic remodeling. Mechanisms underlying hypertrophic remodeling may include increased wall stress due to impaired myogenic response of small arteries in T2DM. The presence of endothelial dysfunction in T2DM may be related to the increased permeability of microvessels to large molecules such as albumin. In addition, vascular dysfunction of the capillary network in T2DM may alter insulin delivery and thus impaired insulin sensitivity. Observed microvascular structural changes in T2DM include thickening of the capillary basement membrane and reduced capillary size. Changes in the extracellular matrix of blood vessels are also observed in the vascular walls of T2DM patients. Although these structural and functional changes have been observed in diabetes, the mechanisms of these changes are not yet fully understood. [20, 21]

2.1.4. Hypertension and diabetes

Abnormally high blood pressure, called hypertension, strains chronically the cardiovascular system and, if left untreated, damages arterial vessels and leads to arteriosclerosis, heart disease, stroke, and kidney failure. Hypertension can be diagnosed when systolic blood pressure (SBP) is above 140 mmHg and/or diastolic blood pressure (DBP) is above 90 mmHg, of which systolic blood pressure is the more reliable and accurate predictor of risk associated with hypertension. The risk of developing hypertension increases with age, with a lifetime risk of over 80 %. Lowering blood pressure is effective in preventing strokes and other vascular events and lowering SBP by just 2 mmHg reduces deaths from stroke by 6 % and deaths from heart disease by 4 %. Drug treatment of hypertension is recommended if non-pharmacological approaches prove ineffective. [15 p. 315-316, 22].

Hypertension is a well-known complication of diabetes, and diabetes is a well-known complication of hypertension. Both diabetes and hypertension can cause various complications without symptoms. Type 2 diabetes and hypertension are well-established risk factors for cardiovascular disease (CVD), and people with T2DM and hypertension have an increased risk of CVD mortality. This increased risk is thought to be due to the synergistic effect on large and small blood vessels simultaneously, which reduces the compensatory collaterality that protects organs from the adverse effects of damage to either vascular bed. As the main function of the vasculature is to deliver oxygen and nutrients to tissues, the functional changes that occur in T2DM and hypertension significantly alter the hemodynamic stress on the heart and other organs. And the interaction between these two conditions can also lead to the development of stroke and myocardial infarction due to the progression of arteriosclerosis. [19, 20]

The increase in blood pressure is preceded the endothelial dysfunction and vascular remodeling, through which the resistance vessels narrow, and this promotes the elevation in blood pressure and the increase in vascular resistance. The blood pressure elevation is observed in resistance vessels that undergo vascular remodeling if the functional vasoconstriction remains at a constant level. The advanced vascular endothelial dysfunction promotes the progression of vascular remodeling and thus a cycle can develop. The presence of coexisting risk factors (e.g., hypertension, diabetes, and dyslipidemia) promotes more advanced vascular endothelial dysfunction and ultimately produces damage to various organs. The development of arteriosclerosis involves oxidation stress, inflammation, vasoactive materials, cytokines, chemokines, and growth factors that can affect each other. [19]

2.2. Autonomic Nervous System

The human nervous system can be divided anatomically into two major parts: the central and peripheral nervous systems. The central nervous system (CNS) is the brain and spinal cord, and the peripheral nervous system (PNS) is the nerves and ganglia outside the CNS. The nervous system can also be divided into two parts mostly based on a functional difference in responses: the somatic and autonomic nervous systems. The somatic nervous system (SoNS) is associated with conscious perception and voluntary motor responses and the autonomic nervous system (ANS) is associated with involuntary responses of the body, such as those related to homeostasis. In addition to the endocrine system, the ANS is an important part of the body's homeostatic mechanisms, and it can be divided into two divisions. The two divisions are the sympathetic nervous system (SNS) and the parasympathetic nervous system (PSNS). The sympathetic system is associated with the fight or flight response, and the parasympathetic system is referred to as rest and digest. The interaction and balance between the sympathetic and parasympathetic divisions, or homeostasis, leads to sympathovagal balance, which is responsible for, among other things, modulating the sinus node, promoting heart rate regulation, altering systolic and diastolic volumes, and promoting control of vascular smooth muscle cells, thereby affecting peripheral vascular resistance. Most of the organs under the autonomic regulation receive connections from both sympathetic and parasympathetic divisions. The division of the autonomic nervous system, therefore, does not mean that its different parts are independent units, but that it functions as a whole. [9, 10 p. 328 – 350, 11]

The sympathetic nervous system is activated during stress and physically demanding situations, for example, to improve the body's physical performance and prepare it for demanding tasks. Due to the interconnection of sympathetic ganglia, the effect extends to all target organs of the sympathetic nervous system. Activation of the sympathetic nervous system, in general, accelerates the activity of the target organs. The parasympathetic nervous system, on the other hand, is activated during rest and recovery, when, for example, digesting food and replenishing the body's resources is more important than using resources. In normal situations, the parasympathetic nervous system plays a more dominant role in the regulation of target organs. Parasympathetic activity, for example, reduces the pumping force of the heart and lowers blood pressure. Most parasympathetic nerve fibers pass through the vagus nerve. Parasympathetic ganglia are not connected, so its effects may therefore be limited to a single target organ. Both divisions are equally important and chronic changes in the balance between the two, cause autonomic dysfunction. And because cardiovascular autonomic dysfunction is potentially arrhythmogenic, it can predispose to atrial and ventricular arrhythmias and sudden cardiac death. [9, 10 p. 328 – 350, 11]

Heart rate variability (HRV) is the variation between each heartbeat in relation to time. It is highly influenced by the autonomic nervous system and as such is an indicator of ANS function and therefore is used to analyze it. The duration of consecutive heartbeats is not fixed and reflects the combined activity of sympathetic and parasympathetic divisions, the greater the variation, the greater the parasympathetic activity. High HRV reflects the individual's ability to adapt continuously to changes in the microenvironment (although, higher HRV is not always better because pathological conditions can produce HRV) and low HRV is a marker of cardiovascular risk. Measuring HRV is convenient because it is non-invasive, painless, and cost-effective. But, although HRV indices and their interpretations are

well established in the literature, their reference values are still not standardized. In 1996, the European Society of Cardiology and the North American Society of Pacing and Electrophysiology published guidelines setting out standardized values for HRV measurements and their clinical correlations. However, some of the ranges were from studies with small sample sizes and were not adjusted for potential confounding factors such as gender, age, or environmental factors. They should therefore be considered as estimates. However, despite criticism and the lack of standardized reference values, HRV remains a method widely associated with health and the body's ability for self-regulation, adaptability, or resilience, as well as early detection of autonomic changes and increased cardiovascular risk. Moreover, HRV has been reported as a tool for identifying cardiovascular disease risk even in individuals with no history of cardiovascular disease. [11, 13, 14]

2.2.1. Autonomic nervous system regulation and diabetes

Several studies have evaluated the assessment of heart rate variability in T2DM, but there have been conflicting results reported. In general, studies show that individuals with T2DM have reduced heart rate variability at rest and during postural changes compared to age-matched controls. Some evidence suggests that heart rate variability may be a predictor of diabetes-related complications. In a recent meta-analysis main finding was that T2DM patients had a strong decrease in HRV, in both sympathetic and parasympathetic activity, compared to non-T2DM persons. This decrease in HRV, which is shown in most of the time and frequency parameters, can be explained by the adverse metabolic effects of blood glucose levels on HRV, although it has been suggested that acute episodes of hyperglycemia cause more harm than chronic poor glycemic control. Dyslipidemia and hypertension are also associated with decreased HRV in T2DM. Many diseases or conditions have been linked with a decrease in parasympathetic activity and sympathetic activity increase, but in this meta-analysis, they demonstrated that in T2DM both divisions were decreased in activity, compared to non-T2DM persons. One explanation for this could be that T2DM is a metabolic disease causing cardiac autonomic neuropathy that affects both sympathetic and parasympathetic fibers. They also did find an association between total cholesterol and an increase in both the low frequency (LF) and high frequency (HF) bands. Also, they demonstrated that an increase in systolic blood pressure was linked with shorter RR intervals and a decrease in HF. They also found a significant relationship between body mass index (BMI) and HRV. However, the severity of obesity-related diseases is particularly related to fat distribution, especially its visceral localization, and HRV parameters have previously been correlated with sagittal abdominal diameter, anterior forearm skinfold thickness, and waist-hip ratio. This meta-analysis also demonstrated a decrease in both LF and HF with age and male gender, but these had a minor role on the HRV parameters compared to the variables linked to T2DM. [4, 12]

2.3. Thermoregulation

Humans regulate their temperature within certain limits, although the ambient temperature, for example, can vary widely. The highest temperatures are in the brain and inside the chest and abdominal cavity and are called the core temperature, which is closely regulated. Surface temperatures, on the other hand, can vary widely

depending on ambient temperature and surface blood flow. The core temperature represents a dynamic balance between the factors that increase and decrease body heat, including radiation, conduction, convection, and evaporation, which produce heat loss, and the basic metabolism, muscle activity, hormones, the thermic effect of food, changes in posture and the environment, which produce heat gain. The integration of mechanisms that modify heat transfer to the periphery regulates evaporative cooling and alters the body heat production to maintain temperature balance, and the temperature regulation is fine-tuned by circulatory adjustments. Heat is retained by the rapid movement of blood into the body's deep cavities and parts of the muscle mass, thus optimizing insulation from subcutaneous fat and other body surfaces. In contrast, the increase in internal heat dilates peripheral blood vessels as warm blood flows to the cooler periphery. The effort to maintain temperature balance is so powerful that it triggers sweating in the heat or increases oxygen consumption due to shivering in severe cold. [10 p. 260-266, 15 p. 611-639]

In response to thermal stress, humans trigger several critical thermoregulatory responses, such as piloerection, shivering, sweating, and profound changes in skin blood flow. All these efferent responses are controlled by higher brain centers, primarily the preoptic/anterior hypothalamus, which is considered the main integration and control center for thermoregulation. A specialized group of neurons in the hypothalamus acts as a thermostat, usually carefully set and adjusted to 37 °C ± 1 °C, continuously making temperature adjustments to compensate for deviations from the temperature norm. The hypothalamus cannot “turn off” heat, but it triggers responses to protect the body from either a build-up or loss of heat. The body’s thermoregulatory mechanisms are activated by thermal receptors in the skin that provide input to the central control center and by changes in the blood temperature, which perfuse the hypothalamus directly to stimulate neurons. Peripheral thermoreceptors, which respond to rapid changes in heat and cold, are mainly free nerve endings in the skin, especially on the face. In general, cold receptors exist more than warm receptors. Cold receptors are usually located close to the skin surface and play an important role in triggering regulatory responses to the cold environment. Skin thermoreceptors act as an “early warning system” that relays sensory information to the hypothalamus and cortex. This direct line of communication triggers appropriate heat-saving or heat-releasing physiologic adjustments, and the individual also makes a conscious effort to seek relief from the thermal challenge. In addition to receiving peripheral input, cells in the anterior hypothalamus detect small changes in blood temperature. Increased activity of these cells stimulates other areas of the hypothalamus to initiate coordinated responses for heat conservation or heat loss. In contrast to peripheral receptors that detect cold, the temperature of the blood passing through the hypothalamus is the primary monitoring system for assessing body warmth. [10 p. 260-266, 15 p. 611-639, 23]

2.3.1. Thermoregulation in heat stress and heat loss

The body’s thermoregulatory mechanisms protect primarily against overheating and the mechanisms for heat loss are the same whether the heat load is internal (metabolic heat) or external (environmental heat). Under the heat load, the heat stress triggers a series of well-coordinated cardiovascular responses that are essential to promote heat transfer between the body and the environment to maintain thermal homeostasis. These cardiovascular responses include a considerable increase in cardiac output and

redistribution of blood, which together contribute to a substantial increase in skin blood flow, thereby the circulatory system can be represented as the “workhorse” to maintaining thermal balance. The hypothalamus triggers an increase in heat loss following the afferent input from central and peripheral thermoreceptors through an increase in skin blood flow (i.e., vasodilation) and sweating. Vasodilation opens skin blood vessels, resulting in increased blood flow to the skin, which raises skin temperature and thus increases the gradient of dry heat exchange between the skin and the external environment. However, heat loss is only activated when the mean body temperature has exceeded a certain threshold. Heat loss responses then increase in proportion to the increase in mean body temperature, the linear component of which represents the thermosensitivity. When heat loss responses reach maximum values, heat loss no longer increases even if the mean body temperature continues to rise, and a continued rise in mean body temperature can lead to heat-related illness and/or injury. The onset threshold, thermal sensitivity, and maximum capacity of heat loss responses associated with skin vasodilatation and sweating can have a significant impact on the amount of heat stored. [4, 10 p. 260-266, 15 p. 611-639, 23]

The body loses heat through four physical processes: radiation, conduction, convection (air movement), and evaporation (sweating). Radiative heat transfer is usually the most significant form of heat loss. In radiation, heat radiates from warm surfaces toward cold surfaces and, because the human body generally remains warmer than the environment, the net exchange of radiant heat is transferred through the air to solid, cooler objects in the environment. Heat transfer by conduction refers to the direct transfer from one molecule to another through a liquid, solid, or gas. Conduction heat loss is then associated with warming air molecules and cooler surfaces in contact with the skin. Conduction is an effective form of heat loss, but it is usually of little importance because heat is only conducted from the soles of the feet in the standing position. The wind carries heat away from the skin and clothing surface and can multiply heat loss, this is called convection or convective heat loss. If air movement or convection is slow, the air next to the skin warms and acts as an "insulation zone". Conversely, if cooler air is constantly replacing warmer air around the body on a windy day or when running, heat loss increases because convection is constantly replacing the insulation zone. The cooling effect of airflow forms the basis of the wind chill - index. This index describes the combined effect of wind and temperature on bare skin. The evaporation of water from the skin and respiratory tract absorbs a lot of heat, making it an effective means of removing heat from the body. Heat loss is further facilitated by convective airflow, which moves moist, humid air away from the skin surface. Each liter of water evaporated removes 580 kcal from the body and transfers it to the environment. There are about 2-4 million sweat glands on the surface of the body. During heat stress, these eccrine glands, controlled by cholinergic sympathetic nerve fibers, secrete large amounts of hypotonic saline solution. Sweat evaporates from the skin and has a cooling effect. Effective thermal defense exists when evaporative cooling is combined with a large skin blood flow. The cooled peripheral blood then flows to deeper tissues to absorb additional heat on its return to the heart. Sweating causes loss of water and electrolytes, which triggers hormonal changes to retain salts and fluid. In addition to the heat loss through sweat evaporation, about 350 ml of insensible sweat, i.e., the diffusion of water, seeps through the skin every day. The moist mucous membranes of the respiratory tract also evaporate about 300 ml of water daily. Evaporation is the main protection against overheating. As the ambient temperature rises, conduction, convection, and radiation reduce their effectiveness in

removing heat loss from the body. When the ambient temperature exceeds the body temperature, the body gains heat through these three heat transfer mechanisms. In such an environment (or when conduction, convection, and radiation are unable to remove the high metabolic heat load), sweating of the skin and respiratory tract is the only way to remove heat. [10 p. 260-266, 15 p. 611-639]

The total amount of sweat evaporating from the skin and/or respiratory tract is influenced by three factors: surface exposure to the environment, temperature and relative humidity of the surrounding air, and the convective air currents around the body. The relative humidity is the most important factor in determining the efficiency of evaporative heat loss. The relative humidity is the ratio of water in ambient air at a given temperature to the total amount of moisture that air could contain, expressed as a percentage. For example, relative humidity of 40 % means that ambient air contains only 40 % of the moisture capacity of the air at that temperature. At high humidity, the ambient vapor pressure approaches that of moist skin (around 40 mmHg). In this case, evaporation is greatly reduced, although large amounts of sweat accumulate on the skin and roll off. This form of sweating represents a useless loss of water, which can cause dehydration and overheating. Constant drying of the skin, for example with a towel, prevents evaporative cooling. Evaporation, not sweat, cools the skin. Humans can tolerate relatively high ambient temperatures if relative humidity remains low. Most people find a hot, dry desert climate more comfortable than a cooler but more humid tropical climate. [15 p. 611-639]

2.3.2. Thermoregulation in cold stress and heat production

A normal heat transfer gradient flows from the body to the environment. In general, there is no physiological stress involved in core temperature regulation. However, in extreme cold, excessive heat loss can occur (especially at rest), where the body's heat production increases while heat loss slows down to minimize any decline in core temperature, and this may cause physiological stress on humans. During cold exposure, sympathetic thermoregulatory reflexes, which are responsible for maintaining core temperature during cold exposure, are activated when the average skin temperature falls from a thermo-neutral temperature of about 34°C. Stimulation of the cold receptors in the skin constricts peripheral blood vessels, which immediately reduces the flow of warm blood to the cooler surface of the body and directs it to the warmer core. Peripheral blood flow is reduced when smooth muscle cells in the walls of small blood vessels contract under the control of the sympathetic nervous system. This control of the cutaneous blood flow is crucial for thermoregulation in humans. During exposure to cold, the reduction in skin blood flow reduces convective heat loss and increases the insulating effect of the skin, muscles, and subcutaneous fat, minimizing changes in core temperature and preventing hypothermia. Skin blood flow averages 250 ml/min in a thermoneutral environment, but under intense cold stress, this flow can approach zero. The reorganization of the circulation in the cold usually raises blood pressure by about 20-40 mmHg, and cooling can also constrict myocardial blood vessels, making it more difficult to supply oxygen to the myocardium. A person with excess body fat who is exposed to cold stress will benefit greatly from this heat-saving mechanism. In leaner individuals with a normal body fat content, regulation of skin blood flow usually provides effective thermoregulation at ambient temperatures between 25-29 °C. [15 p. 611-639, 23]

Metabolic heat production can be increased by shivering and non-shivering thermogenesis and the response to cold is regulated by the internal mean temperature, not the body's heat production per se. Increased heat production by shivering activates the skeletal muscles, which have the greatest capacity of all body tissues to increase the metabolism and thus heat production. Maximal heat production through shivering can increase up to fivefold from baseline, or to ~ 40 % of maximal aerobic capacity, and shivering often results in greater oxygen consumption under cold stress than in a thermoneutral environment. Non-shivering thermogenesis occurs mainly via metabolically active brown adipose tissue, and this physiological response is particularly important in mild cold exposure. [4, 15 p. 611-639]

Two "calorigenic" hormones in the adrenal medulla; adrenaline and noradrenaline, increase heat production during cold exposure. Prolonged cold stress also stimulates the release of thyroxine, a thyroid hormone that increases resting metabolic rate. [15 p. 611-639]

2.3.3. Thermoregulation and diabetes

Factors such as aging and diabetes may delay or raise the onset threshold and reduce the thermosensitivity and the maximum capacity of heat loss responses, which may allow a higher mean temperature to rise during heat stress. Most studies on type 2 diabetes and thermoregulatory capacity have been conducted in the context of defining the neuropathy severity and diabetes-related complications, and therefore have only assessed the local heat loss responses in the hands and feet. These studies have generally reported impaired skin blood flow responses in people with type 2 diabetes as a result of pharmacological stimuli, local skin heating, and whole-body heating. Importantly, these effects appear to depend on physical condition, such that in type 2 diabetics who exercise, the reduction in skin vasodilatation is reduced, although in people with type 2 diabetes the maximum skin blood flow is reduced regardless of condition. However, these diabetes-related changes in skin blood flow appear to be closely related to the duration of diabetes and/or the occurrence of associated complications. Although little is known about the central and peripheral mechanisms underlying diabetes-related skin circulatory responses, a study has found that a lower vasodilatation threshold was the primary factor explaining lower skin blood flow, indicating that regulation of skin blood flow is mediated by central nervous system mechanisms. [4]

Local sweating responses have also been commonly reported to be impaired in people with T2DM compared to their healthy controls, and changes in regional sweating responses have also been observed, such that there is relative lower body anhidrosis with hyperhidrosis in the upper body. The primary factors associated with reduced sweating are long-term diabetes, poor glycemic control, and neuropathy, which appear to play an important role in altering the peripheral properties of sweat glands. [4]

It also cannot be ignored that type 2 diabetes is often associated with one or more other health conditions (obesity, hypertension, cardiovascular disease) that may further affect an individual's ability to dissipate heat during heat stress. It has been shown that obesity is associated with impaired heat tolerance and reduced activation of the skin blood flow and sweating heat dissipation responses. In hypertensive individuals, blood pressure rises more during heat stress due to an increase in peripheral resistance, which may limit heat loss due to reduced skin blood flow, which may ultimately lead to a

more pronounced rise in core temperature. In individuals with cardiovascular disease, heat stress is associated with a reduction in exercise capacity and an increase in disease-related symptoms, making them more susceptible to the disease. [4]

Previous evidence suggests that hyperinsulinemia, which is known to occur in people with type 2 diabetes due to their impaired insulin sensitivity, may be associated with moderate skin vasodilation at rest. However, in people with type 2 diabetes, skin blood flow appears to be lower than in age-matched controls. While this may be considered beneficial as it minimizes heat dissipation during exposure to cold, type 2 diabetes is also associated with significant disadvantages in vascular responsiveness to cold. This has been demonstrated in studies that showed reductions in local, reflex, and centrally mediated mechanisms that can determine skin blood flow. Furthermore, this reduced responsiveness is at least partly due to a reduction in the control of vascular diameter by the sympathetic nervous system. Overall, there is some evidence that people with type 2 diabetes may be less able to prevent the drop in core temperature associated with exposure to cold. Studies have suggested that diabetes resembles advanced aging (i.e., diabetes tends to accelerate the changes associated with aging). The elderly are known to have a reduced ability to defend their core temperature during cold exposure, even during relatively mild cold exposure. This has been linked to a number of factors, including blunting of sympathetic outflow to the skin, reduced production and release of vasoconstrictor neurotransmitters, and changes in thermoafferent signaling. [4]

Glycemic control during thermal stress is one factor in thermoregulation in type 2 diabetics. Hypoglycemia is known to cause sympathetic activation, which is reflected in a marked increase in sweating, blood flow of the extremities, heart rate, and blood pressure. And while this may lead to a decrease in core temperature at rest, autonomic nervous system dysfunction may eliminate any potential benefits during whole-body heat stress. Similarly, periods of hyperglycemia may also have a significant negative effect on core temperature regulation. Hyperglycemia, in particular, can lead to an increase in plasma osmolality, which has been independently linked to a decrease in sweating and skin blood flow. People with type 2 diabetes are also at increased risk of dehydration due to increased hyperglycemia and/or medication use. This happens via osmotic diuresis, which can lead to hypovolemia without adequate fluid replacement. [4]

2.4. Cardiovascular Signals

Cardiovascular signals are an important source of information for monitoring the progress of physiological and pathological processes in the body. The connection between cardiovascular signals can be described as follows. Baroreceptors, which are blood pressure sensors located in the aortic arch and internal carotid arteries, contribute to short-term HRV. When inhaled, HR rises. BP rises about 4-5 s later. The baroreceptors detect this rise and are triggered more quickly. When exhaling, the heart rate decreases and BP drops 4-5 s later. The baroreflex contributes to this acceleration and deceleration of the heart, called respiratory sinus arrhythmia (RSA). It also links heart rate, blood pressure, and vascular tone. The oscillation of one cardiovascular function causes similar oscillations in other functions. Baroreceptor triggering due to changes in blood pressure activates mechanisms that alter heart rate and vascular tone. An increase in blood pressure causes a decrease in heart rate and vascular tone, while a decrease in blood pressure causes an increase in both. [13]

As with all signals that can be measured in humans, cardiovascular signals have a complexity that is due to human physiology, which is reflected in the signals. This complexity causes large inter-subject variability and exposes the signals to artifacts and noise due to physiological activity other than that being measured. In this study, three signals are analyzed, namely, HRV derived from electrocardiogram (ECG), BP variation derived from blood pressure, and cutaneous blood flow measured with Laser Doppler Flowmetry (LDF).

2.4.1. Electrocardiogram

The electrocardiogram (ECG) is perhaps the most known and used biomedical signal and it is the representation of the electric activity of the heart. It measures very small millivolt changes from the heart to the skin, and these voltage changes are associated with different periods of cardiac activity. It can be recorded with surface electrodes attached to the chest and/or limbs and together the connections form a three-dimensional electrical picture of the heart. The rhythm of the heart, as beats per minute, can be estimated by counting the readily identifiable waves. These waveshapes are altered by cardiovascular diseases and abnormalities like arrhythmias, infarction, or conduction problems. The ECG is therefore a very important signal and useful in heart rhythm monitoring and the diagnosis of cardiovascular diseases. [10 p. 136, 16 p. 14-28]

The standard electrocardiograph uses 3, 5, or 12 leads, the greater the number of leads, the more information the ECG provides. The conventional 12-lead electrocardiograph uses 10 electrodes that are placed on the person's skin, six on the chest, and four on the limbs, these electrodes together provide 12 simultaneous curves offering spatial information about the electrical activity of the heart. Each component, segment, and interval are labeled on the ECG and correspond to important electrical events, showing the relationship between these events and the contraction of the heart. [9, 10 p. 136-137]

The repetitive electrical depolarization and repolarization pattern of the heart muscle is represented by the ECG. The schematic form of the phases in the ECG is shown in Figure 3. On the ECG there are five prominent points: the P wave, the QRS complex, and the T wave. The depolarization of the atria is represented by the small P wave, the depolarization of the ventricles is represented by the large QRS complex, and the repolarization of the ventricles is represented by the small T wave. The repolarization of the atria is masked under the QRS complex and therefore is not showing in the ECG. [9, 24 p.176-178]

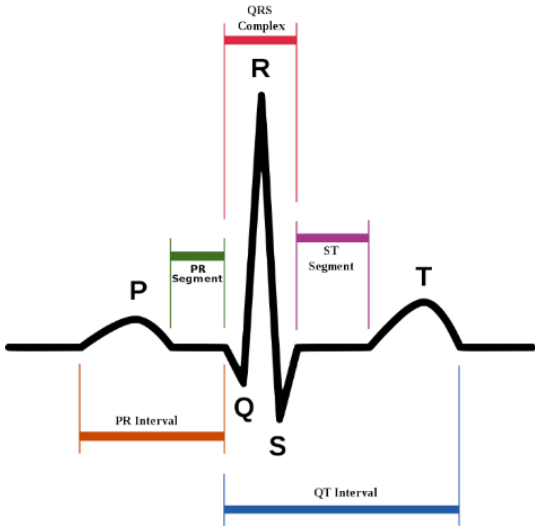

Figure 3. Phases of the electrical activity of the heart detected by ECG. [25]

2.4.2. Heart rate and HRV

The heart rate is the number of heartbeats per minute. Heart rate variability (HRV) is the fluctuation in the time intervals between adjacent heartbeats. A healthy heart is not a metronome, and HRV shows that the heart rate changes slightly from one beat to the next, even under similar conditions. The magnitude of variation depends on the activity of the autonomic nervous system, which regulates sinus rhythm. Therefore, by monitoring the heart, changes in autonomic nervous system activity can also be indirectly measured. On the other hand, other factors like a person's age, sex, state of health, time of day, body composition, respiratory rhythm, and blood pressure affect the heart rate variability either by increasing or decreasing and modifying the heart rate variability and therefore, its values are individual. Heart rate variability has been shown to reflect autonomic nervous system function and balance. Increased sympathetic activity, indicative of stress and strain, reduces the amount of heart rate variability. In turn, parasympathetic nervous activation, indicative of rest and recovery, increases it. [13, 14, 26]

HRV can be evaluated using linear or non-linear methods. In this thesis, linear methods are used because they can better evaluate short-term measurement periods. The linear methods can be divided into two groups: those analyzed in the time-domain and those analyzed in the frequency-domain. Time-domain indices of HRV quantify the amount of variability between successive heartbeats observed during the measurement period. Frequency-domain measurements assess the distribution of absolute or relative power over frequency bands. [11, 13]

HRV parameters. The time-domain: NN (normal-to-normal R-peaks) intervals, mean on NN intervals, the difference between the longest and the shortest NN interval, standard deviations of NN intervals (SDNN), the root mean square of successive NN interval difference (RMSSD), number of interval differences of successive NN intervals greater than 50 milliseconds (NN50), and the percentage of successive NN intervals differing by more than 50 milliseconds (pNN50). The RMSSD, NN50, and pNN50 are associated with high-frequency power (HF) and therefore the parasympathetic activity, whereas the low-frequency (LF) band has a significant impact on the SDNN. SDNN is, however, more accurate when calculated over 24

hours than over shorter periods. The frequency-domain: ultra-low-frequency (ULF; ≤ 0.003), requires a long recording period (at least 24 h), very low frequency (VLF; 0.003– 0.04 Hz), which is comprised of rhythms with periods between 25 and 300 seconds, the LF (0.04–0.15 Hz) is comprised of rhythms with periods between 7 and 25 seconds and is affected by breathing from about 3 to 9 bpm, and the HF (0.15–0.4 Hz) is influenced by breathing from 9 to 24 bpm. The LF/HF ratio may estimate the ratio between the sympathetic nervous system (SNS) and parasympathetic nervous system (PSNS) activity, i.e., the sympathovagal balance. [13, 26]

Awareness of the recording context and the subject variables can help in the interpretation of both long and short-term HRV measurements. Important contextual factors include the length of the recording period, the method of detection or recording, the sampling rate, artifact removal, respiration, and whether paced breathing is involved. Important subject variables are age, sex, heart rate, and health status. In addition, the effects of posture, movement, and frequency of physical activity can all affect measurements subtly or even greatly by altering ANS activation, respiratory mechanics, and emotions. [13]

2.4.3. Blood Pressure

Hydrostatic pressure is the force exerted by a fluid due to gravitational pull, usually against the wall of the container in which it is located. One form of hydrostatic pressure is blood pressure, the force exerted by the blood upon the walls of the blood vessels or the chambers of the heart. Blood pressure may be measured in capillaries and veins, as well as the vessels of the pulmonary circulation; however, the term blood pressure without any specific descriptors typically refers to systemic arterial blood pressure. [9]

Blood pressure is one of the vital signals used to detect a wide range of abnormalities. Typical blood pressure measurements are limited to systolic and diastolic pressure (rather than the whole signal). However, when the whole blood pressure signal is collected, much more information can be extracted from the data. Typical blood pressure signal measurements can be classified into extravascular and intravascular measurements. Typical blood pressure measurement is a popular sphygmomanometer and stethoscope system that is considered the gold standard for extravascular blood pressure measurement systems. Today, however, semi-automatic blood pressure measuring devices are commonly used, most of which measure blood pressure using oscillometry. Intravascular blood pressure measurement is often measured by inserting an arterial catheter. Catheter insertion is often used to measure the entire blood pressure signal, as opposed to recording only SBP and DBP in sphygmomanometer and stethoscope systems or semi-automatic devices. Another way to get continuous blood pressure is to measure finger arterial pressure with a device that uses a volume-clamp method, this method was also used in this study. This is a non-invasive method, where a small, inflatable, cuff is placed around the finger. The cuff uses photoplethysmographic technology for continuous blood pressure monitoring. [24 p. 237-238, 27]

The schematic form of the phases in the BP is shown in Figure 4. On the BP signal, there can be observed different points representing a different phases in a cardiac cycle. The systolic peak (green triangle) is a result of the ejection of blood from the left ventricle to the aorta reaching a peak, the dicrotic notch (blue triangle) is a result of the closure of the aortic valve, and the diastolic peak (purple triangle) is a result of a reflected pulse from the lower body. [16 p. 38]

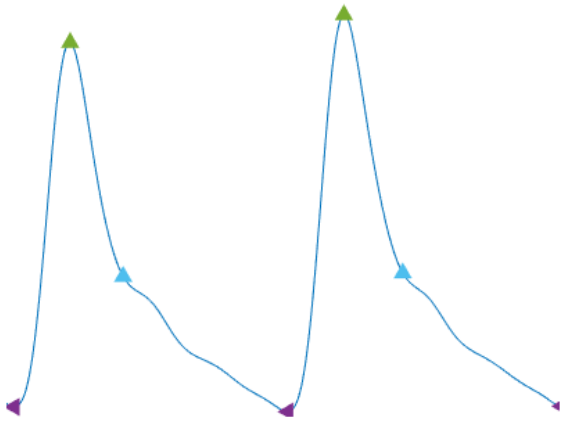

Figure 4. Blood pressure waveform.
▲systolic pressure, ▲dicrotic notch, ▲the diastolic pressure.

2.4.4. Laser Doppler Flowmetry

Laser Doppler flowmetry (LDF) is a method developed specifically to assess microvascular blood flow from the cutaneous microvasculature and it provides a continuous estimate of skin blood flow. It can provide information on the heat exchange between the body and the environment, especially under heat stress, where blood flow increases, in some cases up to 8 liters per minute, thus allowing optimal regulation of the body's core temperature. LDF measurement is a non-invasive, easy-to-set-up measurement measured with probes attached to the skin, from which the vascular bed is readily accessible. LDF has found wide applications in the analysis of microcirculation reactions to different physiological and pharmacological stress tests because it can have excellent temporal resolution and because it provides only a relative index of perfusion in the time-domain. These reactivity tests include mental stress, orthostatic stress, post-occlusive reactive hyperemia, local thermal warming, and pharmacological tools such as iontophoresis of vasoactive agents, and are usually coupled with the skin blood flow in the time-domain to gain insight of the vasodilatory capacity and the mechanisms underlying vascular control. These reactivity tests can also be used to estimate the relative change in spectral energy in any frequency band as a result of a reactivity test. [28, 29, 30]

LDF uses electromagnetic light wave, a laser, to detect the Doppler Effect from the peripheral blood vessels. The general principle of this technology is an interaction of monochromatic laser light with tissue and blood vessels utilizing the frequency shift called Doppler shift, which arises in the light that has been scattered by moving red blood cells. By analyzing the shifted frequency of the backscattered light, where the mean velocity of red blood cells is associated with backscatter and the amplitude of the signal is seen as proportional to red blood cell concentration, the information of the blood flow can be determined as follows

$$flow = RBC_{concentration} \times RBC_{velocity}$$

where RBC stands for red blood cell.

It is therefore important to note that laser Doppler flow measurement does not provide a quantitative estimate of blood flow, but rather a qualitative estimate based

on changes in red blood cell flow. The main advantage of laser Doppler flowmetry is the ability to continuously measure red blood cell flow with a high temporal resolution, especially in skin microvasculature. Laser Doppler flowmetry measurement can be used to assess blood flow in the microvasculature *in vivo* but is mainly used in research because it does not provide an absolute value of blood perfusion. However, a few clinical applications have been found useful in monitoring microvascular blood flow, for example after skin replacement surgery. Figure 5 shows a typical signal measured with the LDF with few motion artifacts. [28, 31, 32]

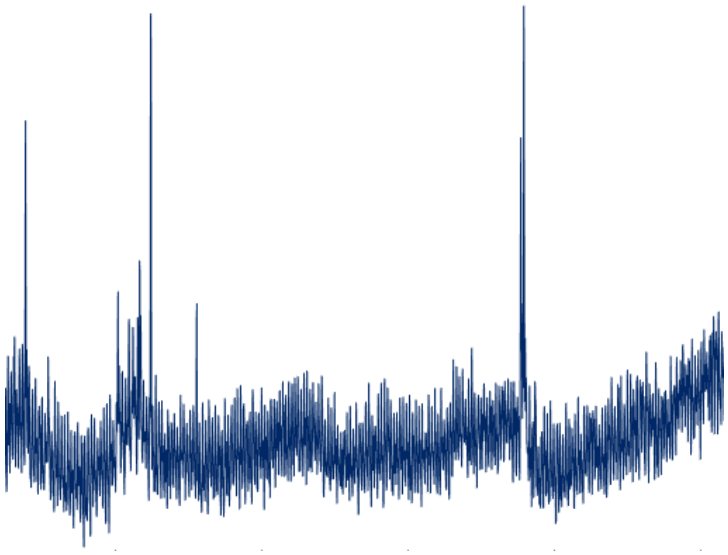

Figure 5. Typical LDF signal with few motion artifacts.

Although the main advantage of the laser Doppler Flowmetry technique is its non-invasiveness and the ability to estimate the microcirculatory blood flow of the tissue locally and the fast changes of perfusion during provocation, it is not without disadvantages. One major disadvantage and limitation of LDF is the motion artifacts due to the movement of both the tissue and the optical fiber. Since LDF measures the movement of scattering objects instead of blood perfusion, it is important that blood perfusion dominates the perfusion signal. This is not necessarily the case if the tissue being measured is moving, as this movement can produce a much larger perfusion signal than the perfusion itself. The small sampling area also poses limitations to the method, as a local measurement of blood flow may not be representative of the limb or whole-body blood flow levels. The small sampling area also makes it difficult to reliably assume that repeated measurements will occur at the same point when probes are removed between measurements, even when efforts to minimize differences in probe placement are taken into account (e.g., photographing or marking the skin). This aspect leads to poor reproducibility of LDF measurements. In addition, the small sampling area makes the measurements highly dependent on the anatomy of the underlying microvasculature, where the distribution and anatomy of superficial veins and arterioles contribute to heterogeneity. This results in high heterogeneity of the measurements between the subjects and within the same subject when measured from different points of the body or at different times. To account for this heterogeneity, several normalization methods have been employed for LDF signals. One of which is normalizing the values as a percentage of the maximal dilation of the sampling area, where the different sites are compared in relation to their maximum dilation capacity.

While this is probably the strongest approach to account for intersite or daily variability in absolute flow values, it should be kept in mind that the mere presentation of data as a percentage of the maximum may mask some important differences between conditions or groups. Also, the maximal response can be affected by the physiological condition, for example, disease state, and this should be taken into consideration when applying this normalization procedure. Lastly, the maximal values are always relative to the method employed to gain maximal response and may not necessarily reflect "true" maximal vasodilation. There is also little interpretive value in reporting blood flow responses relative to the area's maximal response when the interest is in heat dissipation since absolute skin blood flow will affect skin temperature, and therefore, the skin-to-air temperature gradient, which dictates dry heat exchange between the body and the environment. Another normalization method is to normalize the blood flow values relative to a baseline value, but this is highly dependent on the baseline values and the blood flow values can have the same relative increase or decrease in blood flow due to a provocation, but yet still have the absolute values differ between measurements or subjects, for example, threefold. [28]

Another disadvantage is that the depth and volume of most in vivo optical measurement techniques, like LDF, are not known. The measurement volume for most biological tissues is in the area of one cubic millimeter, usually decreasing with increased absorption and scattering. For optical fiber systems, it is increasing with increasing fiber separation. One challenge also behind LDF measurements is biological zero. This occurs during blood vessel occlusion when the blood cells do not move but experience some motion, so-called Brownian motion. The residual signal component at the cessation of tissue perfusion is called biological zero. This is the main reason why the perfusion value never reaches zero even if the blood flow is ceased. These disadvantages and challenges prevent the use of LDF in clinical settings, also the lack of quantitative units (LDF output signal is in perfusion units (p.u) that is relative) and the lack of standardization of measurement protocols are major disadvantages. [28, 33]

2.5. Related Research

As a global public health problem, diabetes and its associated comorbidities have long been studied, both for type 1 and type 2 diabetes, to better understand and manage the disease. The impact of diabetes on the body, and the cardiovascular system, has been investigated through various biomedical signals. The relationship between diabetes and changes in heart rate variability, as well as the effects of diabetes-related comorbidities and obesity on heart rate variability, have been extensively studied [11, 12]. In general, HRV and diabetes studies have calculated different time- and frequency parameters. In most studies, frequency-domain analysis has been performed by Fourier transform, like all the studies reviewed in the articles [11, 12], but wavelet analyses are also seen [34, 35]. In general, studies have found that diabetic patients have decreased HRV, both sympathetic and parasympathetic branch activity. People with diabetes also often have hypertension, the effects of which on vascular changes have been widely studied [19, 20, 36]. Blood pressure variability, and in particular systolic blood pressure variability, has also been extensively studied, but its clinical significance is still unclear [37]. In the study of blood pressure variation, different time periods are used for follow-up, one of which is the very short-term follow-up, which has been used in this study. Most often, time-domain values have been used to quantify

changes in blood pressure variability [37], but there are also many studies where frequency-domain analysis has been used [38]. In the frequency-domain analysis of blood pressure variation, as with the analysis of HRV, the most used analytical method is the Fourier transform [38]. The relationship between diabetes and surface blood flow and the changes in blood flow relative to healthy individuals have been previously studied [29, 30, 39-42]. These studies have also used both the time-domain and the frequency-domain analyses. Most often, wavelet analysis has been used to investigate the surface blood flow in the frequency-domain [30, 40, 42]. Most studies have found a decrease in blood flow in diabetic subjects following local heating relative to healthy subjects, as well as a decrease in frequency-domain parameters such as amplitude and power, especially at frequencies associated with endothelial (0.0095 – 0.021 Hz), neurogenic (0.021 – 0.052 Hz) and myogenic (0.052 – 0.145 Hz) frequencies [30, 40, 42], but also at cardiac (0.6 – 2 Hz) frequency [30].

As outlined above, human cardiovascular signals (also including the respiratory signal) have been extensively studied using frequency-domain analysis, but mostly one or two signals have been studied separately from the other cardiovascular signals. Nevertheless, studies of more than two signals, especially in the frequency-domain, have been carried out. Ticcinelli et al [43] conducted a study in which they analyzed the deterministic properties of the HRV signal together with simultaneously recorded respiratory and microvascular circulatory signals in healthy adolescents, healthy elderly, and elderly with hypertension on medication. They focused on investigating phase coherence and coupling between myogenic activity and cardiorespiratory oscillations using methods to capture time-dependent dynamics, including the Wavelet Transform. They found that the coherence between blood flow and low-frequency oscillations of HRV time series near 0.1 Hz varies significantly between groups, decreases with age, and almost disappears in treated hypertension. Comparing the healthy adolescents and healthy elderly, it was found that the coupling of both respiratory and vascular myogenic activity to heart rhythm decreases significantly with age. Comparing data from healthy elderly and elderly groups with hypertension, it was found that the coupling with vascular myogenic activity is significantly weaker in treated hypertension, suggesting that current antihypertensive drugs do not fully restore microcirculatory mechanisms. Bračič et al [44] conducted a study in which they investigated respiratory, ECG, heart rate variability, blood pressure, and blood flow signals and their frequencies in a time-averaged wavelet transform recorded from healthy young men. They found that although small differences in the frequencies of these signals can be observed, dominant frequency peaks occur in the same frequency range for different signals. With this, they demonstrated that wavelet transform (WT) measurement of cardiovascular signals can detect the regulatory mechanisms reflected from the cardiovascular system at the site of detection, making frequency-domain analysis an important technique for identifying the oscillatory dynamics of the cardiovascular system.

In this thesis, the WT frequency-domain analysis method is used to study the frequency components of three signals in diabetic and healthy individuals measured at the same time from different sites of the body, before, during, and after temperature exposure (warm and cold) to detect how they change and evolve.

3. METHODS

3.1. Setup – The Experimental Study

Participants with advanced T2DM (disease duration ≥ 2 years) and hypertension were included with the following inclusion criteria: BMI 25-30, age 40-70 years, male, HbA1c 53-75 mmol/mol, non-smokers, no active retinopathy. A similar number of age-matched controls without T2DM or hypertension were also included. In the first phase of the project, a total of 10 subjects with T2DM and 10 controls were measured. All subjects underwent autonomic nervous system and peripheral nervous system function tests at the clinic of the neurophysiology of Oulu University Hospital before the actual study measurements. The study was approved by the Ethics Committee of Oulu University Hospital District (EETTMK:199/2016). The study is registered in the Clinical Trials (NCT04698200).

The experimental study was carried out in the thermal laboratories of the Kastelli Research Centre, Oulu, in spring 2021. In the experimental study, subjects were randomly exposed to both cold (+10°C) and hot (+40°C) environmental temperatures while resting for 90 minutes. Exposures were preceded by baseline measurements (30 min) and post-exposure follow-up measurements (30 min) of variables at +22°C. The exposures were chosen to induce thermogenesis in the cold and sweating in the warm. These also include significant changes in surface blood flow. For the exposures, subjects wore a t-shirt, shorts, and socks.

The main variables of the study are blood pressure (central, peripheral, finger blood pressure) and ECG (12-lead, ECG morphology, arrhythmias, heart rate variability). Secondary variables: skin temperatures (14 points), skin blood flow, perspiration efficiency (hot), oxygen consumption (cold), and hematological variables [inflammatory factors (CRP, TNFalpha, IL-6, ET-1), coagulation factors (FVII, vWF, fibrinogen, D-dimer), lipids (cholesterol) and glycemic status (HbA1c)].

3.2. Measurements

ECG was recorded by 12-lead electrode placement continuously throughout the study in the thermal laboratory and 3-lead electrode placement was recorded during each exposure at baseline, intervention, and follow-up for five minutes at a time. In this thesis, the 3-lead recording was used for the analysis of HRV. The electrodes were placed according to the standard 3-lead placement. Blood pressure measurement was performed with a Nexfin® monitor (Edwards LifeSciences Corporation, Irvine, CA, USA) by placing the right size finger cuff on the right middle finger. Blood pressure measurements were performed on each exposure at baseline, intervention, and during follow-up for five minutes at a time. Measurement of skin blood flow was performed with OxyFlo ™ Pro device (Oxford Optronics, UK) with two sensors placed in the left hand of the subject. One sensor was placed on the top of the brachioradialis and the other on the fingertip of the middle finger, on the palm side. Blood flow measurements were performed on each exposure at baseline, intervention, and during follow-up for five minutes at a time. The sensors were placed in the same place during each measurement. The location of the brachioradialis sensor was marked with a pen on the skin, and for the second exposure, the location of the sensor was drawn on a membrane so that the sensor could be placed as close to the same location as possible.

3.3. Analysis

All collected data were initially reviewed with LabChart software (LabChart v8, ADInstruments). The signals from every measurement were then separated into three stages of measurement (baseline, intervention, and recovery) and exported to Matlab (R2021b MathWorks) for further processing of ECG, BP, and LDF.

3.3.1. Pre-Processing of ECG signal

The raw ECG signals were prepared through different pre-processing steps for QRS complex detection and therefore HRV detection. In this thesis, an application of the Pan-Tompkins algorithm was used, where an alternative QRS complex peak detection is used [45], this algorithm was, however, slightly modified throughout the algorithm. The algorithm for QRS detection was proposed by Pan and Tompkins in 1985 for the detection of real-time QRS complexes, it is based on the analysis of the slope, amplitude, and width of the QRS complexes. The algorithm includes a series of steps; filters and methods to perform lowpass, high pass, derivative, squaring, integration, adaptive thresholding, and search procedures. [16 p. 187 – 190]

In this application, the signal is down sampled to 200 Hz, using the Matlab function *resample*. The first step of the algorithm is to remove DC drift from the signal by removing the mean and then normalizing the signal to one by dividing each value of the signal by the maximum. Figures 6 and 7 show the input signal and the signal after the first step, respectively.

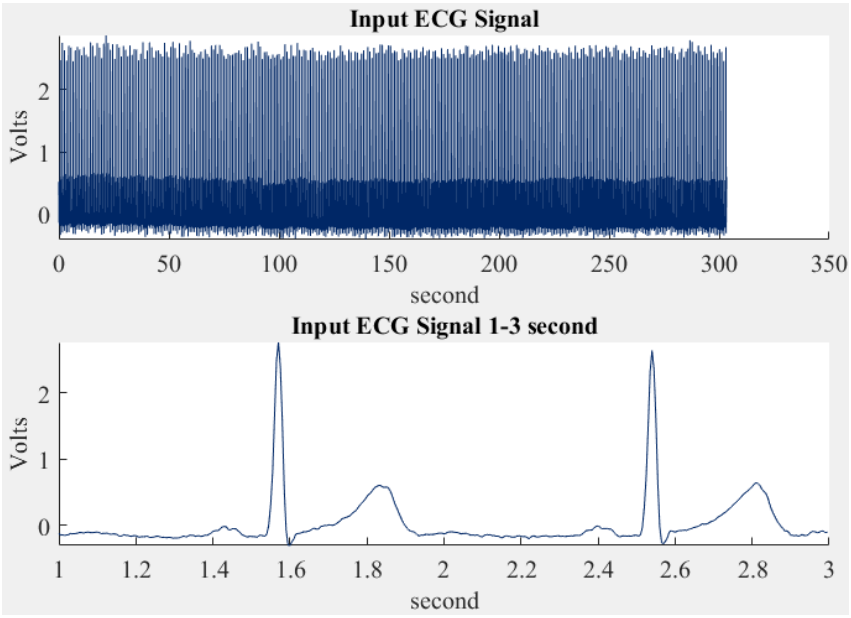

Figure 6. The input signal and close-up.

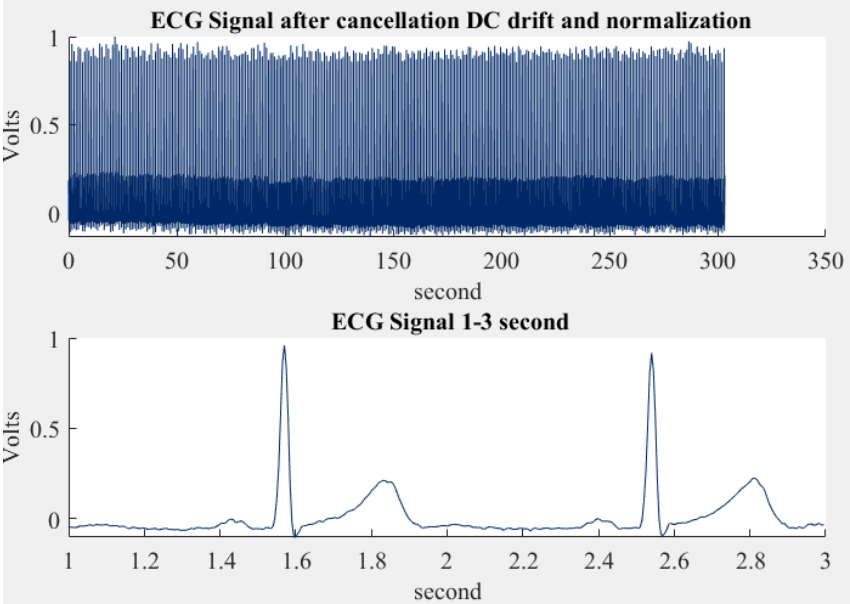

Figure 7. The signal after DC drift cancellation and normalization and close up.

Then bandpass filtering was made, by using low-pass and high-pass filters in cascade, this was done to reduce noise (such as muscle noise and powerline interference) from the signal. The second-order low-pass filter has the transfer function of equation (1).

$$H(z) = \frac{1}{32}\frac{(1-z^{-6})^2}{(1-z^{-1})^2}. \quad (1)$$

The cut-off frequency of the filter is about 11 Hz, and the delay is 5 samples or 25 ms [16 p. 187 – 190]. The difference equation of the filter is as in equation (2).

$$\mathrm{y(n)} = 2n(n-1) - y(n-2) + \frac{1}{32}[x(n) - 2x(n-6) + x(n-12)]. \quad (2)$$

The high-pass filter is implemented as an all-pass filter minus the low-pass filter [16 p. 187 – 190]. The transfer function of the low-pass component is shown in equation (3).

$$Hlp(z) = \frac{(1-z^{-32})}{(1-z^{-1})}. \quad (3)$$

The high-pass filter has the transfer function as shown in equation (4).

$$Hhp(z) = z^{-16} - \frac{1}{32}Hlp(z). \quad (4)$$

The difference equation of the high-pass filter is as in equation (5).

$$p(n) = x(n-16) - \frac{1}{32}[y(n-1) + x(n) - x(n-32)]. \quad (5)$$

The low cut-off frequency of the filter is about 5 Hz, and the delay is 16 samples or 80 ms [16 p. 187 – 190]. Figures 8 and 9 show the signal after the low-pass filter and high-pass filter, respectively.

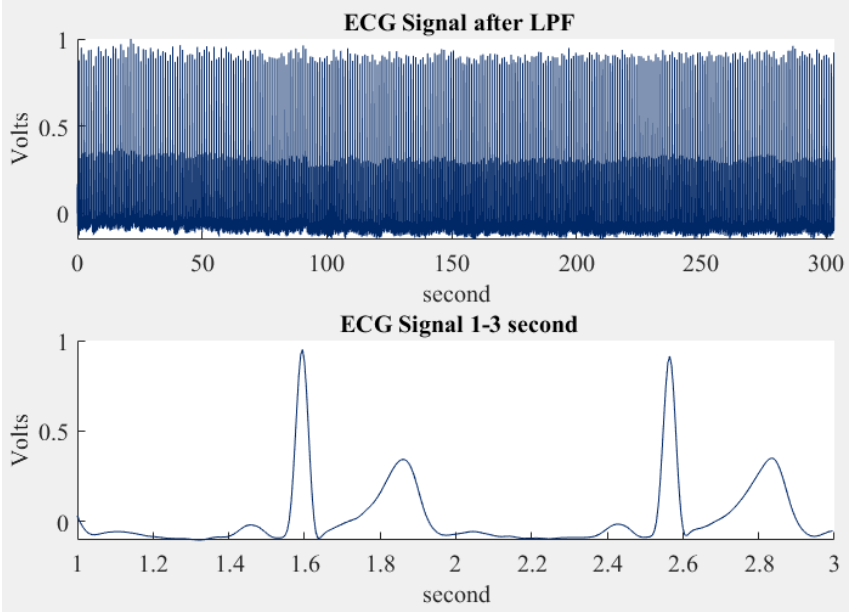

Figure 8. Signal after the low-pass filter and close up.

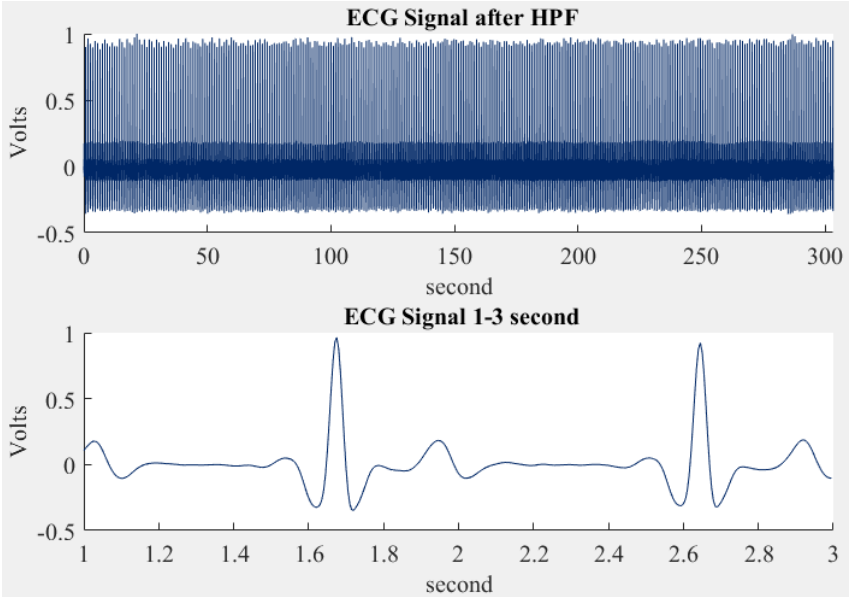

Figure 9. Signal after the high-pass filter and close up.

Then the signal is passed through a derivative operator which provides a large gain to the high-frequency components that distinguish the QRS complexes, and it also suppresses the low-frequency ECG components such as the P and T waves. [16 p. 187 – 190] A five-point derivative is implemented using the transfer function as in equation (6).

$$H(z) = \frac{1}{8}(2 + z^{-1} - z^{-3} - 2z^{-4}). \quad (6)$$

The difference equation is as in equation (7).

$$y(n) = \frac{1}{8}[2x(n) + x(n-1) - x(n-3) - 2x(n-4)]. \quad (7)$$

This derivative approximates the ideal derivative over the range of the dc and 30 Hz, and the delay is 2 samples or 10 ms [16 p. 187 – 190]. Figure 10 shows the signal after the derivative filter.

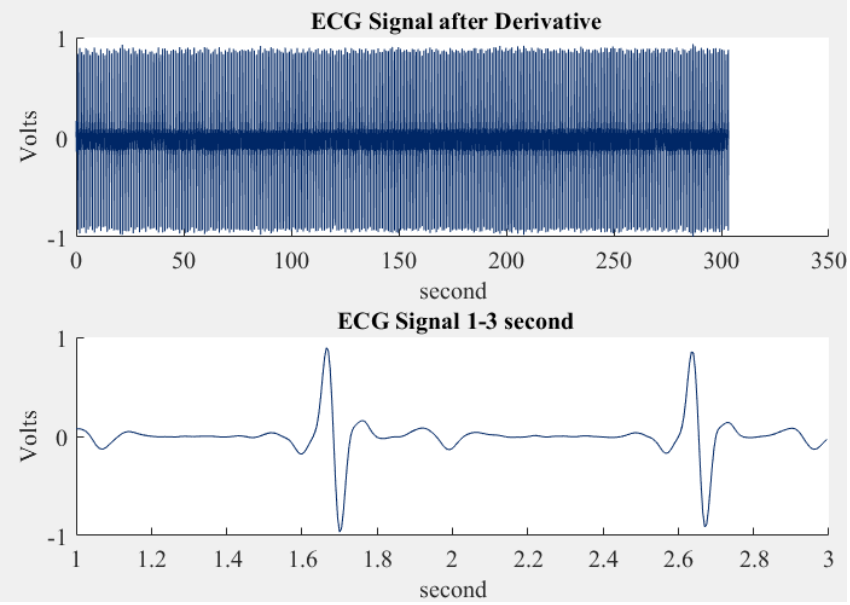

Figure 10. Signal after the derivative filter and close up.

The next operation is the squaring operation, this is done to make the resulting signal positive and to emphasize the large differences within the QRS complexes; the small differences are suppressed, and the high-frequency components are further enhanced [16 p. 187 – 190]. The signal is squared from point to point, and the equation for this operation is as in equation (8).

$$y(n) = [x(n)]^2. \quad (8)$$

The squared signal is then passed through a moving-window integrator of window-length of N = 30 samples (for 200 Hz sampling frequency), the result is a single smooth peak related to the QRS complex on each ECG cycle [16 p. 187 – 190]. The difference equation of the moving window integrator is as shown in equation (9).

$$y(n) = \frac{1}{N}[x(n-(N-1)) + x(n-(N-2)) + \cdots + x(n)]. \quad (9)$$

Figures 11 and 12 show the signal after the squaring operation and window integration, respectively.

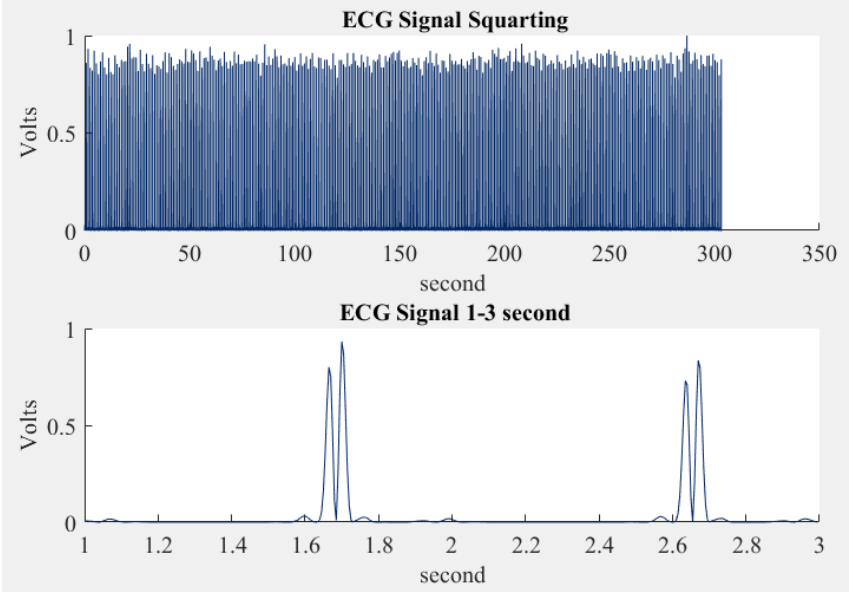

Figure 11. Signal after squaring operation and close up.

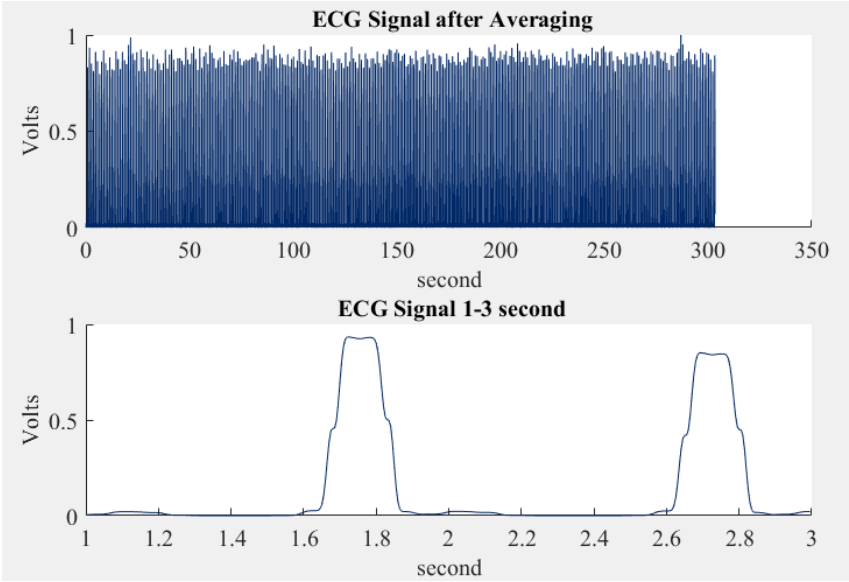

Figure 12. Signal after window integration and close up.

From this result are found the QRS points, this is done differently than in the original Pan-Tompkins algorithm. QRS points are detected by setting two thresholds: the first threshold is set as the peak or maximum amplitude of the signal. The second threshold is set as the mean of the signal, which is considered to represent the noise of the signal. Next, an array of segments is formed, taking into account those signal indices whose signal values are greater than the thresholds multiplied together. The left and right segments are then formed by finding the indices of the boundaries of each segment from the arrays formed. Finally, the minimum and maximum values of these left and right segments are searched for using a simple decision logic that runs through all possibilities. Figures 13 and 14 show the integrated signal and the found QRS points from the signal, respectively.

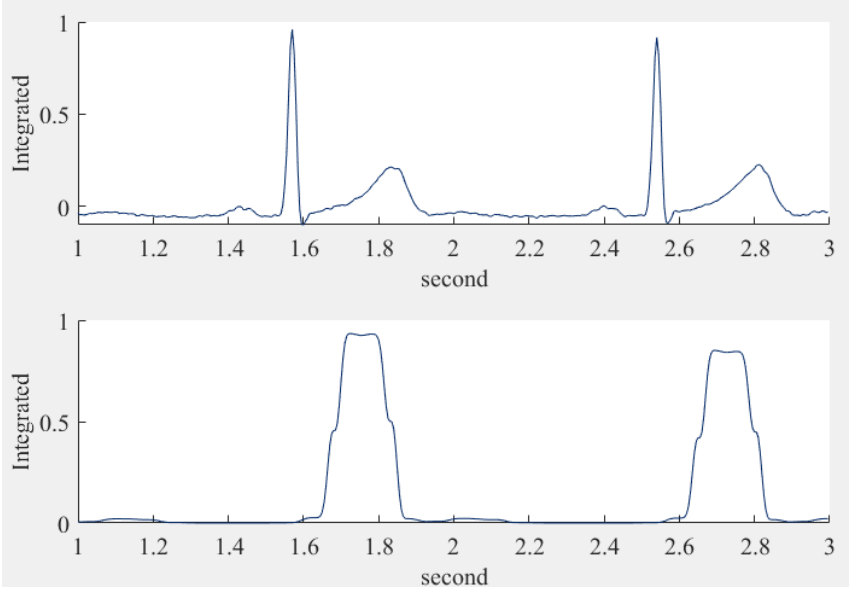

Figure 13. Close up of the integrated signal.

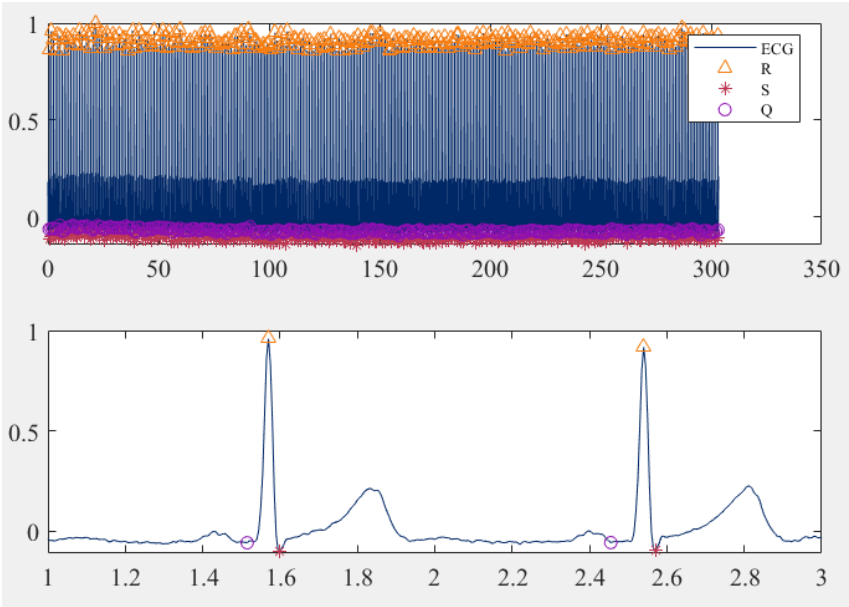

Figure 14. Found QRS points in the signal and close up.

From the R-points found, HRV was extracted by dividing the locations of the R-points by the sampling frequency (200 Hz) and then computing the differences between adjacent elements; the result is also multiplied by 1000 to obtain milliseconds. Before analyzing the HRV signal, pre-processing was made by detecting outliers, i.e., abnormalities in R-peaks. This was done by using the Matlab function *filloutliers*. This function detects and replaces outliers in the given data. The default outlier detection was used, where outliers are defined as elements more than three scaled median absolute deviations (MAD) away from the median. The method for replacing the outliers was chosen to be 'linear', where the detected outlier will be filled by using linear interpolation of neighboring, non-outlier values. Figure 15 shows an example of an extracted HRV, pre-processed, and both signals superimposed from a subject with detectable abnormalities.

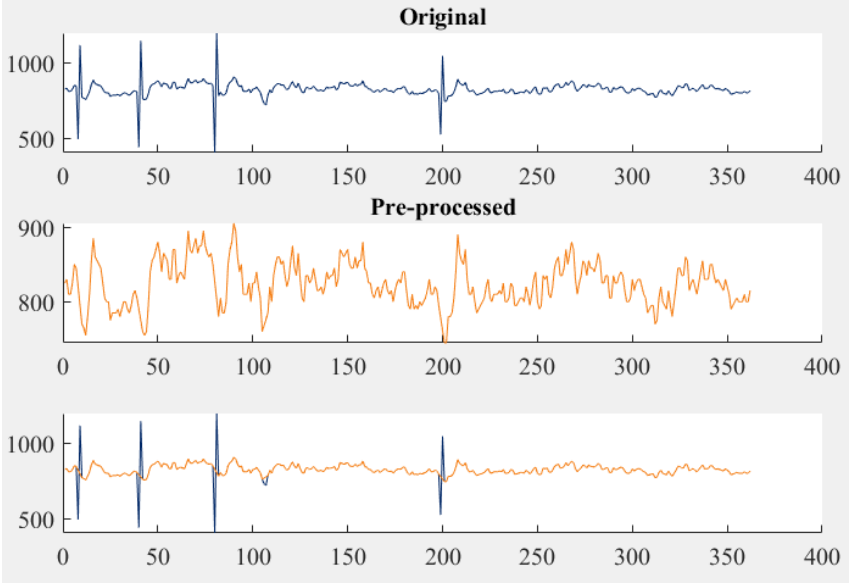

Figure 15. Extracted HRV, pre-processed, and both signals superimposed.

3.3.2. Pre-processing of BP signal

The raw BP signals were also prepared through different pre-processing stages for detection of the different stages in the BP signal and therefore the systolic blood pressure variation detection. In this thesis, the methods described in other studies have been followed to find the different phases in the BP signal [46]. The technique is largely based on derivatives and thresholds defined in [47] and [48]. From the raw BP signal was first found the different phases, and from those have been calculated maximum, minimum, and mean values of SBP and DBP in mmHg. Mean arterial pressure (MAP) is also calculated from the mean values, which by definition is the average arterial pressure during one cardiac cycle, systole and diastole. This value is influenced by cardiac output and systemic vascular resistance [49].

The signal was then normalized before further analysis. The Z-score technique, as shown in equation (10), is used in this thesis to get amplitude-limited data.

$$z = \frac{x-\mu}{\sigma}, \tag{10}$$

where x is the signal, μ is the mean of the signal, and σ is the standard deviation of the signal. Figure 16 shows the raw BP signal and after the normalization.

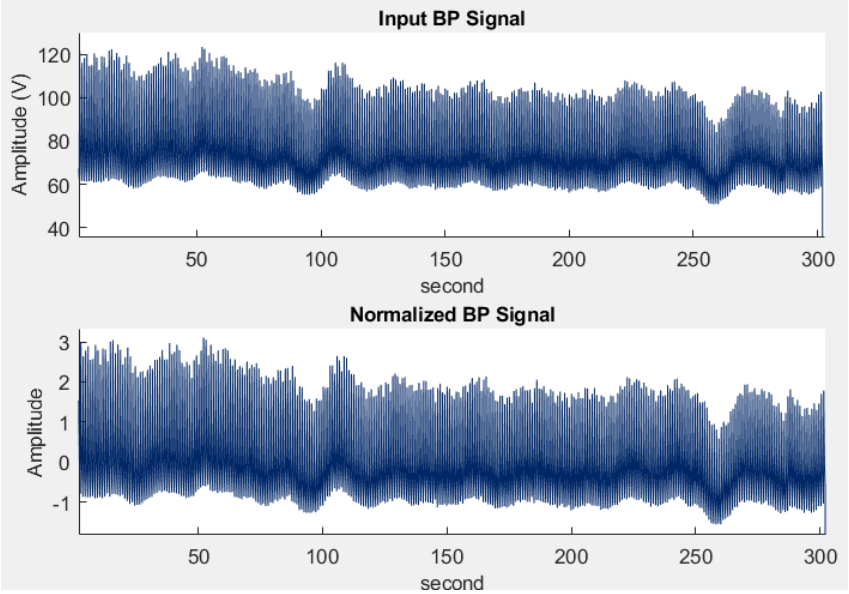

Figure 16. The raw BP signal and the normalized BP signal.

After the normalization, the different phases of the BP signal were again annotated using the algorithm. The first step of the algorithm is to resample the signal to 200 Hz. Then the signal is filtered with a low-pass filter to remove high-frequency components. The transfer function of the low-pass filter is shown in equation (11).

$$H(z) = \frac{(1-z^{-6})^2}{(1-z^{-1})^2}. \tag{11}$$

The difference equation of the filter is as in equation (12).

$$\mathrm{y(n)} = 2n(n-1) - y(n-2) + [x(n) - 2x(n-6) + x(n-12)]. \tag{12}$$

The denominator coefficient is also multiplied by 36 to remove DC gain. The next step is to find the different phases of the BP signal, i.e., the important features, the diastolic pressure, the dicrotic peak indices, and the systolic pressure. In this work, the different parts of the algorithm to find these important features are only briefly described, as presented by the authors in [46]. The foot index, the diastolic pressure, is defined as the point where the second derivative of the time series is the highest in each interval where a moving average of the second derivative was bigger than an adaptative threshold. This criterion was preferred over others because of its robustness. The dicrotic notch and peak indices are prominent and distinctive features in the BP signal. In the algorithm, the dicrotic notch is defined as the minimum of the subtraction of the signal and the straight line going from systole to diastole. Dicrotic peak indices were defined as the minimum of the second derivative of the time series following the dicrotic notch, relative to a window of radius RR/5 s around itself (RR is the median heartbeat interval computed from the foot indices). These indices are moved to waveform minima and maxima if these exist. The systolic peak is defined as the maximum of the waveform following the foot index, relative to a window of radius 1/8 s around itself. Figure 17 shows the close-up of the algorithm result for different BP phases marked.

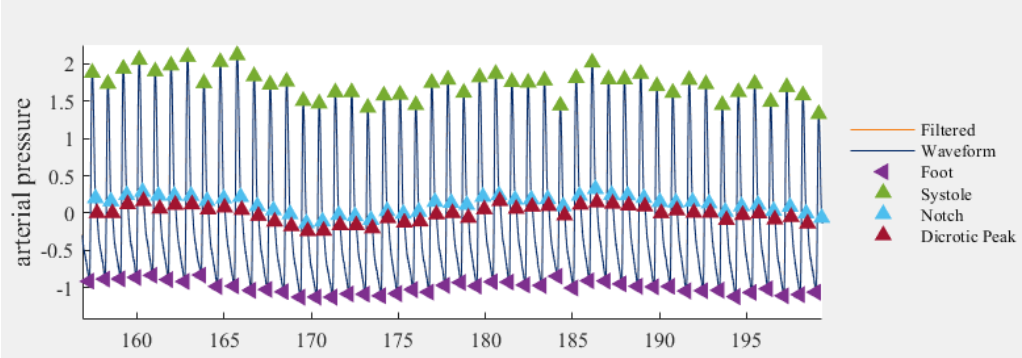

Figure 17. Close up of the algorithm result with different BP phases marked.

From the SBP points found, the SBP variation data was extracted in the same method that HRV was extracted. Before analyzing the retrieved signal, pre-processing was made the same as with HRV, to detect any possible outliers, i.e., abnormalities in SBP-peaks. Possible outliers were replaced with linear interpolation of neighboring, non-outlier values.

3.3.3. Pre-processing of LDF signal

The initial review of the LDF signals showed that the measurement from the finger probe was clear, oscillatory, and uniform across all measurements, therefore it was chosen to be the primary signal used in the analysis. The forearm measurement turned out to be mostly quite sporadic, and thus this was omitted from any further analysis.

The imported LDF signals showed high-frequency artifacts; the acquisition noise, and other high-frequency disturbances, therefore high-frequency filtering was done using the IIR Butterworth filter. Butterworth filter was implemented with Matlab *butter* function, and the cut-off frequency was set at 2,5 Hz. The imported signals also showed baseline wandering, therefore detrending was performed by subtracting third-order polynomial fit from the signal. After detrending the signal was set above zero by subtracting the minimum value from it. These filtering techniques were found to be used for the LDF signals in the literature to prepare them for analysis and these were also found to be working nicely in this work and pre-processing the data appropriately. Figure 18 shows the result of the filtering and detrending of the raw signal.

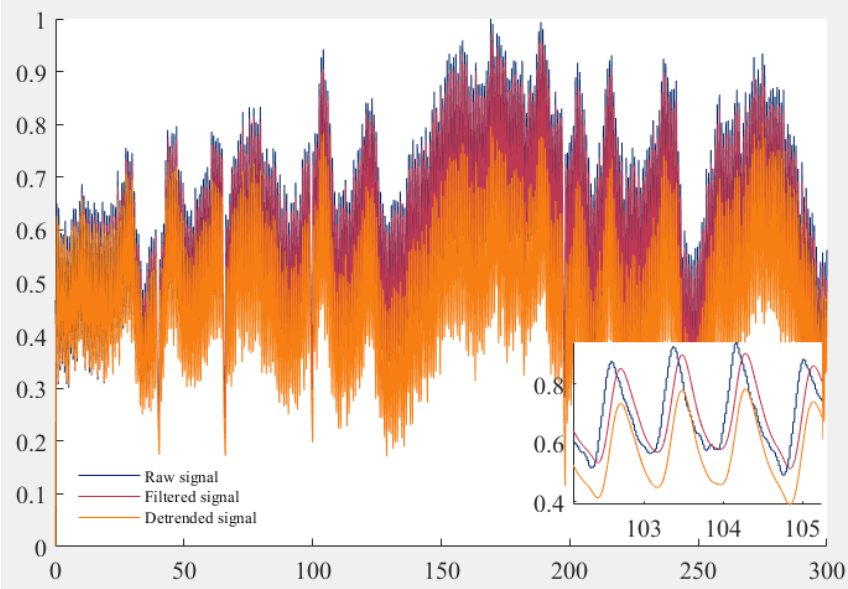

Figure 18. Raw LDF signal, filtered and detrended signal, and close-up from the high-frequency filtering results.

The LDF measurements are sensitive to involuntary movements, and they can result in spike-shaped artifacts in the signal. Results can be compromised by these disturbances; therefore, these were attenuated. This was done by using the Matlab function *filloutliers*. This function detects and replaces outliers in the given data. The method for detecting outliers was chosen to be '*mean*', where outliers are defined as elements more than set threshold standard deviations from the mean. And the method for replacing the outliers was chosen to be 'nearest', where the detected outlier will be filled with the nearest non-outlier. The threshold was set to 2,25, this was chosen through experimenting with different thresholds and this value was determined to give the best outcome within this data. Results from outlier detection and filling in Figure 19. For the frequency-domain analysis, the LDF signals were down sampled to 10 Hz, using the Matlab function *resample*.

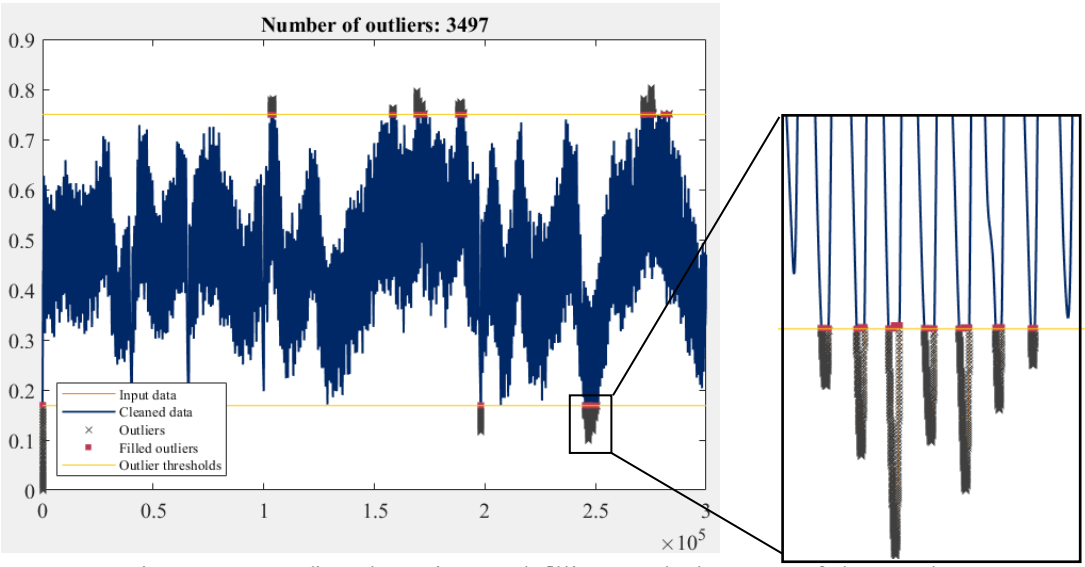

Figure 19. Outlier detection and filling and close-up of the results.

3.3.4. Time-domain analysis

For the time-domain analysis, different parameters were extracted from the pre-processed signals, but the main focus of this thesis is on the frequency-domain analysis, therefore time-domain is presented here very shortly.

From extracted HRV, the heart rate during the measurement was calculated as shown in equation (13), and the mean heart rate was calculated as shown in equation (14).

$$HR = \frac{60}{RR_i} \tag{13}$$

$$\overline{HR} = \frac{1}{N}\sum_{i=1}^{N} HR_i \tag{14}$$

Where N is the total number of heartbeats. The mean RR calculates the mean of the RR intervals from the RR interval sequence as shown in equation (15).

$$\overline{RR} = \frac{1}{N}\sum_{i=1}^{N} RR_i \tag{15}$$

Where the N is the total number of all RR intervals.

The HRV time-domain parameters have been presented in section 2.4.2, and the equations for these parameters are presented here. SDNN, shown in equation (16), is the standard deviation of NN intervals.

$$SDNN = \sqrt{\frac{1}{N-1}\sum_{i=1}^{N}(RR_i - \overline{RR})^2} \tag{16}$$

The RMSSD, shown in equation (17), is the root mean square of successive NN interval differences.

$$RMSSD = \sqrt{\frac{1}{N}\sum_{i=1}^{N-1}(RR_{i+1} - RR_i)^2} \tag{17}$$

The NN50 count, shown in equation (18), is the number of interval differences of successive NN intervals that are greater than 50 milliseconds. And the pNN50, shown in equation (19), is the percentage of these successive NN intervals during the measurement period.

$$NN50 = \sum_{i=1}^{N}\{|RR_{i+1} - RR_i| > 50ms\} \tag{18}$$

$$pNN50 = \frac{NN50}{N} * 100 \tag{19}$$

For the BP signals, the maximum SBP and DBP and the minimum SBP and DBP were extracted, and mean SBP and DBP were calculated as shown in equation (20) and equation (21), and from those were calculated the MAP, as shown in equation (22). From the extracted variation of the systolic BP was calculated the mean SBP variation,

equation (23), and the maximum SBP variation and minimum SBP variation values were extracted.

$$\overline{SBP} = \frac{1}{N}\sum_{i=1}^{N} SBP_i \quad (20)$$

$$\overline{DBP} = \frac{1}{N}\sum_{i=1}^{N} DBP_i \quad (21)$$

$$MAP = \overline{DBP} + \frac{1}{3}(\overline{SBP} - \overline{DBP}) \quad (22)$$

$$\overline{SBPv} = \frac{1}{N}\sum_{i=1}^{N} SBPv_i \quad (23)$$

In the time-domain, LDF signals give very limited information as they provide a relative index of vascular bed perfusion, and they provide therefore information regarding the volume of the blood flow flowing through the measurement area. In the time-domain analysis, data is measured in absolute Blood Perfusion Units (arbitrary), and the values derived from the time-domain in this study are the absolute mean blood perfusion, shown in equation (24), and the absolute maximal blood perfusion. Alone, these measurements cannot provide information as to the mechanisms resulting in such changes. To determine if changes in flow are due to changes in vasomotor tone, blood flow must be normalized to arterial blood pressure and expressed as vascular conductance (term cutaneous vascular conductance (CVC) is used in relation to laser Doppler flowmeter), shown in equation (25). Absolute values of CVC can further be normalized to maximal response CVC gained from the reactivity test and be expressed as a percentage change ($\%CVC_{max}$), shown in equation (26). As no maximal response blood flow testing was performed in this study, the maximum blood flow value was taken from the warm measurement intervention and the cold measurement baseline, both of which were taken the maximum value after pre-processing.

$$\overline{BPU} = \frac{1}{N}\sum_{i=1}^{N} BPU_i \quad (24)$$

$$CVC_{abs} = \frac{\overline{BPU}}{MAP} \quad (25)$$

$$\%CVC_{max} = \frac{CVC_{abs}}{CVC_{max}} * 100 \quad (26)$$

Body fat percentage was determined from four-site skinfold measurements (subscapular, suprailiac, triceps, and biceps) measured with skinfold calipers. Each site was measured three times and the measures were averaged and then summarized. The sum of skinfolds was fitted to the conversion table based on the prediction equation of Durnin & Womersley [50] to get an estimation of the body fat percentage. BMI was calculated as shown in equation (27).

$$BMI = \frac{Weigth\ (kg)}{Height^2(m)} \quad (27)$$

3.3.5. Frequency-domain analysis

The frequency-domain analysis of the dynamic properties of a physiological signal can be assessed by calculating its Fourier transform (FT). In this transformation, the original signal is windowed either to reduce leakage or to achieve time localization (in this case, a short-time Fourier transform is obtained). The choice of window length plays an essential role throughout the analysis. If a shorter window is selected, the very low frequencies become hard to recognize from the amplitude spectra. Taking a longer segment leads to improvement of low-frequency resolution, but on the other hand, it smears the higher frequency components. This choice of window length and shape, which then determines the frequency resolution, becomes difficult. The wavelet analysis is, however, a way of avoiding the choice of window length altogether. [24 p.79-88, 51]

The generalized wavelet analysis is a scale-independent method. The wavelet transform (WT) enables signal oscillations time and frequency content analysis and has the advantage over the FT in providing information on changes in the frequency and power of individual oscillating components over time. Wavelet transform analysis breaks down the steady fluctuating time series into its frequency elements. It is based on an oscillating function of limited duration called a mother wavelet. The Morlet mother wavelet is one of the popular mother wavelets and it has been used in many biomedical signal analyses, such as LDF, electroencephalogram (EEG), and ECG because it has the best time-frequency localization properties of generalized wavelets. It is a Gaussian function modulated with a sine wave with basic frequency ω_0. The choice of ω_0 is a compromise between localization in time and frequency. Wavelet transform can also be averaged over a period of time at a certain frequency to obtain an average scalogram, which is the squared magnitude of the wavelet transform. The continuous wavelet transform of a signal $x(u)$ is defined as in equation (28).

$$w(s,t) = \int_{-\infty}^{\infty} \psi_{s,t}(u)x(u)du \tag{28}$$

where $\psi_{s,t}$ is a wavelet function, as defined in equation (29).

$$\psi_{s,t}(u) = \frac{1}{\sqrt{s}}\psi\left(\frac{u-t}{s}\right) \tag{29}$$

where ψ is the mother wavelet function, t is time, and s is the scale related to the central frequency of $\psi_{s,t}$. The Morlet mother wavelet, which was used in this thesis, is defined in simplified expression as in equation (30).

$$\psi_0(u) = \pi^{-1/4} e^{j\omega_0 u} e^{-u^2/2} \tag{30}$$

where ω_0 is the basic frequency. A larger value of ω_0 will give better frequency localization. [32, 34, 51]

It should be noted that the data obtained from the FT and WT analysis of the signals cannot be directly compared because they are computed differently. Fourier transform-based power spectrum analysis is frequency localized because it is based on sine waves and can give very accurate estimates of the frequencies present in the signal, but not when they are present in time. In contrast, WT can distinguish the frequency content of a signal and where it changes in time. The signal parameters (length and sampling

rate) and the FT parameters (window size and type, and the number of bins) also affect the power spectral density, so they should always be reported alongside the analysis. In this work, WT-based frequency analysis was chosen as the method of analysis because previous work on the analysis of LDF signals has been done with WT and it was desired to continue the analysis of other signals with the same method for better comparability. [29]

Mechanistic information on the processes regulating microvascular perfusion can be obtained by spectral analysis of blood flow measurements obtained with LDF with low-frequency periodic oscillations (0.0095-2 Hz). Spectral studies of the LDF signal have identified five frequency bands in the cutaneous flowmotion spectrum. Each interval is associated with the activity of a specific cardiovascular system structure. The five frequency bands are: 1) The slow oscillations at 0.0095 – 0.021 Hz which reflect vascular tone regulation of endothelial activity. 2) the frequency range of 0.021 – 0.052 Hz which is from the neurogenic sympathetic vasomotor activity, or the metabolic activity, which causes the blood vessel movement. 3) the frequency range of 0.052 – 0.145 Hz which is from the vascular tone regulation of myogenic mechanism which reflects the vascular smooth muscle response to the transmural pressure. This activity is weakly present in the microvascular blood flow signal. 4) the frequency range of 0.145 – 0.6 Hz which reflects the peripheral vascular tone regulation of respiratory activity (thorax movement). 5) the frequency range of 0.6 – 2 Hz which carries the information about the influence of heart pump activity. [51]

In this thesis, these same low-frequency bands have been applied to HRV and BP variation signals, even though they are not usually identified in these signals. If the same frequency bands are compared with the three most common frequency bands of HRV (and BP), the same regulatory mechanisms can be identified. The VLF band (0.003– 0.04 Hz) practically combines the two lowest bands in the LDF band division. VLF band seems to be affected by the heart's intrinsic nervous system and SNS is said to be influencing the amplitude and frequency of its oscillations. The power of VLF may be also generated by physical activity, thermoregulatory, renin-angiotensin, and endothelial influences on the heart. However, there is still uncertainty regarding the mechanisms responsible for the activity in this band in HRV. The LF band (0.04–0.15 Hz) has been mainly said to reflect the baroreceptor activity during rest. Within this frequency band lies the so-called Mayer waves, oscillating at a frequency of 0.1 Hz, and their hemodynamic basis has been linked to sympathetic vasomotor tone. Also, some research data have been in support of the major role of the baroreceptor reflex in the generation of Mayer waves, but some studies have also found that the oscillation at this frequency is still present after the denervation of the baroreceptor. The HF band (0.15–0.4 Hz) is strongly present both in HRV and BP variation signals, and it is generally accepted as a respiratory band [13, 52].

For reliable statistical analysis, the recording should ideally include 10 cycles for each frequency band [26], in this study, however, the individual recording time of each phase was about 5 minutes, which resolves frequencies down to 0.033 Hz therefore in this study, the myogenic band in 0.052 – 0.145 Hz is the lowest frequency interval for reliable statistics. The human heartbeat frequency is on average 1 Hz, ranging from 0.6 Hz in athletes to 1.6 Hz in patients with an impaired cardiovascular system [51], this frequency band is not seen in either HRV or BP variation frequency analysis.

The wavelet transform was done using Matlab software and the wavelet toolbox. The Matlab function for continuous wavelet transform, *cwt*, was used. This function compares the signal to shifted and compressed or stretched versions of a chosen

wavelet and returns the continuous wavelet transform and frequencies of the transform. The used wavelet was the same as in literature, Morlet-wavelet. For the Matlab *cwt* -function the Analytic Morlet (Gabor) Wavelet is supported by the name *'amor'*, which was used in this thesis. In the Matlab function, all parameters are determined inside of the *cwt* -function based on the chosen wavelet. The wavelet transform was done for the frequency range of interest (0.0095 – 2 Hz). The same mother wavelet and frequency range was used in all of the signals. A scalogram of the frequency range and global average wavelet power was plotted (Figure 20) where different bands and their influence on whole power can be seen. This was done with the Matlab function *timeSpectrum*, which gives the time-averaged wavelet spectrum. The global average power (average scalogram) was also retrieved in separate and the different frequency bands were marked with different colors, for clearer separation of the bands (Figure 21). Wavelet transform is calculated with a logarithmic resolution, and therefore the frequency axes are presented logarithmically.

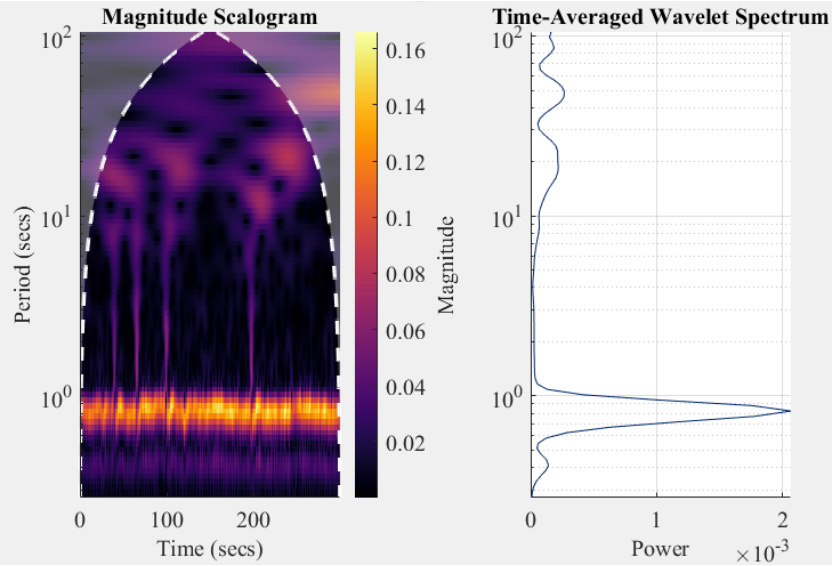

Figure 20. A scalogram of the frequency range and global average wavelet power from an LDF signal

From the frequency bands, peak amplitudes for each frequency band were determined by the detection of local maxima in the average wavelet transform. From every band, the frequency at peak amplitude was also extracted. The mean amplitude of each frequency band was calculated, by taking the mean from the retrieved frequency band amplitudes. The wavelet amplitudes of the signals at each frequency band were normalized to overcome individual variations, this was defined as the ratio of the absolute mean amplitude of the frequency band to that of the same frequency band mean amplitude in the baseline. The absolute mean power within each frequency band and for the total frequency range was calculated using Matlab function *bandpower*, which allows estimating the signal power. The relative power (RP) for each frequency band was defined as the ratio between the mean power within each band and the mean power of the entire spectrum [42], and the relative mean power in percent was calculated as shown in equation (31). Also, the mean power ratios between different frequency bands were calculated.

$$\%RP = \frac{P_i(f_{i1}, f_{i2})}{\overline{P_{total}}} * 100 \quad (31)$$

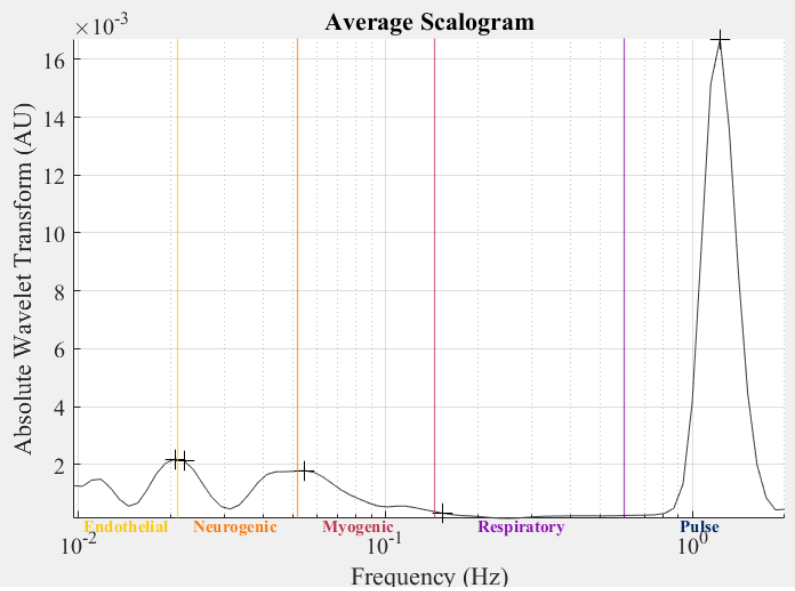

Figure 21. A global average power of an LDF signal, the peak amplitudes marked.

3.3.6. Statistical analysis

The statistical analysis of the data was done with IBM SPSS Statistic (version 28, Chicago, IL) The normality of the data was assessed with the Shapiro-Wilk test before analysis. The student t-test was used to compare means between those with T2DM and controls. Where skewed distribution existed, the Mann-Whitney U test was used. The $p < 0.05$ was considered statistically significant.

4. RESULTS

HRV and BP measurements in the cold exposure were done on all subjects during baseline and recovery, except for one subject in the recovery phase. This was because the subject's blood pressure was very low during the intervention and in the recovery. The intervention measurement was done on 14 subjects. The intervention measurement in the cold exposure was not done on 6 subjects due to earlier termination of the exposure, because the subjects were feeling too cold, and because the recording was very challenging due to shivering. Also, two subjects' baseline measurements were 3 minutes long, one because of low blood pressure and one because of disturbance in signals. For two subjects' the intervention measurements with both HRV and BP were 3 minutes long, one because the blood pressure climbed very high and one because of strong shivering, the shivering was also the reason for one other subject's shorter BP measurement in the cold. For three subjects' the recovery measurement was 3 minutes long, due to technical issues and two because of disturbances in signals. All measured signals were still included in the analysis, regardless of the length, and therefore the total measurement phases in the cold that were analyzed was 53. HRV and BP measurements during the warm exposure were done on all subjects during baseline, intervention, and recovery, except for one subject in the intervention and the recovery phase, because of low blood pressure of the subject. Also, two subjects' baseline measurements were 3 minutes long, and three subjects' recovery measurements were 3 minutes long, due to technical issues. All measured signals were also here included in the analysis, regardless of the length, and therefore the total measurement phases in the warm that was analyzed were 58.

The LDF measurements in the cold exposure were conducted on all subjects during baseline and recovery. The intervention measurement was done on 15 subjects, although with one subject the intervention measurement was about one minute shorter. The intervention measurement in the cold exposure was not done on 5 subjects because of earlier termination of the exposure. The total measurement phases that were included in the analysis were 55. LDF measurements in the warm exposure were done on all subjects in baseline, intervention, and recovery, except for one subject in the recovery phase. This was because of low blood pressure. Also, with one subject the duration of the baseline measurement was below two minutes, and therefore the lowest frequency band (endothelial) was not included. The total measurement phases that were included in the analysis were 59.

4.1. Time-domain results

4.1.1. Cold exposure

The HRV time-domain parameters presented as mean ± SD from the cold exposure are in Table 1. Controls had on average lower body fat percent (25.07) and BMI (25.4) compared with diabetics (31.8 and 30.1, respectively). Mean heart rate was higher in the diabetic group compared with controls. At cold baseline mean heart rate was significantly higher in the diabetics compared with the controls ($p < 0.001$). Both groups had a similar decrease in heart rate. At baseline diabetic group had significantly shorter mean RR intervals compared with the controls ($p < 0.001$). The RR intervals

increased in both groups similarly and further slightly increased in the recovery. The RR intervals were significantly shorter with diabetics also in the intervention ($p = 0.025$) and recovery ($p = 0.003$) compared to controls. The SDNN and RMSSD were at baseline significantly lower in diabetic individuals (SDNN ($p = 0.007$), RMSSD ($p = 0.042$). For both groups, the SDNN and RMSSD increased in the cold exposure, and further slightly increased in the recovery. The NN50 and pNN50 values were larger in controls at baseline, for both groups the parameters increased, controls increase was a bit larger.

Table 1. Time-domain data of the experimental study in response to cold (+10 ˚C) exposure among persons with T2DM (n = 10) and controls (n = 10). The values are represented as mean±SD.

Experimental Group. Diabetics (*n*=10) and Controls (*n*=10)								
	Body fat %	BMI	HR	RR	SDNN	RMSSD	NN50	pNN50
Diab base	31.76 ±6.8	30.1 ±4.9	81.6 ±11.7	752.7 ±114.3	18.6 ±10.1	11.67 ±5.2	0.6 ±1.1	0.17 ±0.3
Diab int	31.76 ±6.8	30.1 ±4.9	72 ±12.1	855.8 ±151.9	31.6 ±12.4	20.72 ±11.0	13.6 ±20.3	4.34 ±7.1
Diab reco	31.76 ±6.8	30.1 ±4.9	71.5 ±11.6	866 ±146.3	32.5 ±12.6	21.77 ±11.6	10.3 ±17.4	3.44 ±6.5
Contr base	25.07 ±3.5	25.4 ±2.2	64.4 ±6.2	947.1 ±89.8	31.7 ±9.0	18.69 ±8.5	6.2 ±10.6	2.14 ±3.7
Contr int	25.07 ±3.5	25.4 ±2.2	56.1 ±4.6	1082 ±85.8	46.1 ±23.6	31.13 ±19.6	26.8 ±39.6	11.59 ±15.1
Contr reco	25.07 ±3.5	25.4 ±2.2	56.5 ±7.7	1097 ±141.5	51 ±24.0	33.65 ±21.3	23.4 ±27.8	11.37 ±15.0

The BP time-domain parameters presented as mean ± SD from the cold exposure are in Table 2. In the cold exposure, baseline mean SYS, DIA, and MAP were higher in the diabetics compared with the controls. The mean SYS increase during the intervention was greater in diabetics and also the decrease in recovery was greater in diabetics. The mean DIA also increased in the cold intervention for both groups similarly, but in the recovery, diabetics had a slight decrease in the mean DIA whereas the controls had a slight increase in mean DIA. This, however, is not on average the common behavior with the controls, but there are few measurements where the difference is quite large and therefore impacted the mean value. MAP increased in the cold for both groups and in the recovery MAP decreased, with diabetics the changes are a bit larger. The mean SBP variation is similar to the mean RR interval, also with significant differences between the two groups, it is also behaving similar way, increasing during the cold intervention, and further slightly increasing in the recovery.

Table 2. Time-domain data of the experimental study in response to cold (+10 ˚C) exposure among persons with T2DM (n = 10) and controls (n = 10). The values are represented as mean±SD.

Experimental Group. Diabetics (*n*=10) and Controls (*n*=10)				
	Mean SYS	**Mean DIA**	**MAP**	**Mean SBPv**
Diab base	122.89±24.9	72.56 ±11.0	89.34 ±14.7	751.83±114.4
Diab int	143.53±26.8	83.67 ±8.8	103.62±13.1	855.88±152.3
Diab reco	135.05±18.4	80.44 ±6.5	98.64 ±7.4	867.1 ±146.5
Contr base	123.55±10.0	70.68 ±7.5	88.3 ±7.6	949.14±9.1
Contr int	137.08±38.3	78.91 ±20.3	98.3 ±26.1	1078.02 ±82.6
Contr reco	132.4 ±20.1	80.36 ±7.2	97.71 ±9.6	1105.72 ±138.8

The LDF time-domain parameters presented as mean ± SD from the cold exposure are in Table 3. In the cold exposure, the absolute maximum BPU decreased in both groups substantially in the intervention and the recovery increased but did not reach the baseline values. The absolute mean BPU also decreased substantially in the cold intervention for both groups and increased slightly in the recovery. The absolute BPU values in general were lower with the diabetics at the baseline. The CVC decreased in the cold intervention for both groups and in the recovery, CVC increased slightly. Controls had larger CVC in the baseline. The $\%CVC_{max}$ decreased considerably for both groups in the cold intervention and the recovery had a slight increase. There were, however, no between-group significant differences in any parameters.

Table 3. Time-domain data of the experimental study in response to cold (+10 ˚C) exposure among persons with T2DM (n = 10) and controls (n = 10). The values are represented as mean±SD.

Experimental Group. Diabetics (*n*=10) and Controls (*n*=10)				
	Max BPU	**Mean BPU**	**CVC**	**% CVCmax**
Diab base	509.84±253.2	384.9 ±222.4	4.5 ±2.9	72.5 ±11.9
Diab int	53.45 ±18.7	20.7 ±10.6	0.2 ±0.1	3.8 ±1.0
Diab reco	141.3 ±160.2	50.5 ±44.7	0.5 ±0.4	11.3 ±15.8
Contr base	774.51±413.4	578.31±366.0	6.5 ±4.2	71.9 ±11.7
Contr int	70.69 ±42.4	24.76 ±14.2	0.3 ±0.1	3.4 ±2.4
Contr reco	108.62±53.5	56.34 ±43.4	0.6 ±0.4	9.1 ±7.7

4.1.2. Warm exposure

The HRV time-domain parameters presented as mean ± SD from the warm exposure are in Table 4. In the warm exposure, the baseline mean heart rate was significantly higher in the diabetics compared with the controls ($p = 0.002$). Controls also did have a large raise (from 63.9 to 78.7 bpm) in the mean heart rate whereas with diabetics the mean heart rate did not rise considerably (from 82.1 to 86.1 bpm). At baseline diabetic group had significantly shorter mean RR intervals compared with the controls ($p = 0.001$), the RR intervals decreased in both groups, and with controls, the decrease was larger. In the recovery, for both groups, the RR intervals increased, but no between-group significant differences were in the intervention or recovery. The SDNN and RMSSD were significantly lower in the diabetic individuals at baseline (SDNN ($p < 0.001$), RMSSD ($p = 0.008$). Both the SDNN and RMSSD decreased in intervention, and increased in the recovery, with the controls the decrease in the intervention was larger, and SDNN was significantly lower in the intervention ($p = 0.022$). For both groups, the NN50 and the pNN50 parameters decreased in the warm exposure.

Table 4. Time-domain data of the experimental study in response to warm (+40 ˚C) exposure among persons with T2DM (n = 10) and controls (n = 10). The values are represented as mean±SD.

Experimental Group. Diabetics (*n*=10) and Controls (*n*=10)								
	Body fat %	BMI	HR	RR	SDNN	RMSSD	NN50	pNN50
Diab base	31.76 ±6.8	30.1 ±4.9	82.1 ±13.2	751.6 ±124.9	14.81 ±7.8	10.54 ±6.0	0.1 ±0.3	0.032 ±0.1
Diab int	31.76 ±6.8	30.1 ±4.9	86.1 ±7.5	706.3 ±66.5	14.08 ±4.7	7.96 ±3.9	0	0
Diab reco	31.76 ±6.8	30.1 ±4.9	82.4 ±9.3	744.1 ±92.2	16.52 ±6.3	9.81 ±5.2	0	0
Contr base	25.07 ±3.5	25.4 ±2.2	63.9 ±7.2	956.8 ±116.3	32.00 ±10.5	19.97 ±11.0	10.40 ±16.2	3.54 ±5.6
Contr int	25.07 ±3.5	25.4 ±2.2	78.8 ±11.7	778.8 ±113.8	21.76 ±7.9	9.67 ±4.3	0.5 ±1.0	0.13 ±0.3
Contr reco	25.07 ±3.5	25.4 ±2.2	72.8 ±10.8	841.8 ±124.5	26.55 ±9.7	11.51 ±5.0	0.5 ±0.8	0.16 ±0.3

The BP time-domain parameters presented as mean ± SD from the warm exposure are in Table 5. In the warm exposure, the mean SYS decreased during the intervention and in the recovery increased nearly to the baseline levels. The mean DIA was at baseline lower in diabetics (p = 0.015). The mean DIA increased slightly in diabetics during the intervention and continued to slightly rise during the recovery, but with controls, the mean DIA decreased during the intervention and increased close to the baseline value during the recovery. MAP was significantly lower in diabetics in the baseline compared to controls (p = 0.026). In the recovery, diabetics had an increase in MAP that exceeded the baseline value. The mean SBP variation was similar to the mean RR interval also in the warm exposure and was behaving also similar way, decreasing during the warm intervention, and increasing in the recovery.

Table 5. Time-domain data of the experimental study in response to warm (+40 ˚C) exposure among persons with T2DM (n = 10) and controls (n = 10). The values are represented as mean±SD.

Experimental Group. Diabetics (*n*=10) and Controls (*n*=10)				
	Mean SYS	**Mean DIA**	**MAP**	**Mean SBPv**
Diab base	114.59±20.3	65.95 ±7.2	82.16 ±9.8	752.09±124.5
Diab int	106.93±17.7	66.03 ±6.2	79.67 ±9.2	706.97±67.1
Diab reco	114.29±15.8	67.85 ±7.7	83.33 ±9.2	745.05±92.4
Contr base	127.78±15.2	74.44 ±6.9	92.22 ±8.8	959.4 ±118.1
Contr int	108.68±7.2	67.95 ±6.0	81.53 ±5.9	777.25±116.6
Contr reco	120.28±8.7	72.24 ±6.9	88.25 ±7.1	841.72±124.9

The LDF time-domain parameters presented as mean ± SD from the warm exposure are in Table 6. In the warm exposure, the absolute maximum BPU increased in both groups substantially during the intervention and in the recovery decreased but did not reach the baseline values. The absolute mean BPU also increased substantially in the warm intervention for both groups and decreased in the recovery period. However, the BPU values with the controls in the baseline do seem to be inconsistent and the absolute values are notably lower with few subjects which impact all the mean values in the baseline. The CVC increased in the warm intervention for both groups and in

the recovery CVC decreased slightly. The $\%CVC_{max}$ was significantly higher in diabetics in the baseline compared to controls ($p = 0.034$).

Table 6. Time-domain data of the experimental study in response to warm (+40 ˚C) exposure among persons with T2DM (n = 10) and controls (n = 10). The values are represented as mean±SD.

Experimental Group. Diabetics (*n*=10) and Controls (*n*=10)				
	Max BPU	**Mean BPU**	**CVC**	**% CVCmax**
Diab base	557.18±295.3	399.82±223.1	4.8 ±2.4	58.1 ±35.2
Diab int	821.33±342.4	609.64±302.3	8.1 ±4.3	72.2 ±11.7
Diab reco	710.23±254.5	522.99±207.6	6.4 ±2.7	65.7 ±25.9
Contr base	412.09±251.2	288.09±206.5	3.1 ±2.1	31.0 ±33.5
Contr int	1086.17 ±347.6	892.64±336.7	10.9 ±4.0	81.0 ±7.0
Contr reco	850.62±613.9	614.13±476.4	7.1 ±5.9	52.4 ±27.4

4.2. Frequency-domain results

4.2.1. HRV from cold exposure

Total spectrum from 0.0095 to 2 Hz. The magnitude scalogram (top) and the average scalogram (bottom) of the HRV at baseline in cold exposure from a diabetic and control subject side by side can be seen in Figure 22. And at intervention from cold in Figure 23. Values of the absolute wavelet transform in the baseline and the intervention can be observed to be considerably lower in diabetics compared to controls. The total mean WT power of the spectrum increased from 5.6×10^3 AU to 27.8×10^3 AU in diabetics and from 33.1×10^3 AU to 456.9×10^3 AU in controls, therefore the increase in controls was larger.

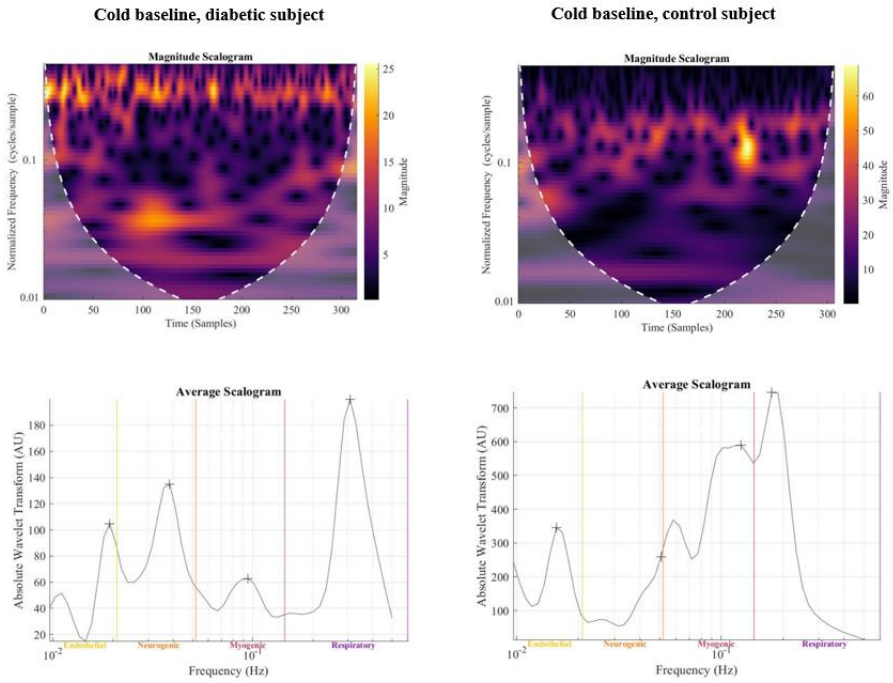

Figure 22. Cold baseline magnitude scalogram (top) and average scalogram (bottom) from a diabetic and control subject.

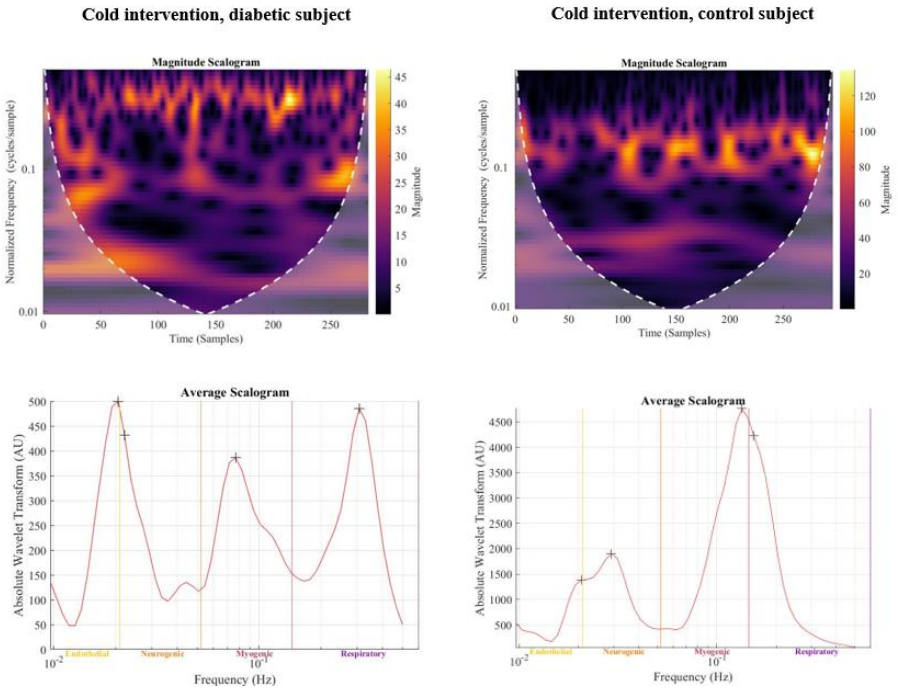

Figure 23. Cold intervention magnitude scalogram (top) and average scalogram (bottom) from a diabetic and control subject.

From a general point of view, the reliability of the lowest detectable frequency values depends on the duration of the original signal as mentioned in Section 3.3.5 therefore, amplitude and power values corresponding to the two lowest frequency bands are not included in this study. The peak amplitudes of the following frequency bands are calculated as the average of the peak amplitude frequencies of the measurements.

The absolute power of the frequency bands from 0.0052 to 2 Hz. The absolute power of the oscillations around 0.054 Hz (myogenic) was significantly lower in diabetics in the baseline in cold exposure ($p = 0.015$) compared to controls. The absolute power increased by 360 % ($4.6 \times 10^3 - 21.2 \times 10^3$) in response to cold intervention in diabetics, and controls the increase was 2000 % ($42.9 \times 10^3 - 89.8 \times 10^3$). The absolute power of the oscillations around 0.2 Hz (respiratory) increased by 700 % ($2.4 \times 10^3 - 19.1 \times 10^3$) in diabetic and in controls the increase was 1500 % ($26.3 \times 10^3 - 42.5 \times 10^3$) (Figure 24). The absolute myogenic power and the absolute respiratory power ratio in the baseline were 4.6 in diabetics and 5.3 in controls and in the intervention 1.7 in diabetics and 3.4 in controls. The change in diabetics was a 61 % decrease and in controls 35 % decrease.

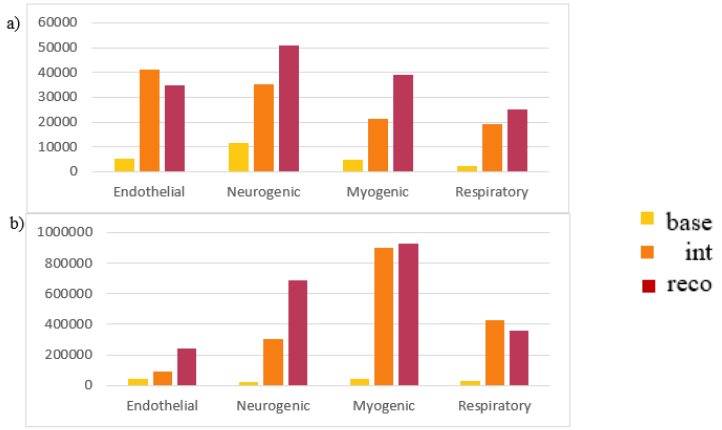

Figure 24. The absolute power of the HRV frequency spectrum from cold exposure diabetics (a) and controls (b).

The relative power of the frequency bands from 0.0052 to 2 Hz. The relative power of the oscillations around 0.054 Hz increased in response to cold by 6 % (0.55 – 0.58) in diabetics, whereas in controls the relative power decreased by 4 % (1.12 – 1.10). The relative power of the oscillations around 0.2 Hz decreased by 34 % (0.93 – 0.62) in diabetics, whereas in controls the relative power increased by 52 % (0.43 – 0.66) (Figure 25).

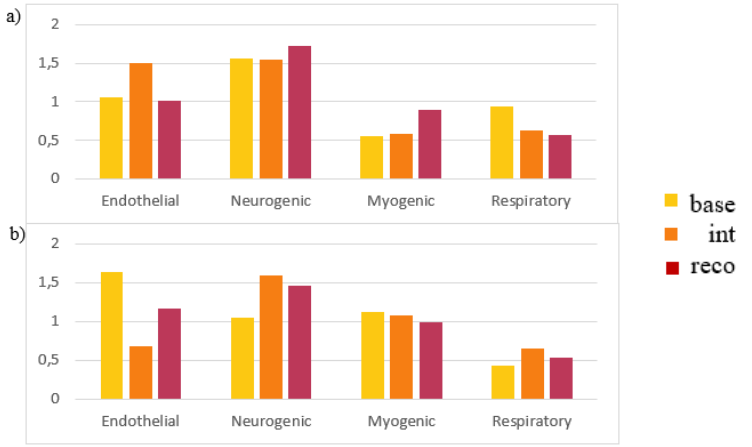

Figure 25. The relative power of the HRV frequency spectrum from cold exposure diabetics (a) and controls (b).

The absolute amplitude of the frequency bands from 0.0052 to 2 Hz. The absolute amplitude of the oscillations around 0.054 Hz was significantly lower in diabetics at baseline in cold exposure ($p = 0.026$) compared to controls. The absolute amplitude increased by 140 % (44.1 – 104.2) in response to cold intervention in diabetics, and in controls, the increase was 180 % (151.2 – 426.3). The absolute amplitude of the oscillations around 0.2 Hz increased by 215 % (29.0 – 91.5) in diabetics and controls, the increase was 220 % (87.0 – 280.2) (Figure 26).

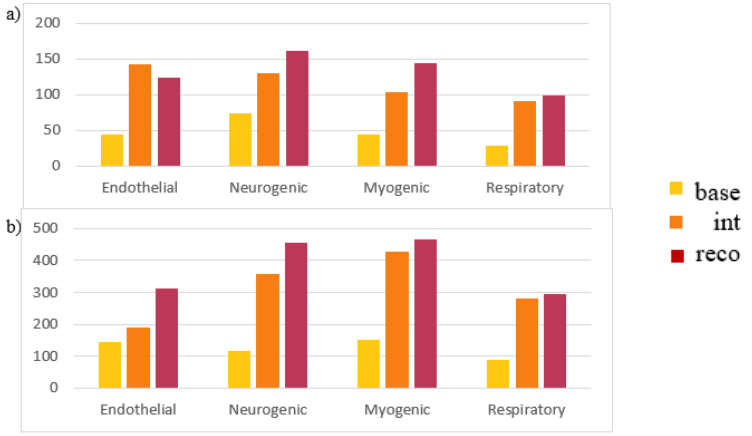

Figure 26. The absolute amplitude of the HRV frequency spectrum from cold exposure diabetics (a) and controls (b).

The relative amplitude of the frequency bands from 0.0052 to 2 Hz. The relative amplitude of the oscillations around 0.054 Hz increased in response to cold by 350 % in diabetics and by 270 % in controls. The relative amplitudes of the oscillations around 0.2 Hz increased by 226 % in diabetics and by 265 % in controls.

The CWT scalogram of the HRV at baseline, intervention, and recovery from cold exposure from the same diabetic and control subjects as the total power figures, can be seen in Figure 27. And from the same representatives, the average scalograms superimposed from cold intervention can be seen in Figure 28.

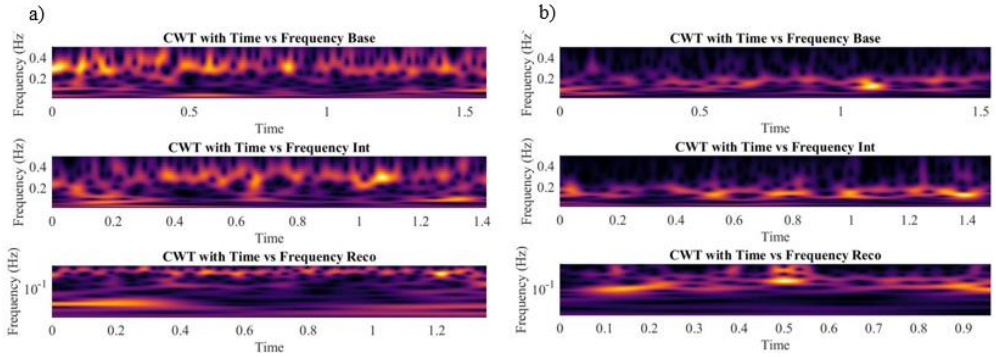

Figure 27. The CWT scalogram of a diabetic subject (a) and a control subject (b) from cold exposure from baseline, intervention, and recovery.

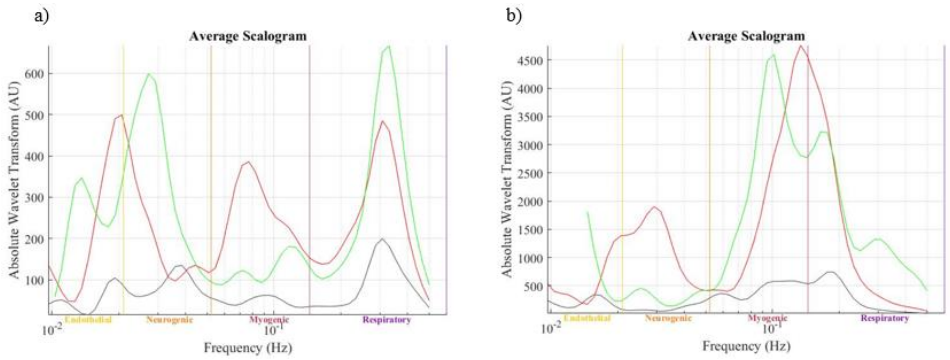

Figure 28. The average scalogram from cold exposure at baseline, intervention, and recovery of the diabetic subject (a) and the control subject (b) superimposed. Black line = baseline, red line = intervention, green line = recovery.

The distribution of the frequency bands in baseline, intervention, and recovery from cold exposure from the same subjects can be seen in Figure 29. From these pie charts can observe that different frequency bands were more pronounced in diabetics than in controls during cold exposure. From these pie charts, it can be seen that myogenic, which is comparable to the LF band, was the dominant band in controls.

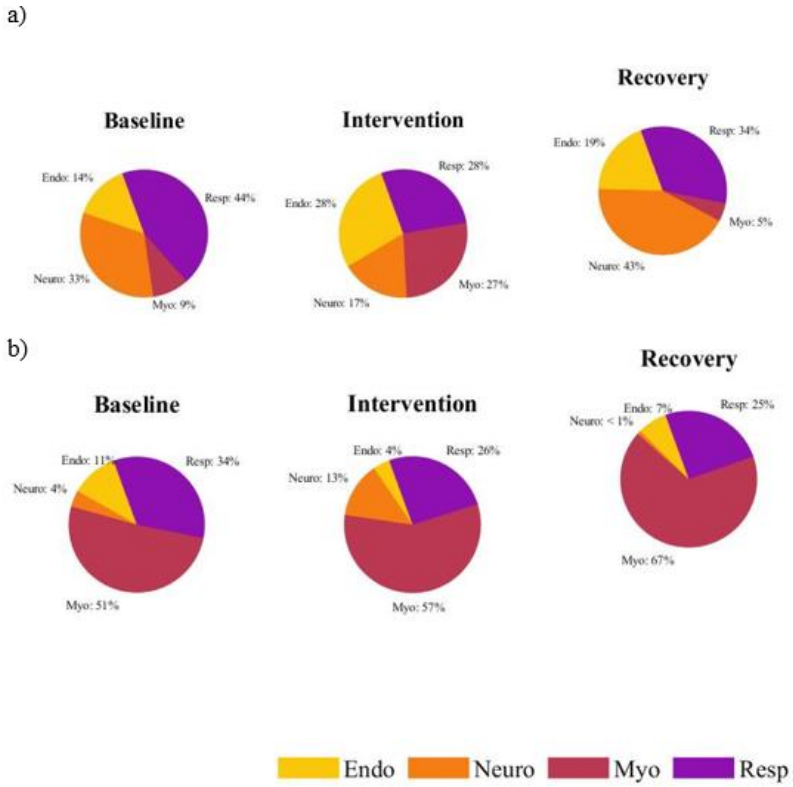

Figure 29. Distribution of frequency bands from the diabetic subject (a) and the control subject (b) from cold exposure.

4.2.2. HRV from warm exposure

The magnitude scalogram (top) and the average scalogram (bottom) of the HRV at baseline in warm exposure from a diabetic and control subject side by side can be seen in Figure 30. And at intervention from warm in Figure 31. Values of the absolute wavelet transform are also lower during warm exposure in diabetics compared to controls. The total mean WT power of the spectrum decreased from 4.5×10^3 AU to 1.2×10^3 AU in diabetics and from 42.6×10^3 AU to 7.3×10^3 AU in controls, therefore the decrease in controls was larger.

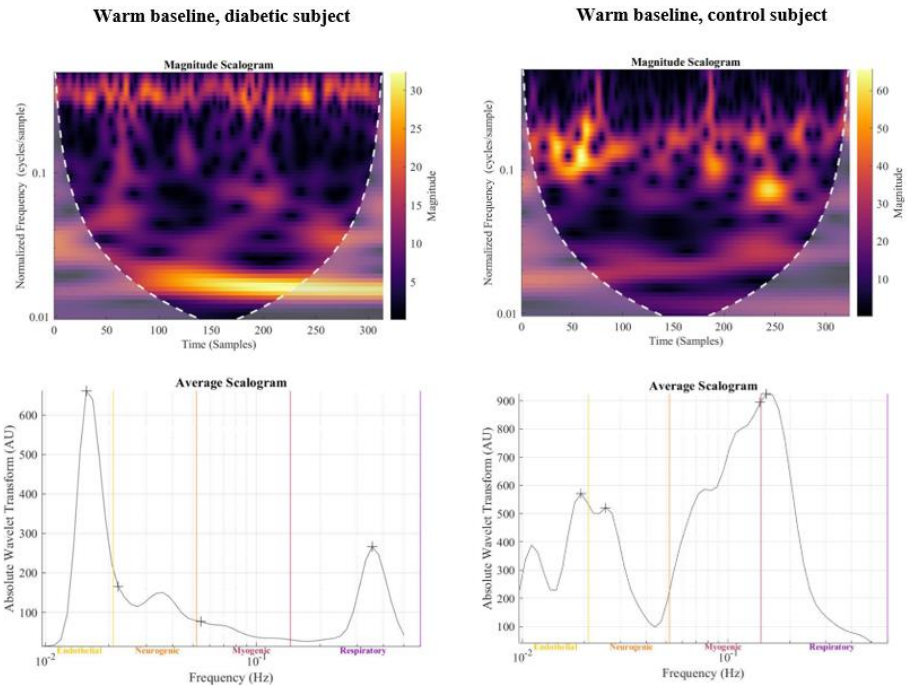

Figure 30. Warm baseline magnitude scalogram (top) and average scalogram (bottom) from a diabetic and control subject.

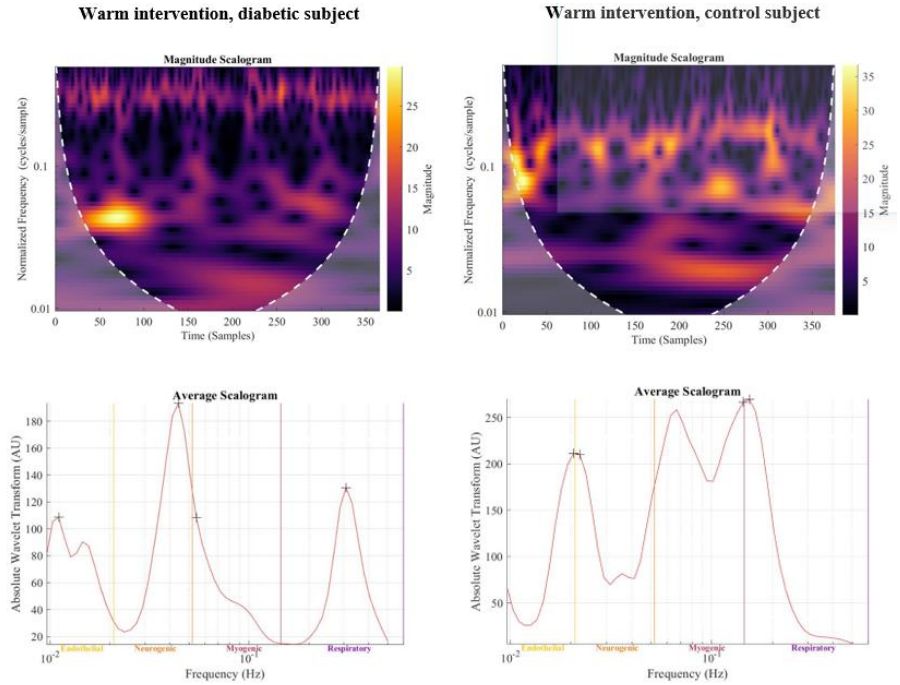

Figure 31. Warm intervention magnitude scalogram (top) and average scalogram (bottom) from a diabetic and control subject.

The peak amplitudes of the following frequency bands are calculated as the average of the peak amplitude frequencies of the measurements.

The absolute power of the frequency bands from 0.0052 to 2 Hz. The absolute power of the oscillations around 0.054 Hz was significantly lower in diabetics in the baseline in warm exposure ($p = 0.002$) compared to controls. Diabetics' absolute power in the warm intervention was also significantly lower ($p = 0.009$). The absolute power

decreased by 7 % ($0.5 \times 10^3 - 0.47 \times 10^3$) in response to warm intervention in diabetics, and controls the decrease was 82 % ($61.0 \times 10^3 - 11.0 \times 10^3$). The absolute power of the oscillations around 0.2 Hz was significantly lower in diabetics in the baseline in warm exposure ($p = 0.010$) compared to controls. The absolute power decreased by 74 % ($2.0 \times 10^3 - 0.52 \times 10^3$) in diabetic and controls the decrease was 96 % ($39.9 \times 10^3 - 1.8 \times 10^3$) (Figure 32). The absolute myogenic power and the absolute respiratory power ratio in the baseline were 1.7 in diabetics and 4.9 in controls and in the intervention 2.1 in diabetics and 26.1 in controls. The change in diabetics was a 26 % increase and in controls 430 % increase.

Figure 32. The absolute power of the HRV frequency spectrum from warm exposure diabetics (a) and controls (b).

The relative power of the frequency bands from 0.0052 to 2 Hz. The relative power of the oscillations around 0.054 Hz decreased in response to warm by 25 % ($0.41 - 0.31$) in diabetics, whereas in controls the relative power increased by 13 % ($0.9 - 1.04$). Relative power was significantly lower in diabetics in intervention in warm exposure ($p = 0.034$) compared to controls. The relative power of the oscillations around 0.2 Hz decreased by 62 % ($0.8 - 0.3$) in diabetics and by 63 % ($0.5 - 0.2$) in controls (Figure 33).

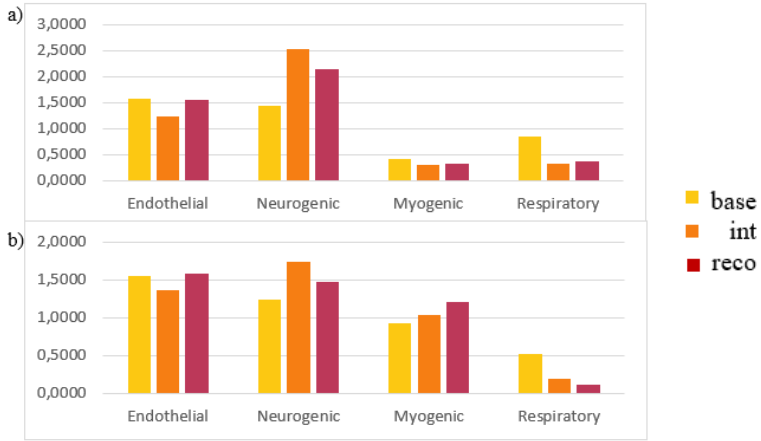

Figure 33. The relative power of the HRV frequency spectrum from warm exposure diabetics (a) and controls (b).

The absolute amplitude of the frequency bands from 0.0052 to 2 Hz. The absolute amplitude of the oscillations around 0.054 Hz was significantly lower in diabetics in the baseline in warm exposure ($p = 0.002$) compared to controls. The absolute amplitude decreased by 19 % ($16.8 - 13.6$) in response to warm intervention in diabetics, and in controls, the decrease was 58 % ($157.1 - 66.2$). The absolute amplitude of the oscillations around 0.2 Hz was significantly lower in diabetics in the baseline in warm exposure ($p = 0.016$) compared to controls. The absolute amplitude decreased by 48 % ($23.4 - 12.1$) in diabetics and controls, the decrease was 81 % ($105.4 - 19.9$) (Figure 34).

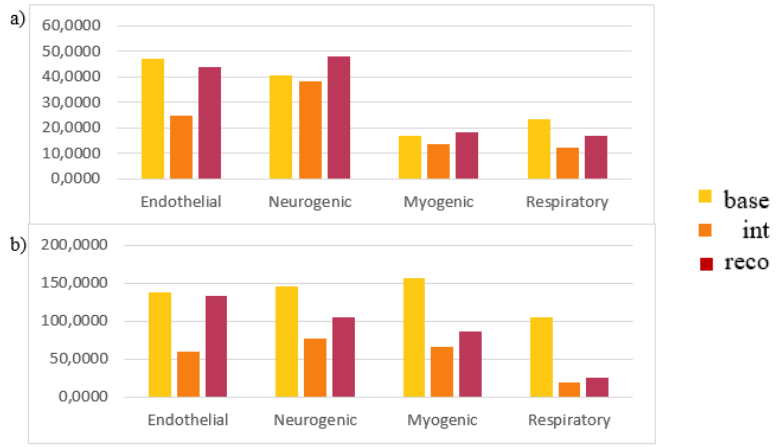

Figure 34. The absolute amplitude of the HRV frequency spectrum from warm exposure diabetics (a) and controls (b).

The relative amplitude of the frequency bands from 0.0052 to 2 Hz. The relative amplitude of the oscillations around 0.054 Hz decreased in response to warm by 27 % in diabetics and by 33 % in controls. The relative amplitudes of the oscillations around 0.2 Hz decreased by 46 % in diabetics and by 72 % in controls.

The CWT scalogram of the HRV at baseline, intervention, and recovery from warm exposure from the same diabetic and control subjects as the total power figures, can be seen in Figure 35. And from the same representatives, the average scalograms superimposed from warm intervention can be seen in Figure 36.

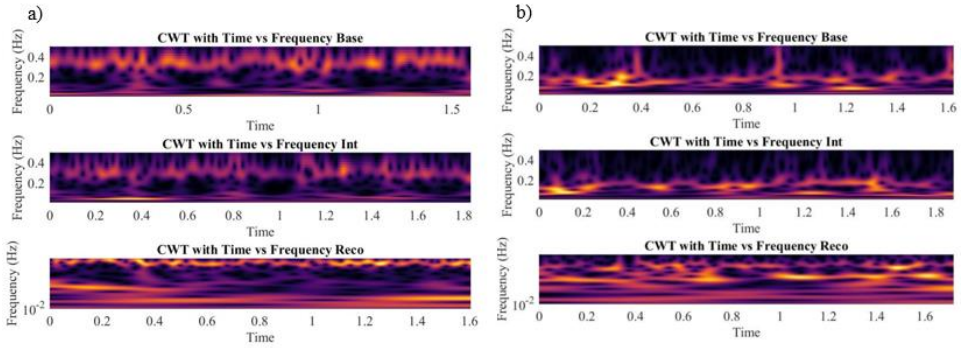

Figure 35. The CWT scalogram of a diabetic subject (a) and a control subject (b) from warm exposure from baseline, intervention, and recovery.

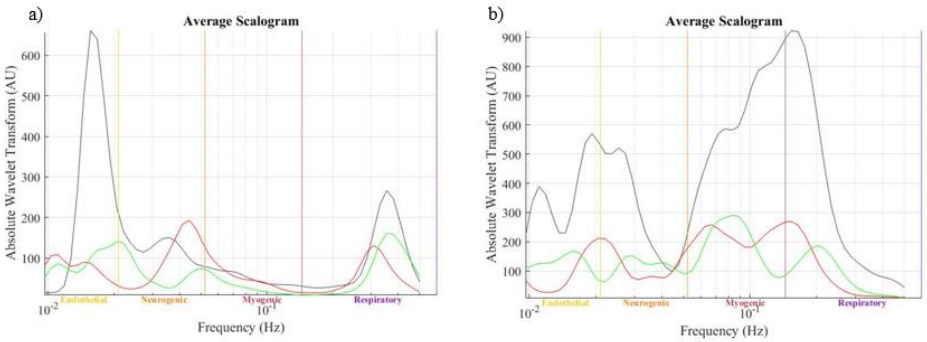

Figure 36. The average scalogram from warm exposure at baseline, intervention, and recovery of the diabetic subject (a) and the control subject (b) superimposed. Black line = baseline, red line = intervention, green line = recovery.

The distribution of the frequency bands in baseline, intervention, and recovery from warm exposure from the same subjects can be seen in Figure 37. From these pie charts can observe that different frequency bands were more pronounced in diabetics than in controls in warm exposure. From these pie charts, it can be seen that myogenic, which is comparable to the LF band, was the dominant band in controls.

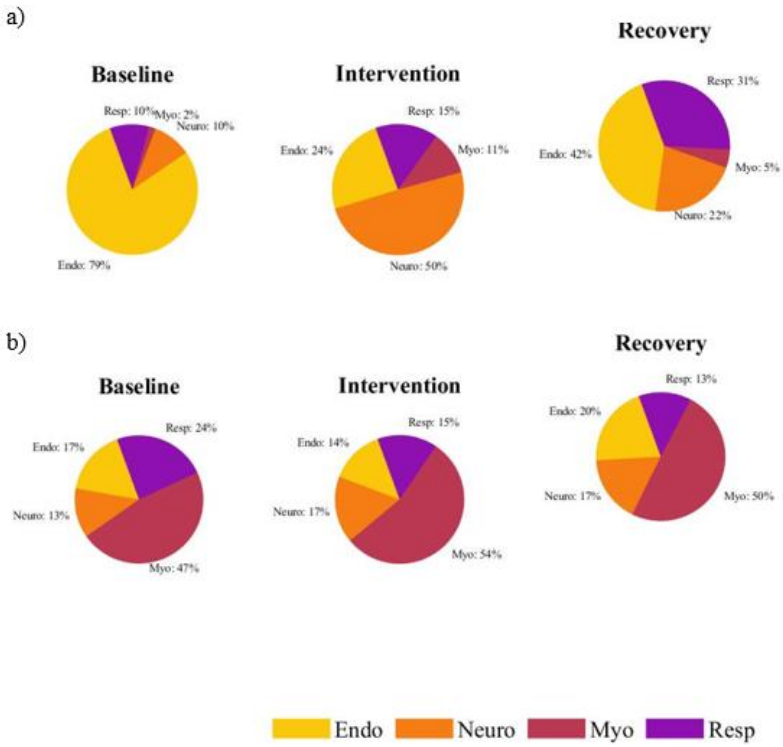

Figure 37. Distribution of frequency bands from the diabetic subject (a) and the control subject (b) from warm exposure.

4.2.3. BP from cold exposure

Total spectrum from 0.0095 to 2 Hz. The magnitude scalogram (top) and the average scalogram (bottom) of the BP at baseline in cold exposure from a diabetic subject and control subject side by side can be seen in Figure 38. And at intervention from cold in Figure 39. Values of the absolute wavelet transform can be observed to be considerably

lower during the cold intervention in diabetics compared to controls. The total mean WT power of the spectrum increased from 6.1×10^3 AU to 27.2×10^3 AU in diabetics and from 33.2×10^3 AU to 462.8×10^3 AU in controls, therefore the increase in controls was larger.

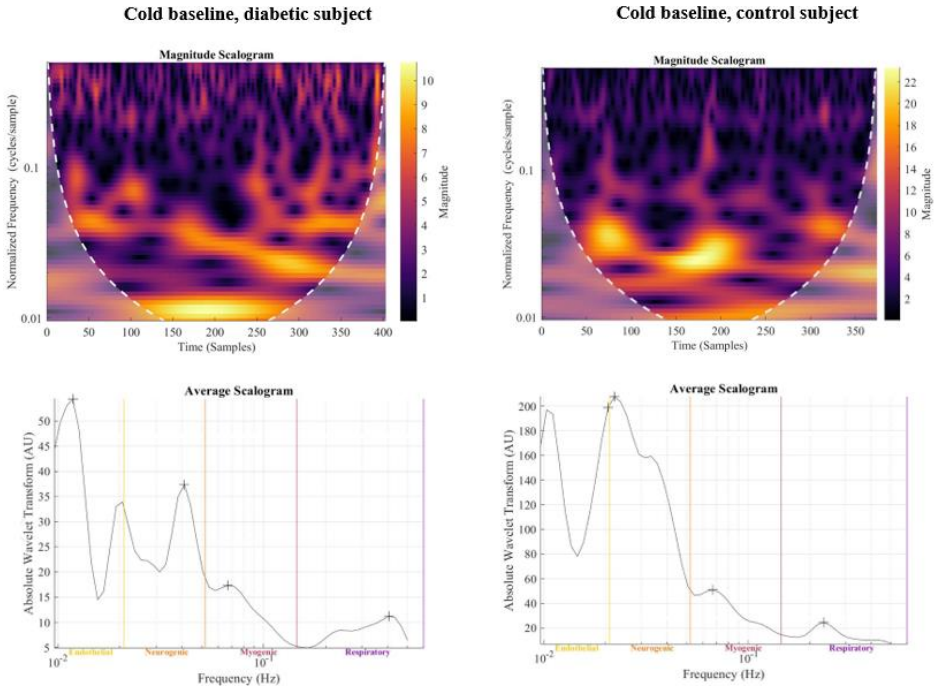

Figure 38. Cold baseline magnitude scalogram (top) and average scalogram (bottom) from a diabetic and control subject.

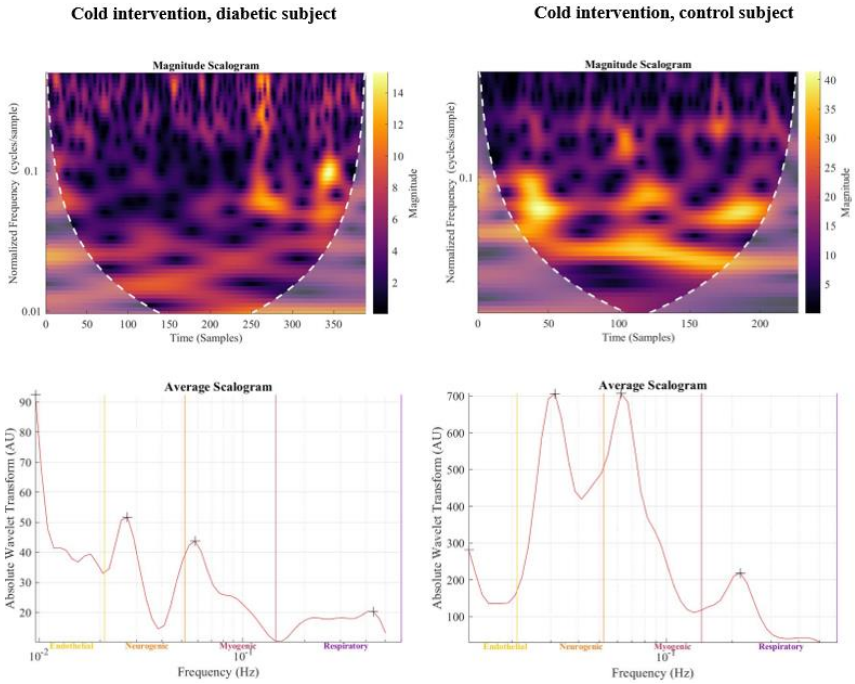

Figure 39. Cold intervention magnitude scalogram (top) and average scalogram (bottom) from a diabetic and control subject.

The peak amplitudes of the following frequency bands are calculated as the average of the peak amplitude frequencies of the measurements.

The absolute power of the frequency bands from 0.0052 to 2 Hz. The absolute power of the oscillations around 0.06 Hz (myogenic) was significantly lower in diabetics in the baseline in cold exposure ($p = 0.016$) compared to controls. The absolute power increased 280 % ($5.7 \times 10^3 - 21.3 \times 10^3$) in response to cold intervention in diabetics, and controls the increase was 1900 % ($41.5 \times 10^3 - 840.7 \times 10^3$). The absolute power of the oscillations around 0.2 Hz (respiratory) increased by 740 % ($2.7 \times 10^3 - 22.6 \times 10^3$) in diabetic and in controls the increase was 1200 % ($28.1 \times 10^3 - 359.4 \times 10^3$) (Figure 40). The absolute myogenic power and the absolute respiratory power ratio in the baseline were 2.49 in diabetics and 4.93 in controls and in the intervention 1.25 in diabetics and 3.78 in controls. The change in diabetics was a 50 % decrease and in controls 23 % decrease.

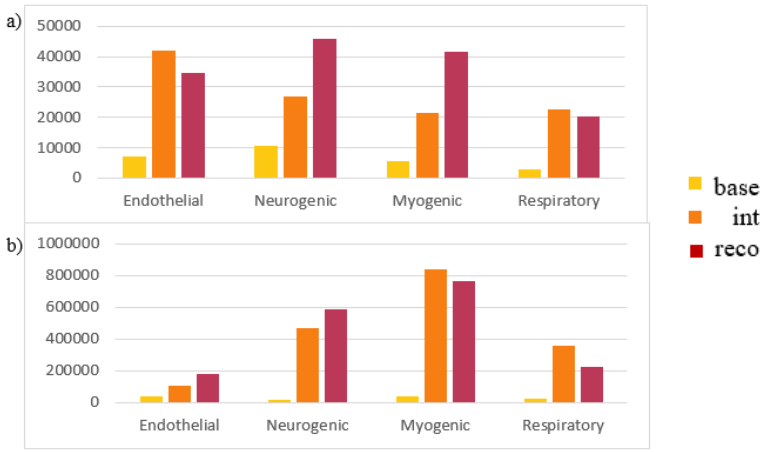

Figure 40. The absolute power of the BP frequency spectrum from cold exposure diabetics (a) and controls (b).

The relative power of the frequency bands from 0.0052 to 2 Hz. The relative power of the oscillations around 0.06 Hz increased in response to cold by 11 % ($0.54 - 0.6$) in diabetics and by 0.4 % ($1.102 - 1.106$) in controls. The relative power of the oscillations around 0.2 Hz decreased by 25 % ($1.18 - 0.88$) in diabetics and by 8.5 % ($0.48 - 0.44$) in controls (Figure 41). The relative power in the respiratory frequency band was significantly lower in controls in the intervention ($p = 0.039$) compared to diabetics.

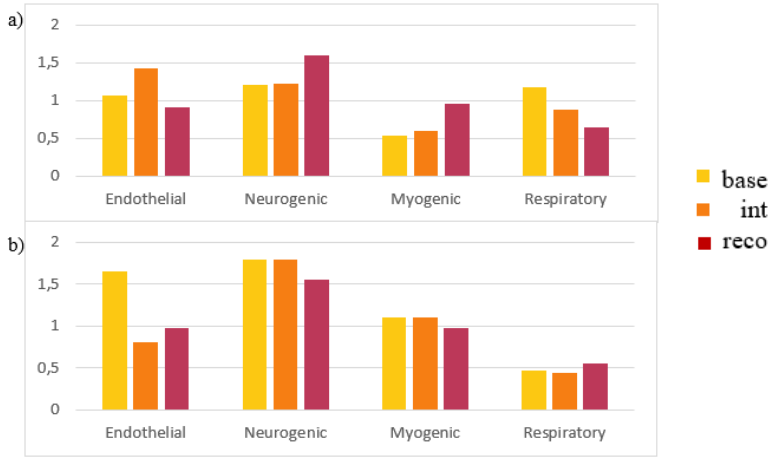

Figure 41. The relative power of the BP frequency spectrum from cold exposure diabetics (a) and controls (b).

The absolute amplitude of the frequency bands from 0.0052 to 2 Hz. The absolute amplitude of the oscillations around 0.06 Hz was significantly lower in diabetics in the baseline in cold exposure ($p = 0.019$) compared to controls. The absolute amplitude increased by 130 % ($47.9 - 109.0$) in response to cold intervention in diabetics, and in controls, the increase was 199 % ($148.5 - 443.8$). The absolute amplitude of the oscillations around 0.2 Hz increased by 230 % ($32.5 - 108.4$ in diabetics and controls, the increase was 180 % ($92.0 - 260.3$) (Figure 42).

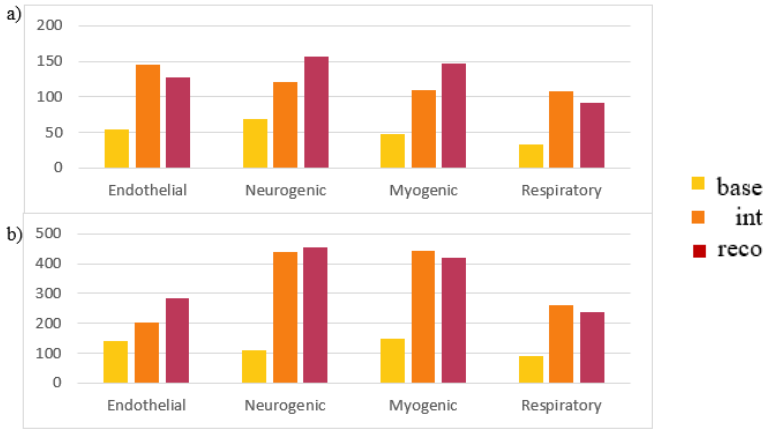

Figure 42. The absolute amplitude of the BP frequency spectrum from cold exposure diabetics (a) and controls (b).

The relative amplitude of the frequency bands from 0.0052 to 2 Hz. The relative amplitude of the oscillations around 0.06 Hz increased in response to cold by 380 % in diabetics and by 280 % in controls. The relative amplitudes of the oscillations around 0.2 Hz increased by 297 % in diabetics and by 255 % in controls.

The CWT scalogram of the BP at baseline, intervention, and recovery from cold exposure from the same diabetic and control subjects as the total power figures, can be seen in Figure 43. And from the same representatives, the average scalograms superimposed from cold intervention can be seen in Figure 44.

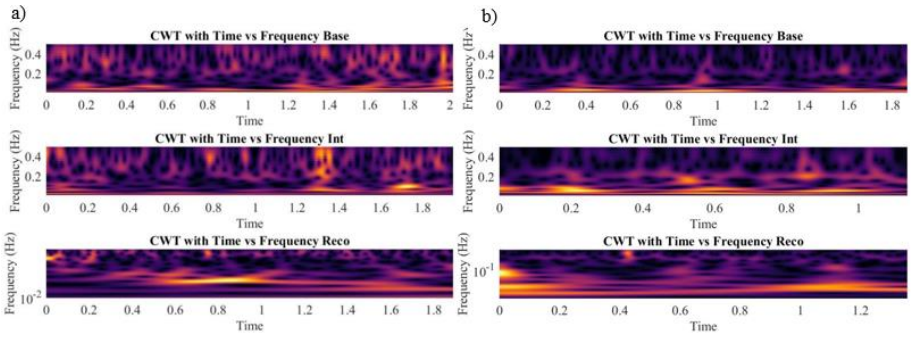

Figure 43. The CWT scalogram of the diabetic subject (a) and the control subject (b) from cold exposure from baseline, intervention, and recovery.

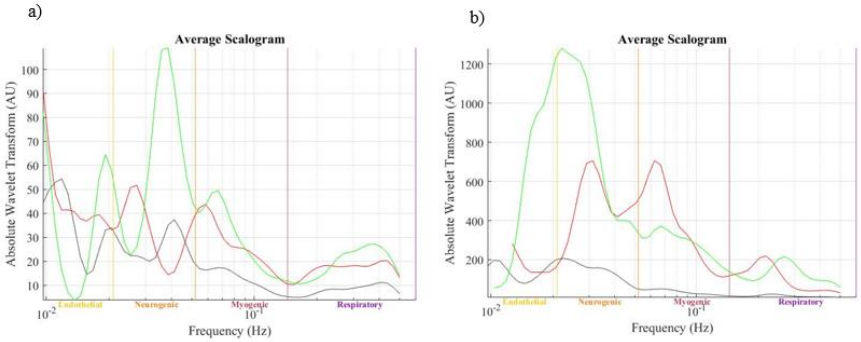

Figure 44. The average scalogram from cold exposure at baseline, intervention, and recovery of the diabetic subject (a) and the control subject (b) superimposed. Black line = baseline, red line = intervention, green line = recovery.

The distribution of the frequency bands in baseline, intervention, and recovery from cold exposure from the same subjects can be seen in Figure 45. From these pie charts can observe that also in BP variation signal, different frequency bands were more pronounced in diabetics than in controls in cold exposure. However, the dominant bands were different than in HRV.

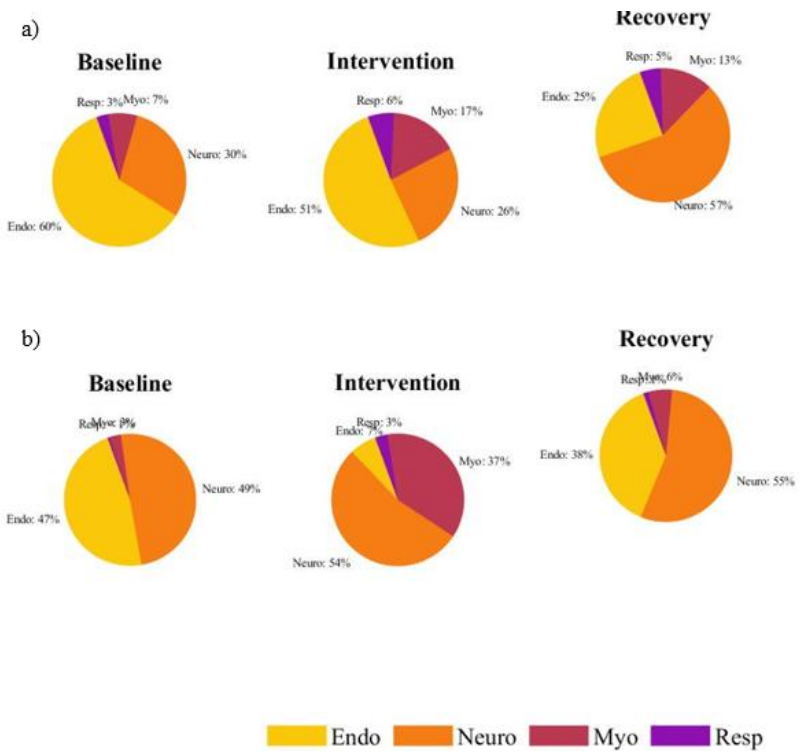

Figure 45. Distribution of frequency bands from the diabetic subject (a) and the control subject (b) from cold exposure.

4.2.4. BP from warm exposure

The magnitude scalogram (top) and the average scalogram (bottom) of the BP at baseline in warm exposure from a diabetic and control subject side by side can be seen in Figure 46. And at intervention from warm in Figure 47. Values of the absolute wavelet transform can be observed to be considerably lower also during the warm intervention in diabetics compared to controls. The total mean WT power of the spectrum decreased from 4.4×10^3 AU to 1.2×10^3 AU in diabetics and from 40.3×10^3 AU to 8.6×10^3 AU in controls.

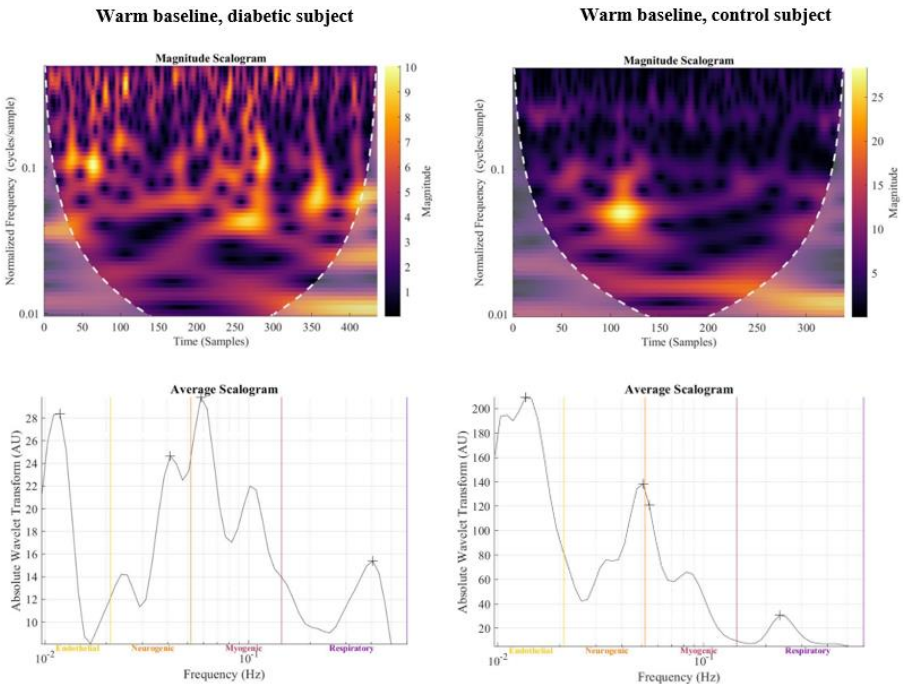

Figure 46. Warm baseline magnitude scalogram (top) and average scalogram (bottom) from a diabetic and control subject.

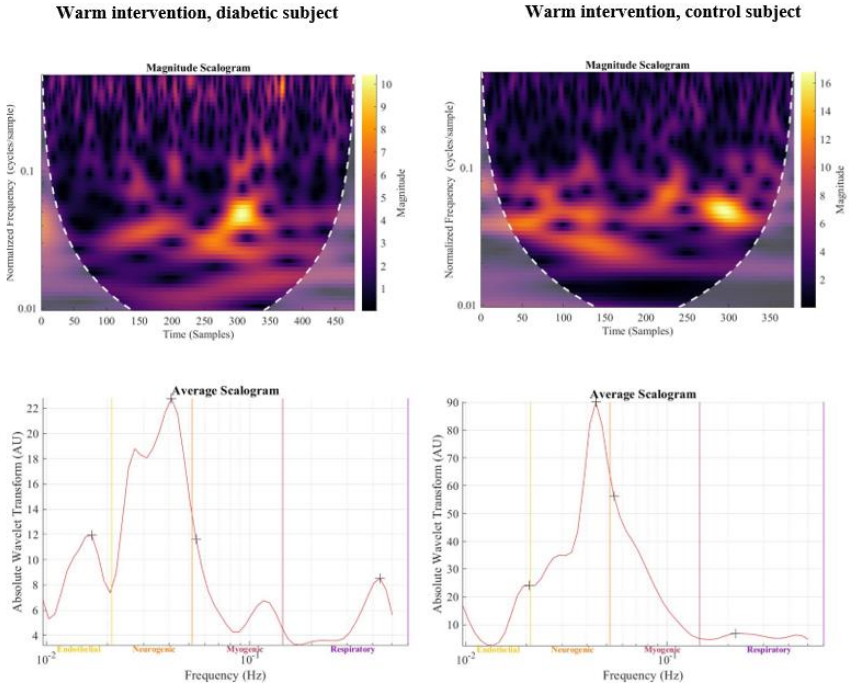

Figure 47. Warm intervention magnitude scalogram (top) and average scalogram (bottom) from a diabetic and control subject.

The peak amplitudes of the following frequency bands are calculated as the average of the peak amplitude frequencies of the measurements.

The absolute power of the frequency bands from 0.0052 to 2 Hz. The absolute power of the oscillations around 0.06 Hz was significantly lower in diabetics in the baseline in warm exposure ($p = 0.003$) compared to controls. The absolute power increased 16 % ($0.46 \times 10^3 - 0.54 \times 10^3$) in response to warm intervention in

diabetics, whereas in controls the absolute power decreased by 72 % ($40.8 \times 10^3 - 11.2 \times 10^3$). The absolute power was also significantly lower in diabetics in the intervention ($p = 0.007$) compared to controls. The absolute power of the oscillations around 0.2 Hz was significantly lower in diabetics at baseline in warm exposure ($p = 0.010$) compared to controls. The absolute power decreased by 81 % ($2.8 \times 10^3 - 0.55 \times 10^3$) in diabetic and in controls the decrease was 96 % ($45.1 \times 10^3 - 1.8 \times 10^3$) (Figure 48). The absolute myogenic power and the absolute respiratory power ratio in the baseline were 1.69 in diabetics and 6.34 in controls and in the warm exposure intervention 1.66 in diabetics and 15.94 in controls. The change in diabetics was a 1.7 % decrease, whereas in controls the power ratio increased by 150 %.

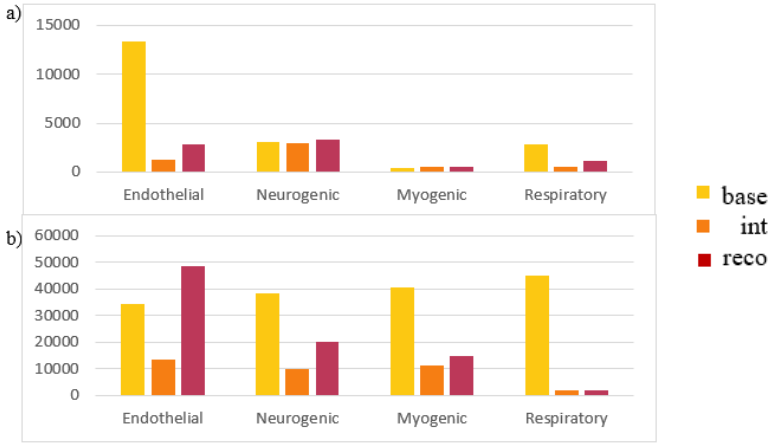

Figure 48. The absolute power of the BP frequency spectrum from warm exposure diabetics (a) and controls (b).

The relative power of the frequency bands from 0.0052 to 2 Hz. The relative power of the oscillations around 0.06 Hz decreased in response to warm by 39 % ($0.62 - 0.38$) in diabetics, whereas in controls the relative power increased by 18 % ($0.83 - 0.98$). The relative power of the oscillations around 0.2 Hz decreased by 51% ($0.84 - 0.41$) in diabetics and 71 % ($0.6 - 0.17$) in controls (Figure 49). The relative power in the respiratory frequency band was significantly lower in controls in the intervention ($p = 0.027$) compared to diabetics.

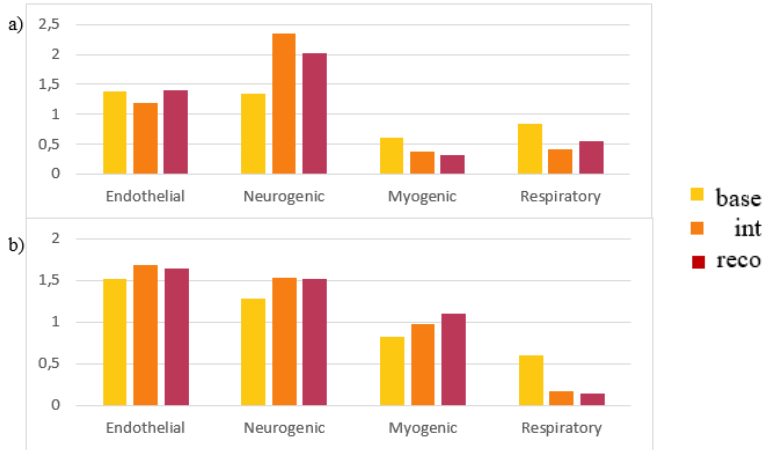

Figure 49. The relative power of the BP frequency spectrum from warm exposure diabetics (a) and controls (b).

The absolute amplitude of the frequency bands from 0.0052 to 2 Hz. The absolute amplitude of the oscillations around 0.06 Hz was significantly lower in diabetics in the baseline in warm exposure ($p = 0.002$) compared to controls. The absolute amplitude decreased by 12 % ($16.8 - 14.8$) in response to warm intervention in diabetics, and in controls, the decrease was 52 % ($140.9 - 67.5$). The absolute amplitude was also lower in diabetics in the intervention ($p = 0.009$) compared to controls. The absolute amplitude of the oscillations around 0.2 Hz was significantly lower in diabetics in the baseline in warm exposure ($p = 0.013$) compared to controls. The absolute amplitude decreased by 47 % ($25.3 - 13.5$) in diabetics and controls, the decrease was 82 % ($126.1 - 22.9$) (Figure 50).

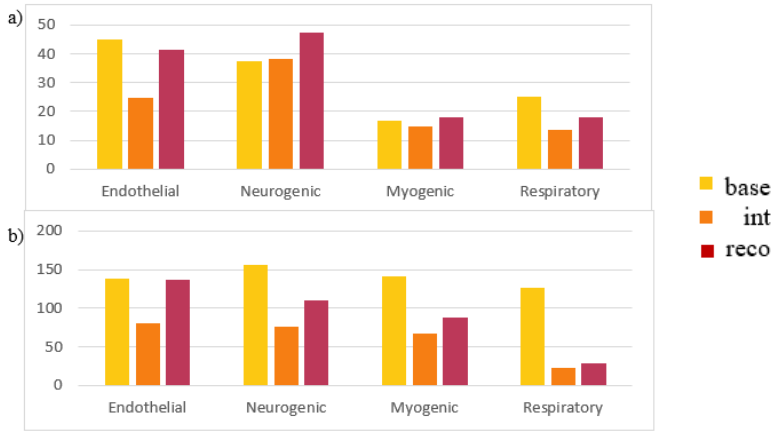

Figure 50. The absolute amplitude of the BP frequency spectrum from warm exposure diabetics (a) and controls (b).

The relative amplitude of the frequency bands from 0.0052 to 2 Hz. The relative amplitude of the oscillations around 0.06 Hz decreased in response to warm by 22 % in diabetics and by 21 % in controls. The relative amplitudes of the oscillations around 0.2 Hz decreased by 43 % in diabetics and by 69 % in controls.

The CWT scalogram of the BP at baseline, intervention, and recovery from warm exposure from the same diabetic and control subjects as the total power figures, can be seen in Figure 51. And from the same representatives, the average scalograms superimposed from warm intervention can be seen in Figure 52.

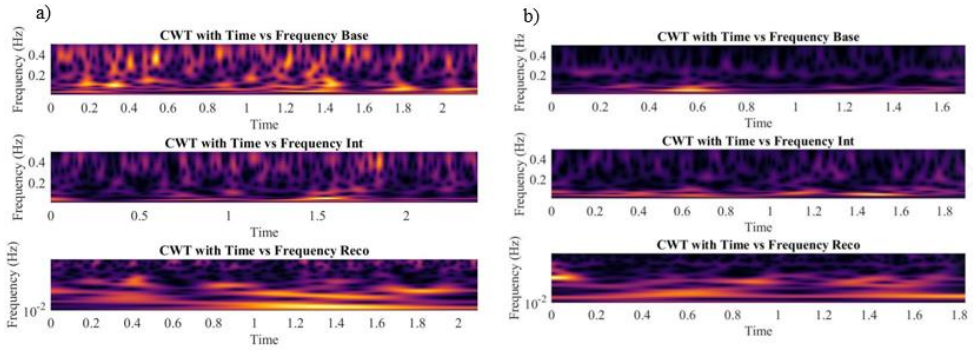

Figure 51. The CWT scalogram of the diabetic subject (a) and the control subject (b) from warm exposure from baseline, intervention, and recovery.

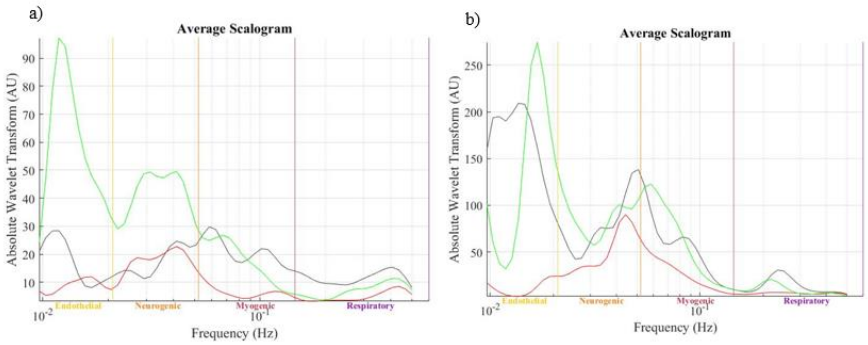

Figure 52. The average scalogram from warm exposure at baseline, intervention, and recovery of the diabetic subject (a) and the control subject (b) superimposed. Black line = baseline, red line = intervention, green line = recovery.

The distribution of the frequency bands in baseline, intervention, and recovery from warm exposure from the same subjects can be seen in Figure 53. From these pie charts can observe that also in BP variation signal, different frequency bands were more pronounced in diabetics than in controls in warm exposure. However, the dominant bands were different than in HRV.

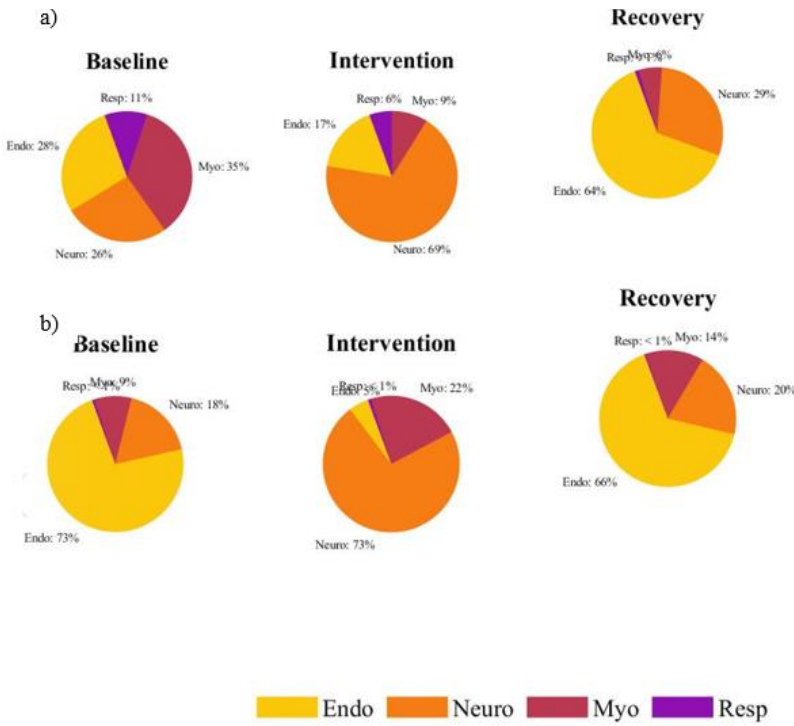

Figure 53. Distribution of frequency bands from the diabetic subject (a) and the control subject (b) from warm exposure.

4.2.5. LDF from cold exposure

Total spectrum from 0.0095 to 2 Hz. The 3D magnitude scalogram (top) and the average scalogram (bottom) of the LDF at baseline in cold exposure from a diabetic and control subject side by side can be seen in Figure 54. And at intervention from cold in Figure 55. Values of the absolute wavelet transform can be observed to be

lower during the cold baseline and intervention in diabetics compared to controls. The total mean WT power of the spectrum decreased from 4.9×10^{-7} AU to 3.12×10^{-10} AU in diabetics and from 4.8×10^{-6} AU to 1.0×10^{-9} AU in controls. The decrease in total WT power for both groups was similar in the cold intervention.

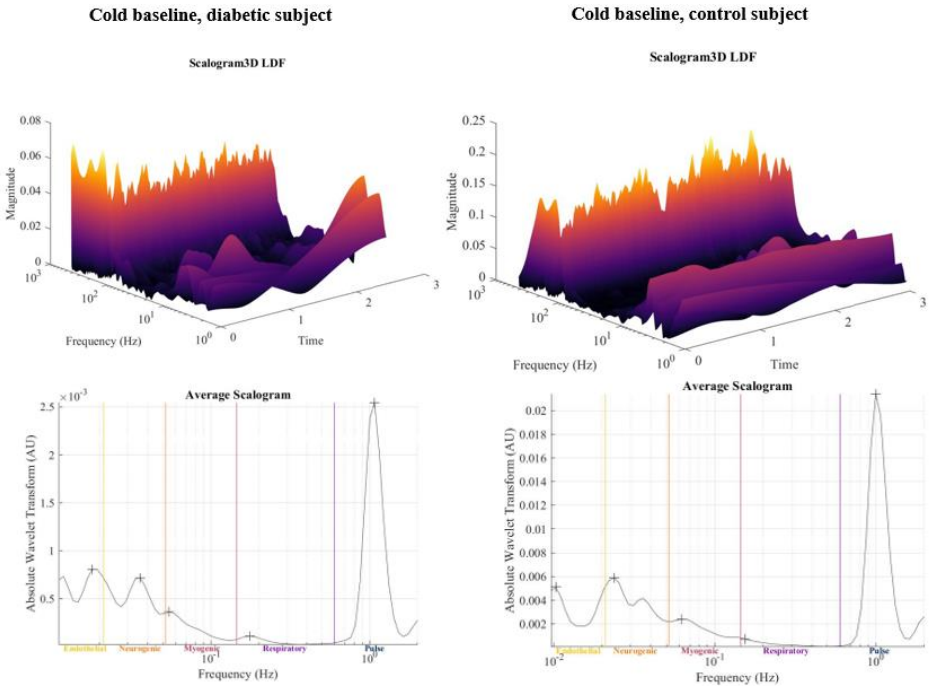

Figure 54. Cold baseline 3D magnitude scalogram (top) and average scalogram (bottom) from a diabetic and control subject.

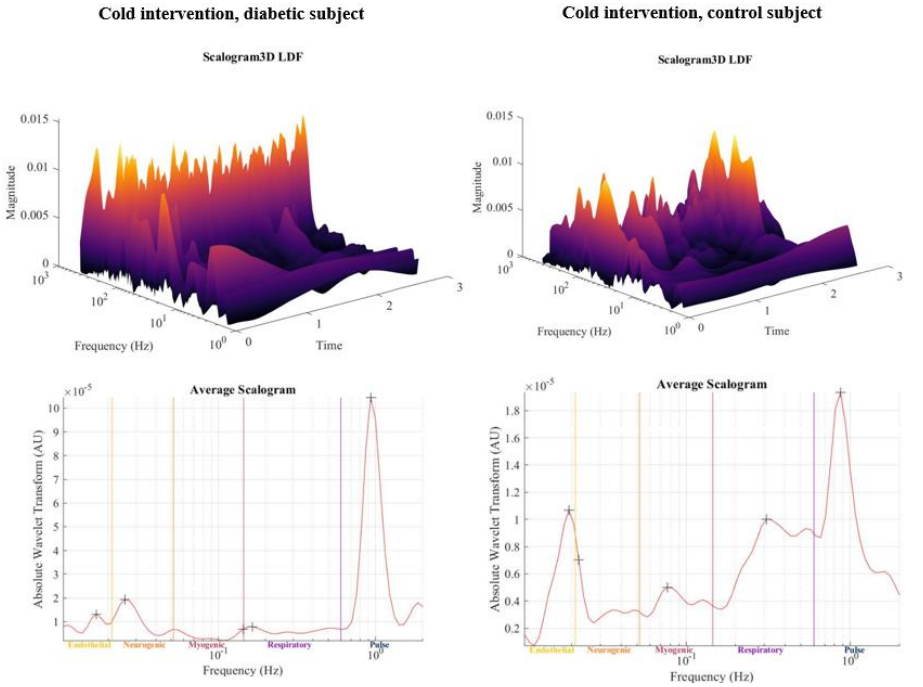

Figure 55. Cold intervention 3D magnitude scalogram (top) and average scalogram (bottom) from a diabetic and control subject.

The peak amplitudes of the following frequency bands are calculated as the average of the peak amplitude frequencies of the measurements.

The absolute power of the frequency bands from 0.0052 to 2 Hz. The absolute power of the oscillations around 0.05 Hz (myogenic) decreased 100 % ($4.8 \times 10^{-8} - 2.7 \times 10^{-11}$) in response to cold intervention in diabetics, and controls, the decrease was the same 100 % ($5.2 \times 10^{-7} - 6.5 \times 10^{-10}$). The absolute power of the oscillations around 0.2 Hz (respiratory) decreased by 99 % ($5.2 \times 10^{-9} - 3.5 \times 10^{-11}$) in diabetic and in controls the decrease was the same 99 % ($2.7 \times 10^{-8} - 3.2 \times 10^{-10}$). The absolute power of the oscillations around 0.9 Hz (pulse) decreased by 100 % ($1.6 \times 10^{-6} - 1.2 \times 10^{-9}$) in diabetic and by 100 % ($1.3 \times 10^{-5} - 3.1 \times 10^{-9}$) in controls (Figure 56). There were no between-group significant differences in any absolute power parameters. The absolute myogenic power and the absolute respiratory power ratio in the baseline were 13.7 in diabetics and 35 in controls and in the cold exposure intervention 2.6 in diabetics and 2.4 in controls. The change in diabetics was therefore 83 % decrease and in controls 93 % decrease. The absolute respiratory power and the absolute pulse power ratio in the baseline were 0.03 in diabetics and 0.009 in controls and in the intervention 0.15 in diabetics and 0.41 in controls. The change in diabetics was a 430 % increase and in controls 4460 % increase.

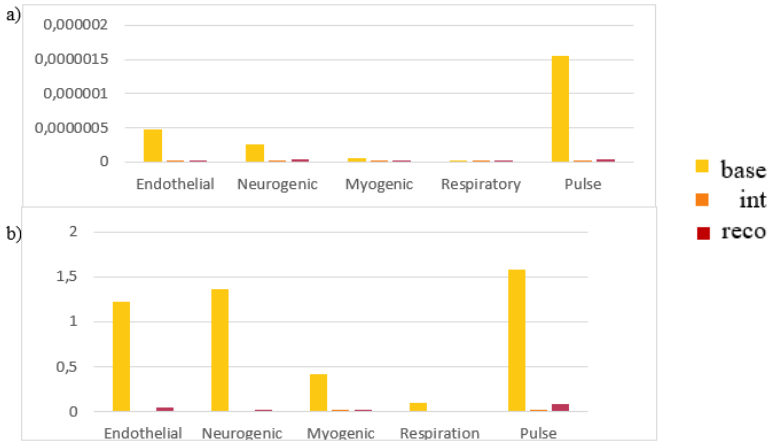

Figure 56. The absolute power of the LDF frequency spectrum from cold exposure diabetics (a) and controls (b).

The relative power of the frequency bands from 0.0052 to 2 Hz. The relative power of the oscillations around 0.05 Hz increased in response to cold by 180 % (0.13 − 0.37) in diabetics and by 480 % (0.09 − 0.56) in controls. The relative power of the oscillations around 0.2 Hz increased by 370 % (0.07 − 0.33) in diabetics and by 1800 % (0.03 − 0.48) in controls, whereas a small change was observed for the frequency around 0.9 Hz decrease by 11 % (3.28 − 2.93)in diabetics and increase of 2,5 % (2.41 − 2.47) in controls (Figure 57). There were no between-group significant differences in any relative power parameters.

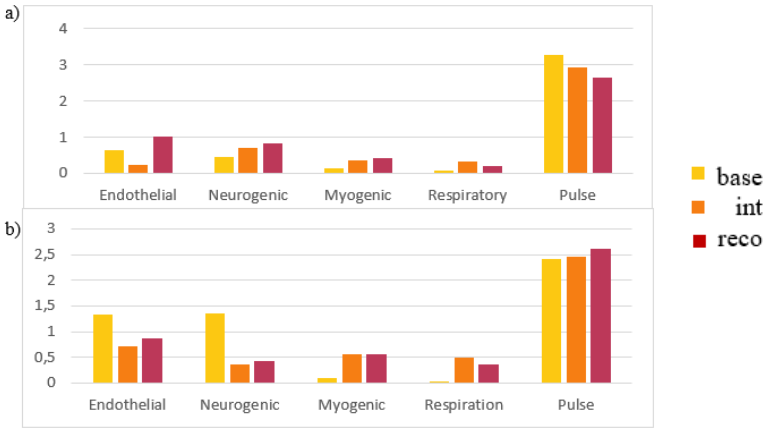

Figure 57. The relative power of the LDF frequency spectrum from cold exposure diabetics (a) and controls (b).

The absolute amplitude of the frequency bands from 0.0052 to 2 Hz. The absolute amplitude of the oscillations around 0.05 Hz decreased 97 % (0.15 − 0.005) in response to cold intervention in diabetics, and in controls, the decrease was 96 % (0.42 − 0.02). The absolute amplitude of the oscillations around 0.2 Hz decreased by 94 % (0.06 − 0.005) in diabetics and controls, the decrease was 88 % (0.1 − 0.01), whereas the absolute amplitude of the oscillations around 0.9 Hz increased by 97 % (0.65 − 0.01) in diabetics and by 98 % (1.58 − 0.03) in controls (Figure 58). There were no between-group significant differences in any absolute amplitude parameters.

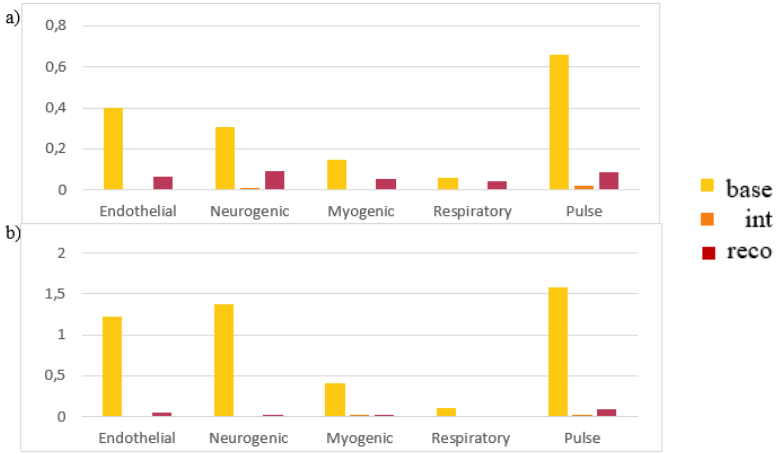

Figure 58. The absolute amplitude of the LDF frequency spectrum from cold exposure diabetics (a) and controls (b).

The relative amplitude of the frequency bands from 0.0052 to 2 Hz. The relative amplitude of the oscillations around 0.05 Hz decreased in response to cold by 97 % in diabetics and by 92 % in controls. The relative amplitudes of the oscillations around 0.2 Hz decreased by 88 % in diabetics and by 83 % in controls. The relative amplitude of the oscillations around 0.9 Hz decreased by 98 % in diabetics and 97 % in controls.

The CWT scalogram of the LDF at baseline, intervention, and recovery from cold exposure from the same diabetic and control subjects as the total power figures, can be seen in Figure 59. And from the same representatives, the average scalograms superimposed from cold intervention can be seen in Figure 60.

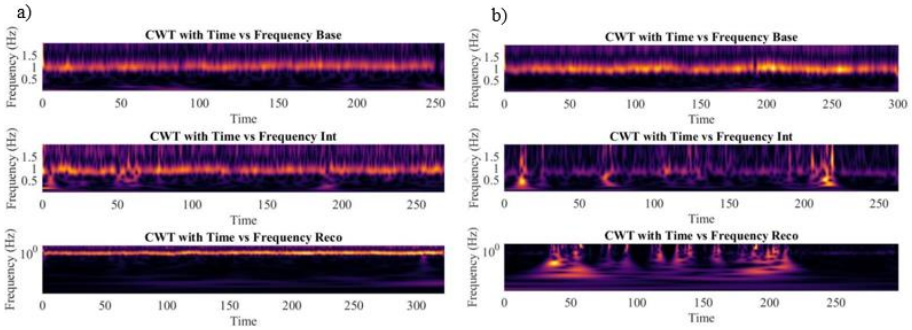

Figure 59. The CWT scalogram of the diabetic subject (a) and the control subject (b) from cold exposure from baseline, intervention, and recovery.

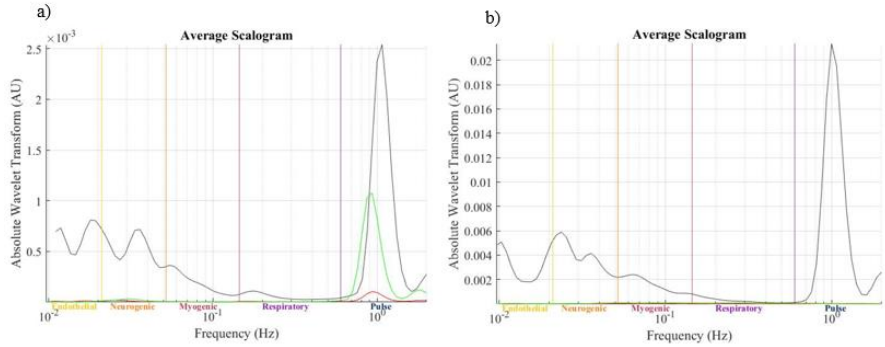

Figure 60. The average scalogram from cold exposure at baseline, intervention, and recovery of the diabetic subject (a) and the control subject (b) superimposed. Black line = baseline, red line = intervention, green line = recovery.

The distribution of the frequency bands in baseline, intervention, and recovery from cold exposure from the same subjects can be seen in Figure 61. From these pie charts can observe that also in the LDF signal, different frequency bands were more pronounced in diabetics than in controls in cold exposure, but at baseline the distribution of the bands between the groups was similar. The dominant bands were also different than in HRV or BP variation signals.

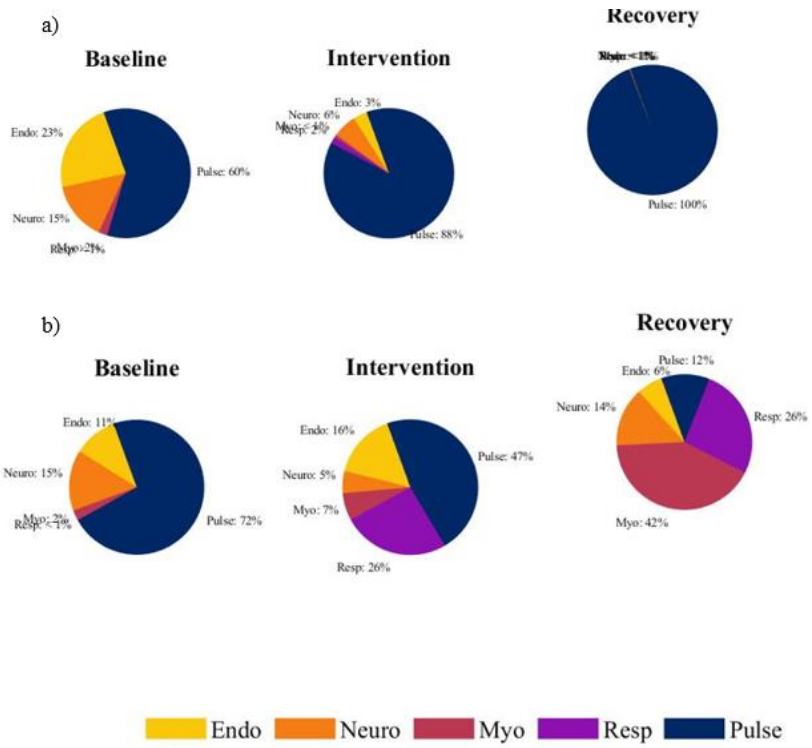

Figure 61. Distribution of frequency bands from the diabetic subject (a) and the control subject (b) from cold exposure.

4.2.6. LDF from warm exposure

The 3D magnitude scalogram (top) and the average scalogram (bottom) of the LDF at baseline in warm exposure from a diabetic and control subject side by side can be seen in Figure 62. And at intervention from warm in Figure 63. The total mean WT power of the spectrum increased in warm from 2.0×10^{-6} AU to 4.4×10^{-6} AU in diabetics and from 1.1×10^{-6} AU to 1.9×10^{-6} AU in controls. The increase of total WT power for diabetics was larger compared to controls in the warm intervention.

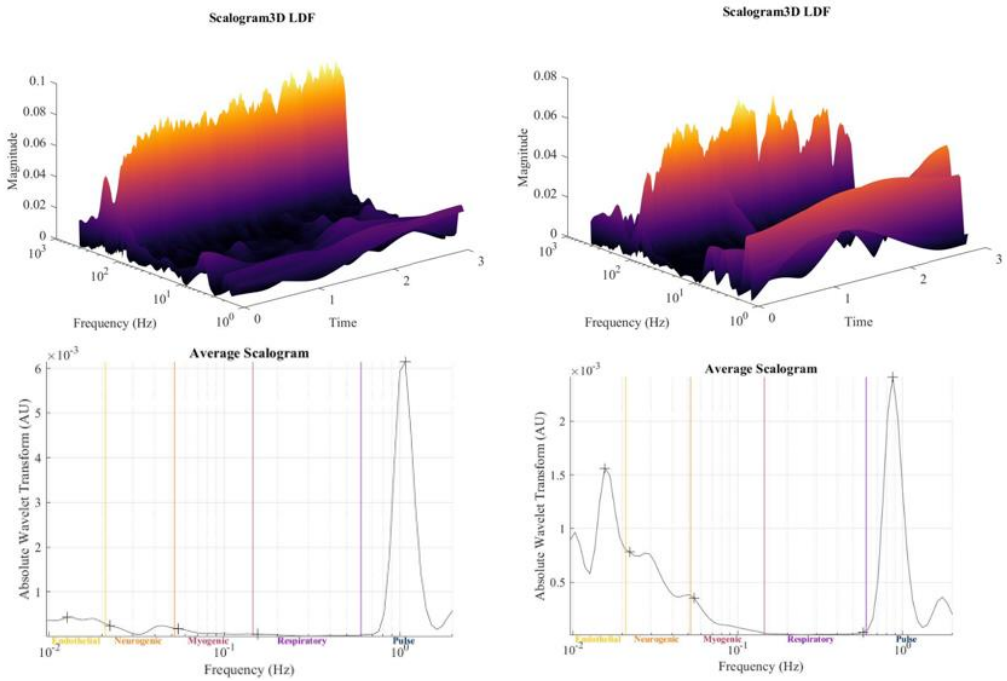

Figure 62. Warm baseline 3D magnitude scalogram (top) and average scalogram (bottom) from a diabetic and control subject.

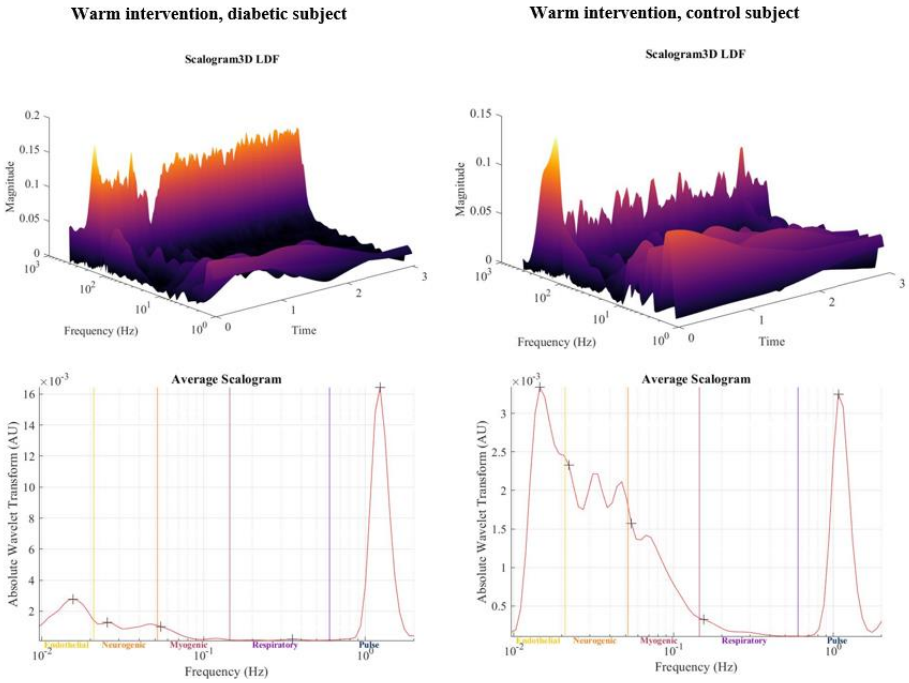

Figure 63. Warm intervention 3D magnitude scalogram (top) and average scalogram (bottom) from a diabetic and control subject.

The peak amplitudes of the following frequency bands are calculated as the average of the peak amplitude frequencies of the measurements.

The absolute power of the frequency bands from 0.0052 to 2 Hz. The absolute power of the oscillations around 0.05 Hz increased 350 % ($7.4 \times 10^{-7} - 3.4 \times 10^{-6}$) in response to warm intervention in diabetics, and controls the increase was considerably smaller by 30 % ($1.2 \times 10^{-6} - 1.5 \times 10^{-6}$). The absolute power of the

oscillations around 0.2 Hz was significantly lower in diabetics in the baseline in warm exposure ($p = 0.034$) compared to controls. The absolute power increased by 260 % ($2.1 \times 10^{-8} - 7.6 \times 10^{-8}$) in diabetic and controls the increase was again, considerably smaller by 60 % ($2.6 \times 10^{-8} - 4.1 \times 10^{-8}$), whereas the absolute power of the oscillations around 0.9 Hz increased by 90% ($3.6 \times 10^{-6} - 6.8 \times 10^{-6}$) in diabetics and decreased by 20 % ($1.8 \times 10^{-6} - 1.4 \times 10^{-6}$) in controls (Figure 64). There were no between-group significant differences in any relative power parameters. The absolute myogenic power and the absolute respiratory power ratio in the baseline were 13.5 in diabetics and 50.7 in controls and in the intervention 11.5 in diabetics and 40 in controls. The change in diabetics was therefore 14.5 % and in controls 20 % decrease. The absolute respiratory power and the absolute pulse power ratio in the baseline were 0.01 in diabetics and 0.006 in controls and in the cold exposure intervention 0.09 in diabetics and 0.6 in controls. The change in diabetics was a 770 % increase and in controls 10 000 % increase.

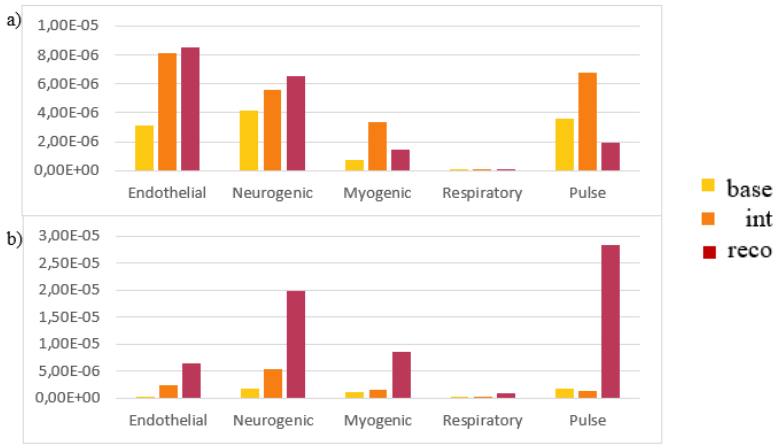

Figure 64. The absolute power of the LDF frequency spectrum from warm exposure diabetics (a) and controls (b).

The relative power of the frequency bands from 0.0052 to 2 Hz. The relative power of the oscillations around 0.05 Hz increased in response to warm by 130 % ($0.19 - 0.44$) in diabetics and by 210 % ($0.24 - 0.74$) in controls. The relative power of the oscillations around 0.2 Hz increased by 180 % ($0.03 - 0.08$) in diabetics and by 1500 % ($0.01 - 0.22$) in controls, whereas the relative power of the oscillations around 0.9 Hz decreased by 35 % ($3.26 - 2.13$) in diabetics and by 62 % ($2.85 - 1.07$) in controls (Figure 65). There were no between-group significant differences in any relative power parameters.

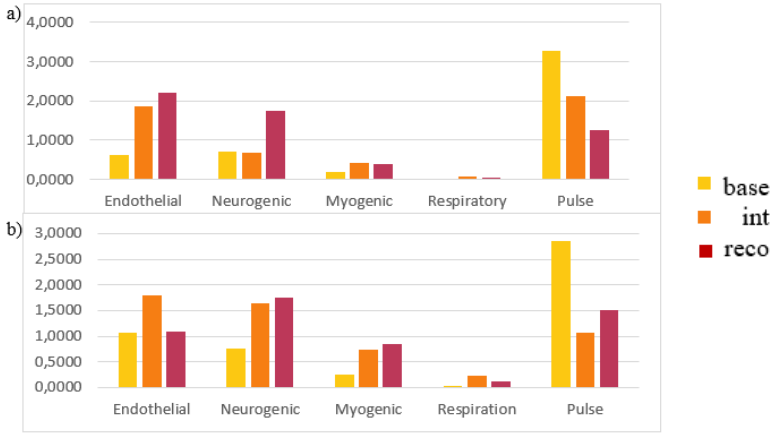

Figure 65. The relative power of the LDF frequency spectrum from warm exposure diabetics (a) and controls (b).

The absolute amplitude of the frequency bands from 0.0052 to 2 Hz. The absolute amplitude of the oscillations around 0.05 Hz increased 82 % (0.42 – 0.72) in response to warm intervention in diabetics, and in controls, the increase was 117 % (0.39 – 0.86). The absolute amplitude of the oscillations around 0.2 Hz was significantly higher in diabetics in the baseline in warm exposure ($p = 0.034$) compared to controls. The absolute amplitude increased by 210 % (0.08 – 0.17) in diabetics and controls, the increase was 150 % (0.05 – 0.15), whereas the absolute amplitude of the oscillations around 0.9 Hz increased by 13 % (0.97 – 1.1) in diabetics and by 11 % (0.62 – 0.68) in controls (Figure 66). There were no between-group significant differences in any absolute amplitude parameters.

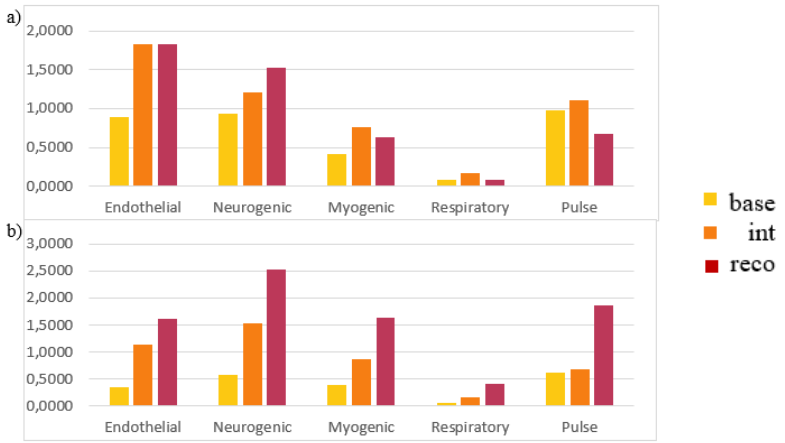

Figure 66. The absolute amplitude of the LDF frequency spectrum from warm exposure diabetics (a) and controls (b).

The relative amplitude of the frequency bands from 0.0052 to 2 Hz. The relative amplitude of the oscillations around 0.05 Hz increased in response to warm by 300 % in diabetics and by 1270 % in controls. The relative amplitudes of the oscillations around 0.2 Hz increased by 210 % in diabetics and by 780 % in controls, whereas the relative amplitude of the oscillations around 0.9 Hz increased by 39 % in diabetics and 86 % in controls.

The CWT scalogram of the LDF at baseline, intervention, and recovery from warm exposure from the same diabetic and control subjects as the total power figures, can

be seen in Figure 67. And from the same representatives, the average scalograms superimposed from warm intervention can be seen in Figure 68.

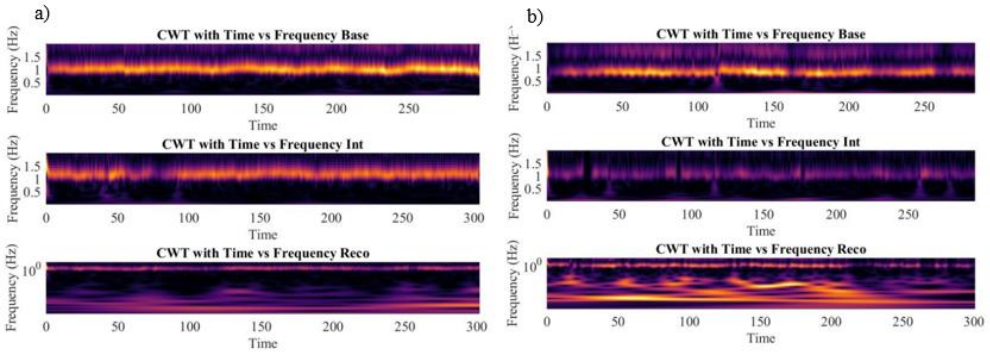

Figure 67. The CWT scalogram of the diabetic subject (a) and the control subject (b) from warm exposure from baseline, intervention, and recovery.

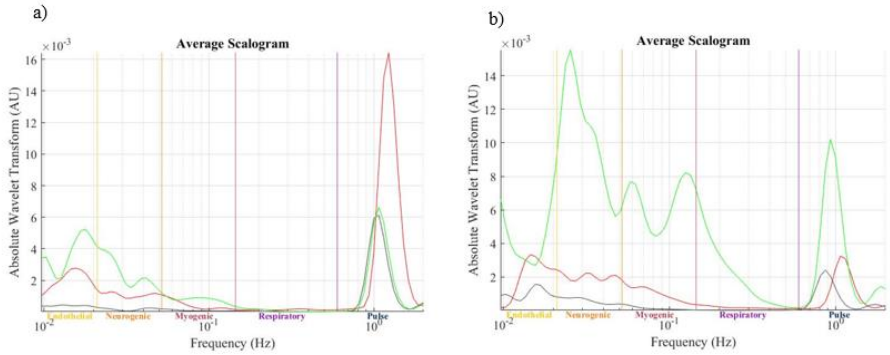

Figure 68. The average scalogram from warm exposure at baseline, intervention, and recovery of the diabetic subject (a) and the control subject (b) superimposed. Black line = baseline, red line = intervention, green line = recovery.

The distribution of the frequency bands in baseline, intervention, and recovery from warm exposure from the same subjects can be seen in Figure 69. From these pie charts can observe that also in the LDF signal, different frequency bands were more pronounced in diabetics than in controls in warm exposure. The dominant bands were also different than in HRV or BP variation signals.

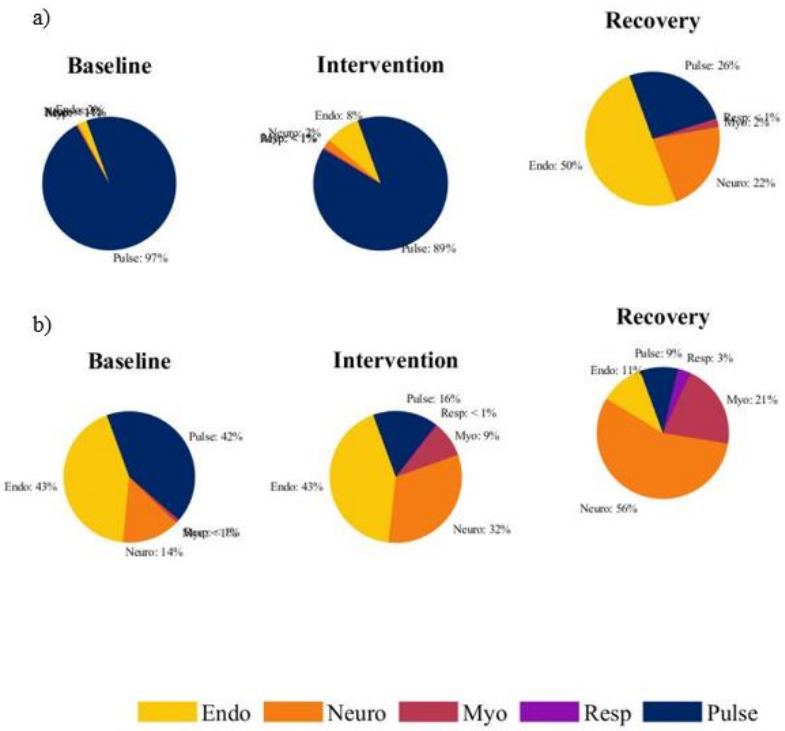

Figure 69. Distribution of frequency bands from the diabetic subject (a) and the control subject (b) from warm exposure.

5. DISCUSSION

The main objective of this thesis was to assess whether there are differences in heart rate, blood pressure, and tissue blood flow parameters between T2DM patients and controls during a thermal challenge in cold (+10 ˚C) and warm (+40 ˚C) environments and whether these possible differences are reflected in the amplitude and/or power of low-frequency oscillations. The signals were also examined in the time-domain to gain insight of the changes between the groups, but these results are only briefly discussed in this thesis. A deeper analysis and interpretation were omitted as the focus was on the analysis of the frequency oscillations of the signals.

5.1. Cold exposure

The results of this study demonstrated that the resting heart rate of T2DM patients was significantly higher and RR intervals shorter at baseline in cold exposure. In the cold exposure, RR intervals increased in both groups similarly. SDNN, RMSSD, NN50, and pNN50 were significantly lower in diabetics at baseline, and these values increased in cold exposure in both groups, with a slightly greater increase in NN50 and pNN50 in the controls. The results showed that mean systolic blood pressure and mean diastolic blood pressure increased during cold exposure in both groups, but the change in SYS was slightly greater in the diabetics. MAP increased during the cold intervention in both groups and decreased during recovery, but the changes were slightly greater in diabetics. The mean SBP variation is similar to the mean RR interval, and they also behaved similarly. The absolute mean BPU decreased considerably in the cold intervention for both groups. And although the perfusion increased during recovery it did not return to baseline levels. BPU values were generally lower in diabetics at baseline and intervention, which is similar to other studies showing that diabetics on average have lower blood perfusion [4]. In cold recovery, diabetics had a greater increase in mean BPU compared to controls, with a 164% increase in BPU compared to a 54% increase in controls.

Total frequency spectrum from 0.052 – 2 Hz. The total power of the frequency range was considerably lower in diabetics than in controls both in the HRV and BP spectra, which is similar to findings in [12], and it increased more in cold in controls than in diabetics. In the LDF spectrum, total power was lower in diabetics at cold baseline and intervention, but its decrease in the cold was similar between groups.

Frequency interval from 0.052 – 0.145 Hz. The results demonstrated that at this frequency interval in general, the amplitude and power of the diabetics were lower at baseline and intervention measurements. There were also significant differences in the absolute amplitude and absolute power of HRV and BP at baseline. Lower values in this frequency range in diabetics are consistent with other studies on HRV [12]. The increase or decrease was consistently greater in controls, except the decrease in LDF was similar between groups both in absolute amplitude and power.

In this thesis, the results show that BP amplitude and power increased in cold (both absolute and relative) in both groups, absolute and relative amplitude of HRV increased in cold in both groups and absolute power increased, considerably more in controls, and relative power increased in diabetics but decreased slightly in controls. For LDF, absolute and relative amplitude decreased in cold in both groups, and absolute power also decreased in both groups, but relative power increased, more in controls. Relative amplitudes were calculated in this thesis relative to the absolute baseline amplitude, and during the work, it was found that a better way to calculate

this might have been relative to the mean amplitude of the whole spectrum (0.0095 – 2 Hz), in the same way, that relative power was calculated.

The origin of this frequency has been attributed to sympathetic activation [51]. In HRV and BP studies, this band can be compared to the LF band, and the power of the band has been used to indicate SNS activity, but the band may be produced by both SNS and PSNS activity [14, 26, 38] and also produced by BP regulation via baroreceptors [13]. It is, therefore, interesting that in this study, results demonstrate that in cold diabetics LF relative power increase but in controls, it decreases.

Frequency interval from 0.145 – 0.6 Hz. The results demonstrated that in this frequency interval, the amplitude and power of diabetics were mostly lower at baseline and in the intervention measurements. There was also a significant difference between diabetics and controls in the relative power of BP in cold intervention. Lower values in this frequency range in diabetics are consistent with other studies on HRV [12]. The increase or decrease was consistently greater in controls, except for the absolute and relative amplitude of BP increased slightly more in diabetics than in controls, and the relative power of BP decreased more in diabetics. Also, the absolute and relative amplitude and absolute power of LDF decreased slightly more in diabetics.

In this thesis, the results show that the absolute and relative amplitude and absolute power of HRV and BP increase in the cold in both groups. In BP, relative power decreases in both groups, with a greater decrease in diabetics. And in HRV, relative power decreases in diabetics, while it increases in controls. In LDF, absolute and relative amplitude and absolute power decrease almost equally in both groups, but relative power increase considerably in both groups, even more in controls.

The origin of this frequency has been accepted as the respiratory band [13]. In HRV studies, this band can be compared to the HF band, and the power of the band has been used to indicate PSNS activity [13, 26]. In this frequency band, it is also interesting that results in this study demonstrate that in cold, HF relative power increases in controls, but in diabetics HF relative power decreases. For LF/HF ratio, originally based on 24-hour recordings and used to estimate sympathovagal balance [13, 26], is controversial from this point of view because the LF band does not directly reflect SNS activity. And especially, when recorded for 5 minutes of rest in the sitting upright position, it has been shown that the primary contributors to the LF band are PSNS and baroreflex activity [13]. Interestingly, the results of this study show that the LF/HF ratio decreases in cold, more in diabetics, and increases in warm, considerably more in controls.

Frequency interval from 0.6 – 2 Hz. This frequency interval was only seen in the LDF signal because the BP and HRV signals originate from the heart and the human heart beats at about 1 Hz frequency. In this band, diabetics had lower absolute amplitude and power and relative amplitude at baseline and intervention in cold, but relative power at baseline and intervention was higher in diabetics. The increase or decrease in absolute amplitude and absolute power was greater in controls. Relative amplitude increased slightly more in diabetics than in controls, and relative power increased in controls, while it decreased in diabetics. Cooling-induced vasoconstriction has been shown to decrease the normalized power of this frequency interval in the LDF signal [29]. Interestingly, in controls, cold exposure shows a very slight increase in normalized power, whereas it decreases in diabetics.

5.2. Warm exposure

The results of this study demonstrated that the resting heart rate of T2DM patients was significantly higher and RR intervals shorter at baseline in warm exposure. The warm exposure resulted in decreased RR interval, which was greater in controls. SDNN, RMSSD, NN50, and pNN50 were significantly lower in diabetics at baseline. In the warm exposure, these values decreased in both groups, with the percentage decrease in SDNN and RMSSD being considerably greater in the controls (diabetics' decrease was 5 % and 24.5 %, respectively, and controls 32 % and 51.6 %, respectively). During warm exposure, SYS and DIA decreased in controls and increased during recovery almost back to baseline values. In diabetics, SYS decreased during the intervention and increased again during recovery, but DIA increased slightly during the intervention and also continued to increase during recovery. In warm, MAP decreased during the intervention in both groups and increased during recovery, but the decrease during intervention was greater in controls. During recovery, MAP increased slightly above the baseline value in diabetics. During the intervention, the absolute mean BPU increased considerably in both groups and decreased during the recovery. But the BPU values of the controls at baseline appear to be inconsistent, with absolute values being considerably lower in some subjects, affecting the baseline mean values. This highlights the problem of heterogeneity in LDF measurements, as the same subjects have had much higher values at the cold baseline, but for some reason, these values are not repeated in the warm baseline. It might have been helpful to have been able to normalize the values to the maximum perfusion to improve the comparability between the subjects.

Total frequency spectrum from 0.052 – 2 Hz. In the warm, because controls had inconsistencies in baseline measurements, it appears that controls had lower total power at baseline, but diabetics had, however, higher total power in the intervention than controls. In both groups, total LDF power increased during the warm intervention due to increased blood flow, consistent with other studies [29].

Frequency interval from 0.052 – 0.145 Hz. At this frequency interval in general, the amplitude and power of the diabetics were lower at baseline and intervention measurements. There were also significant differences in the absolute amplitude and absolute power of HRV and BP in warm exposure at baseline and intervention between diabetics and controls. Lower values in this frequency range in diabetics are consistent with other studies on HRV [12] and on LDF amplitude and power [29, 40, 42]. The increase or decrease was consistently greater in controls, except the increase in LDF in absolute power was considerably greater in diabetics than in controls. There was also an increase in BP absolute power in diabetics, whereas it decreased in controls.

In this thesis, the results show that in warm in BP, absolute and relative amplitude decreases in both groups, but there was a difference in absolute and relative power. The absolute power increases and the relative power decrease in diabetics, and interestingly, in controls these go the other way around, i.e., absolute decreases and relative power increases. For HRV, absolute and relative amplitude decrease, as does absolute power, but relative power decreases in diabetics and increases in controls. For LDF, all parameters increase in warm in both groups.

In LDF studies, the amplitude of this band has been associated with smooth muscle activity in peripheral blood vessels, with an increase in amplitude associated with a greater contribution to the regulation of blood flow [30]. This was also seen in this study, with an increase in amplitude with warm exposure. Power, primarily relative power, has also been associated with smooth muscle activity as a predictor of

vasocontraction (increase) or vasodilation (decrease) [29]. This was observed in this study, where relative power increased in both groups in the cold, with a greater increase in controls. However, in this study, relative power was not found to decrease with warm exposure but increased in both groups. However, it is difficult to say how much the inconsistency with the controls baseline measurements has affected this frequency range power and hence relative power.

Frequency interval from 0.145 – 0.6 Hz. The results demonstrated that in this frequency interval, the amplitude and power of diabetics were mostly lower at baseline and in the intervention measurements in warm. There was also a significant difference between diabetics and controls in the absolute amplitude and power of HRV and BP at baseline and in the relative amplitude of HRV and BP in the intervention and in the relative power of BP in intervention. Also at baseline, the absolute amplitude and power of LDF differed significantly between diabetics and controls. Lower values in this frequency range in diabetics are consistent with other studies on HRV [12] and on LDF amplitude and power [29, 42]. The increase or decrease was consistently greater in controls, except the increase in the absolute power of LDF in the intervention was considerably greater in diabetics than in controls, even though the controls' baseline values were most likely affected by the inconsistency.

In this thesis, the results show that in warm BP and HRV absolute and relative amplitude and absolute and relative power decrease in both groups, all decreasing more in controls. In LDF, all parameters increase in both groups, and the increase in absolute power was considerably greater in diabetics, but the increase in relative power was considerably greater in controls.

In LDF studies, this channel has been associated with the respiratory band and carries information on the influence of thorax movement on peripheral blood flow [30]. Increased activity is observed in this study in relative power, which is similar to the response in [30] in warm exposure.

Frequency interval from 0.6 – 2 Hz. The results demonstrated that in this frequency interval in warm absolute amplitude and power and relative power at baseline and intervention were higher in diabetics, but the relative amplitude was lower in diabetics. The increase or decrease in relative amplitude and relative power was greater in controls, but the absolute amplitude increased more in diabetics, and absolute power increased in diabetics while it decreased in controls, which may be affected by the inconsistency. In warm, this frequency interval power has been observed to increase [30], but in this study, the results demonstrate that in diabetics the absolute power increases while relative decreases, and in controls both decreases.

Overall, the results demonstrated that diabetics had higher HR, but other time-domain parameters can be said to be lower than controls in all measurement phases, except for DIA and MAP in cold, $\%CVC_{max}$ in warm exposure, and mean BPU in warm baseline (which affects CVC in the warm baseline), due to the inconsistency discussed earlier. The higher DIA value and behavior in warm in diabetics could be due to endothelial dysfunction and vascular remodeling due to hypertension, resulting in higher vascular resistance [19]. In general, it can also be said that the response to cold was similar in both groups, but in warm the difference with baseline was greater in controls, and therefore it could be said that the diabetics' response to warm exposure was poorer than in controls. However, the inconsistent LDF baseline measurements of controls should be taken under consideration. The poorer response of diabetics is however consistent with the hypothesis that diabetics, with comorbidities, may gain a higher thermal load than the age-matched controls, leading to a greater risk of heat-

related illnesses [4]. This is also consistent with the synergistic negative effect of aging that may also impair cardiovascular function in diabetics [4]. Generally, in the frequency-domain, the effect of thermal exposure at these frequency bands is similar for most parameters in both diabetics and controls, but the amplitude and power values were greater in controls and the increase or decrease during exposures tended to be greater in controls. These results may indicate that diabetics are less responsive during thermal stress compared to healthy controls and may suggest that diabetics are less able to initiate thermoregulatory processes during acute exposure to extreme environmental thermal conditions and may at least partly explain the increased heat-related complications in diabetics [4].

However, there are some limitations in this study. The number of subjects studied was relatively small and may not accurately reflect the overall population. Also, the controls' baseline measurement in warm with LDF may not accurately reflect the true perfusion, which should be taken under consideration when reviewing the results. In addition, the short duration of the measurement results in most of the data being minimized, which also removes valuable information needed to understand the subject's overall condition. Short duration measurements also affect pre-processing results, as most of the data may be filtered out if the data are noisy, which is a reasonable expectation for subjects under stress. In this study, the individual recordings were not always of good quality, probably mainly due to other concurrent measurements and subjects' movements, as well as the stressful and unusual situation. The duration of the measurement also affected the interpretation of the low-frequency oscillations, and therefore the two lowest bands were not included in the results of this study. It should also be noted that comparing studies is challenging, especially for LDF, as the study design, instrumentation, measurement area and measurement time can be very different.

Future research ideas would be to overcome the above limitations, in particular the short recording time. A longer recording time would allow the two lowest frequency bands to be reliably included in the analysis and would also improve the pre-processing results, as discussed above. It would also be interesting to conduct a similar study with a larger number of subjects. Another dimension to add to the analysis could be the regularity and randomness methods derived from information theory, which have been applied to ECG, EEG, and LDF signals, for example.

6. CONCLUSION

The objective of this thesis was to explore the low-frequency oscillatory characteristics of the cardiovascular system based on tissue blood flow, heart rate, and blood pressure parameters in diabetic and healthy subjects in response to acute exposures to heat and cold. The main goal of this thesis was to explore if these parameters change in T2DM patients compared to the control group during the thermal challenge and whether these differences are reflected in the amplitude and/or power of low-frequency oscillations between the groups. In addition, the parameters were analyzed in the time-domain.

In this thesis the cardiovascular system and its function are described in the theory section, it is also described from the perspective of diabetes and how the disease affects cardiovascular function. As the experimental study focused on the effect of thermal challenge, human thermoregulation is also described and how it has been shown to change with diabetes. The methods section of this thesis describes the signals used and the pre-processing activities and how these signals are studied in this thesis in the time-domain, frequency-domain, and statistically. The results and the discussion of the results conclude this thesis.

The signals were analyzed using wavelet transform and divided into five frequency intervals based on previous studies of LDF signals, these being associated with different cardiovascular system structures, namely endothelial, neurogenic, myogenic, respiratory, and cardiac. The cardiac frequency interval was not seen in the frequency analysis of HRV or BP variation. As presented in this thesis, for reliable statistical analysis the recording should ideally include 10 cycles for each frequency band. In this experimental study, the individual recording time of each phase was about 5 minutes, therefore the myogenic band in 0.052 – 0.145 Hz was the lowest frequency interval for reliable statistics and the two lowest frequency intervals were omitted from the results. The results of this thesis showed that, in general, all calculated parameters in both the time-domain and frequency-domain were lower in diabetics compared with controls. Also, the change as a result of exposure to cold and warm, was generally lower in diabetics, which suggests that the thermoregulatory response is different between diabetic and control groups. Overall, the results of this thesis suggest that there is a difference between T2DM patients and controls in the parameters of these signals, and the difference is reflected in the time-domain parameters as well as in the amplitude and power parameters of the frequency-domain.

7. REFERENCES

[1] World Health Organization. 2020. Diabetes. Available at: https://www.who.int/health-topics/diabetes#tab=tab_1. Accessed 3.2.2022.

[2] Finnish Institute for Health and Welfare. 2020. Diabetes. Available at: https://thl.fi/en/web/chronic-diseases/diabetes. Accessed 3.2.2022

[3] American Diabetes Association. 2020. Diabetes. Available at: https://www.diabetes.org/diabetes. Accessed 3.2.2022.

[4] Kenny, G. P., Sigal, R. J., & McGinn, R. (2016). Body temperature regulation in diabetes. Temperature (Austin, Tex.), 3(1), 119–145. DOI: https://doi.org/10.1080/23328940.2015.1131506

[5] Cho NH, Shaw JE, Karuranga S, Huang Y, da Rocha Fernandes JD, Ohlrogge AW, Malanda B. (2018). IDF Diabetes Atlas: Global estimates of diabetes prevalence for 2017 and projections for 2045. Diabetes Research Clinical Practice. 2018 Apr;138:271-281. DOI: 10.1016/j.diabres.2018.02.023. Epub 2018 Feb 26. PMID: 29496507. Accessed 2.3.2022.

[6] WHO Regional Office for Europe. 2011. Diabetes epidemic in Europe. Available at: https://www.euro.who.int/en/health-topics/noncommunicable-diseases/diabetes/news/news/2011/11/diabetes-epidemic-in-europe. Accessed: 2.3.2022.

[7] Lam HCY, Chan JCN, Luk AOY, Chan EYY, Goggins WB. (2018). Short-term association between ambient temperature and acute myocardial infarction hospitalizations for diabetes mellitus patients: A time series study. PLoS Medicine 15(7): e1002612. DOI: https://doi.org/10.1371/journal.pmed.1002612

[8] University of Oulu. Center for Environmental and Respiratory Health Research (CERH). Available at: https://www.oulu.fi/en/university/faculties-and-units/faculty-medicine/center-environmental-and-respiratory-health-research

[9] Betts G. J., et al. 2013. Anatomy and Physiology. OpenStax. Houston, Texas. USA. Available at: https://openstax.org/details/books/anatomy-and-physiology (Web version latest update 2021/07/28). Accessed: 10.2.2022.

[10] Leppäluoto, J., Rintamäki, H., Vakkuri, O., Vierimaa, H. and Lauri, T. 2019. Anatomia ja fysiologia – Rakenteesta toimintaan. 9., revised edition. E-book. Helsinki: Sanoma Pro Oy. Accessed: 3.3.2022. Requires access rights. Adobe Digital Editions.

[11] Duque A, Mediano MFF, De Lorenzo A, Rodrigues Jr LF. (2021). Cardiovascular autonomic neuropathy in diabetes: Pathophysiology, clinical

assessment and implications. World Journal of Diabetes; 12(6): 855-867. DOI: 10.4239/wjd.v12.i6.855

[12] Benichou T, Pereira B, Mermillod M, Tauveron I, Pfabigan D, Maqdasy S, et al. (2018). Heart rate variability in type 2 diabetes mellitus: A systematic review and meta–analysis. PLoS ONE 13(4): e0195166. DOI: https://doi.org/10.1371/journal. pone.0195166

[13] Shaffer F and Ginsberg JP. (2017). An Overview of Heart Rate Variability Metrics and Norms. Frontiers in Digital Health 5:258. DOI: 10.3389/fpubh.2017.00258

[14] Ishaque S, Khan N and Krishnan S. (2021). Trends in Heart-Rate Variability Signal Analysis. Frontiers in Digital Health 3:639444. DOI: 10.3389/fdgth.2021.639444

[15] McArdle WD, Katch FI and Katch VL. (2010). Exercise Physiology – Nutrition, Energy, and Human Performance. 7th Edition. Philadelphia, Lippincott Williams & Wilkins, a Wolters Kluwers business.

[16] Rangayyan Rangaraj M. (2002). Biomedical Signal Analysis. A case-Study Approach. Institute of Electrical and Electronics Engineers, Inc. New York, John Wiley & Sons.

[17] The heart. Modified. Available at: https://pixabay.com/fi/images/search/human%20heart/. CC0. Accessed: 11.2.2022

[18] Human circulation system. Available at: https://pixabay.com/fi/images/search/human%20circulation%20system/. CC0. Accessed: 11.2.2022

[19] Ohishi M. (2018). Hypertension with diabetes mellitus: physiology and pathology. Hypertension Research 41:389-393. DOI: https://doi.org/10.1038/s41440-018-0034-4

[20] Strain WD. and Paldánius PM. (2018). Diabetes, cardiovascular disease and the microcirculation. Cardiovascular Diabetology 17:57. DOI: https://doi.org/10.1186/s12933-018-0703-2

[21] Tang Y. and He Y. (2018). Numerical modelling of fluid and oxygen exchanges through microcirculation for the assessment of microcirculation alterations caused by type 2 diabetes. Microvascular Research 117:61-73. DOI: https://doi.org/10.1016/j.mvr.2018.01.006

[22] Hypertension. Current Care Guideline. Working group set up by the Finnish Medical Society Duodecim and the Finnish Hypertension Society. Helsinki: The Finnish Medical Society Duodecim, 2020. Available at: www.kaypahoito.fi Accessed: 7.3.2022

[23] Greaney Jl., Kenney WL, and Alexander LM. (2016). Sympathetic regulation during thermal stress in human aging and disease. Autonomic Neuroscience 196:81-90. DOI: 10.1016/j.autneu.2015.11.002

[24] Najarian K. and Splinter R. (2012). Biomedical Signal and Image Processing. Second Edition. Taylor & Francis Group, LLC. Florida, CRC Press.

[25] Atkielski, A. 2012. Sinus Rhythm Labels. Edited 16.7.2021. Available at: https://urly.fi/W3Q. CC0. Accessed: 17.3.2022.

[26] Malik, M., Bigger, J. T., Camm, A. J., Kleiger, R. E., Malliani, A., Moss, A. J. & Schwartz, P. J. (1996). Heart rate variability, Standards of measurement, physiological interpretation, and clinical use. Task Force of The European Society of Cardiology and The North American Society of Pacing and Electrophysiology. European Heart Journal (1996) 17, 354-381. DOI: https://doi.org/10.1161/01.CIR.93.5.1043

[27] Balzer, F. et al. (2016). Comparison of the non-invasive Nexfin® monitor with conventional methods for the measurement of arterial blood pressure in moderate risk orthopedic surgery patients. Journal of International Medical Research. 44(4), 832-843. DOI: 10.1177/0300060516635383

[28] Chaseling, G. K., Crandall, C. G., & Gagnon, D. (2020). Skin blood flow measurements during heat stress: technical and analytical considerations. American Journal of Physiology. Regulatory, Integrative and Comparative Physiology, 318(1), R57-R69. DOI: 10.1152/ajpregu.00177.2019

[29] Clough, G. F., Kuliga, K. Z., and Chipperfield, A. J. (2017). Flow motion dynamics of microvascular blood flow and oxygenation: Evidence of adaptive changes in obesity and type 2 diabetes mellitus/insulin resistance. Microcirculation (New York, N.Y. 1994), 24(2), e12331-n/a. DOI:10.1111/micc.12331

[30] Mizeva, I., Zharkikh, E., Dremin, V., Zherebtsov, E., Makovik, I., Potapova, E., and Dunaev, A. (2018). Spectral analysis of the blood flow in the foot microvascular bed during thermal testing in patients with diabetes mellitus. Microvascular Research, 120, 13-20. DOI: 10.1016/j.mvr.2018.05.005

[31] Fredrikson. I., Fors, C. and Johansson, J. (2007). Laser Doppler Flowmetry – a Theoretical Framework. Department of Biomedical Engineering, Linköping University.

[32] Bagno, A. & Martini, R. (2015). Wavelet analysis of the Laser Doppler signal to assess skin perfusion. Annual International Conference IEEE Engineering in Medicine and Biology Society 2015:7374-7. DOI: 10.1109/EMBC.2015.7320095.

[33] Rajan, V., Varghese, B., van Leeuwen, T. G., & Steenbergen, W. (2009). Review of methodological developments in laser Doppler flowmetry. Lasers in Medical Science, 24(2), 269-283. DOI:10.1007/s10103-007-0524-0

[34] Neto, O.P., Oliveira Pinheiro, A., Pereira, V.L., Pereira, R., Baltatu, O.C., and Campos, L.A. (2016). Morlet wavelet transforms of heart rate variability for autonomic nervous system activity. Applied and Computational Harmonic Analysis, 40(1), 200-2006. DOI: 10.1016/j.acha.2015.07.002

[35] Li. K., Rüdiger, H., and Ziemssen, T. (2019). Spectral Analysis of Heart Rate Variability: Time Window Matters. Frontiers in Neurology, 10:545. DOI: 10.3389/fneur.2019.00545

[36] Petrie, J.R., Guzik, T.J. and Touyz, R.M. (2017). Diabetes, Hypertension, and Cardiovascular Disease: Clinical Insights and Vascular Mechanisms. Canadian Journal of Cardiology, 34, 575-584. DOI: 10.1016/j.cjca.2017.12.005

[37] Rosei, E.A., Chiarini, G., and Rizzoni, D. (2020). How important is blood pressure variability? European Heart Journal Supplements, 22(Supplement E), E1-E6. DOI: 10.1093/eurheartj/suaa061

[38] Parati, G., Saul, J.P., Di Rienzo, M., and Mancia, G. (1995). Spectral Analysis of Blood Pressure and Heart Rate Variability in Evaluating Cardiovascular Regulation. Hypertension 26(6), 1276–1286. DOI: 10.1161/01.HYP.25.6.1276

[39] Bandini, A., Orlandi, S., Manfredi, C., Evangelisti, A., Barrella, M., Bevilacqua, M., and Bocchi, L. (2013). Modelling of Thermal Hyperemia in Skin of Type 2 Diabetic Patiens. Journal of Healthcare Engineering, 4(4), 541-554. DOI: 10.1260/2040-2295.4.4.541

[40] Jan, Y-K., Shen, S., Foreman, R.D., and Ennis, W.J. (2013). Skin blood flow response to locally applied mechanical and thermal stresses in the diabetic foot. Microvascular Research, 89, 40-46. DOI: 10.1016/j.mvr.2013.05.004

[41] Kulikov, D., Glazkov, A., Dreval, A., Kovaleva, Y., Rogatkin, D., Kulikov, A., and Molochkov, A. (2018). Approaches to improve the predictive value of laser Doppler flowmetry in detection of microcirculation disorders in diabetes mellitus. Clinical Hemorheology and Microcirculation, 70(2), 173-179. DOI: 10.3233/CH-170294

[42] Hu, H., Hsiu, H., Sung, C., & Lee, C. (2017). Combining laser-Doppler flowmetry measurements with spectral analysis to study different microcirculatory effects in human prediabetic and diabetic subjects. Lasers in Medical Science, 32(2), 327-334. 10.1007/s10103-016-2117-2

[43] Ticcinelli, V., Stankovski, T., Iatsenko, D., Bernjak, A., Bradbury, A.E., Gallagher, A.R., Clarkson, P.B.M., McClintock, P.V.E., and Stefanovska, A. (2017). Coherence and Coupling Functions Reveal Microvascular Impairment in Treated Hypertension. Frontiers in Physiology, 8:749. DOI: 10.3389/fphys.2017.00749

[44] Bračič, M., McClintock, P., and Stefanovska, A. (2000). Characteristic frequencies of the human blood distribution system. American Institute of Physics Conference Proceedings, 502, 146-153. DOI: 10.1063/1.1302378

[45] Uysal, F. QRS Detection Using Pan-Tompkins algorithm. Available at: https://cnx.org/contents/YR1BUs9_@1/QRS-Detection-Using-Pan-Tompkins-algorithm. Accessed: 21.2.2022

[46] Laurin, A. BP_Annotate. Available at: https://www.mathworks.com/matlabcentral/fileexchange/60172-bp_annotate/. Accessed: 21.3.2022

[47] Pan, J. & Tompkins, W.J. (1985). A real-time QRS detection algorithm. IEEE Transactions on Biomedical Engineering, 32, 230–236. DOI: 10.1109/TBME.1985.325532

[48] Sun, J., Reisner, A. and Mark, R. (2006). A signal abnormality index for arterial blood pressure waveforms. In Proceedings of the 2006 Computers in Cardiology, Valencia, Spain, 2006; pp. 13–16.

[49] DeMers D, and Wachs D. Physiology, Mean Arterial Pressure. [Updated 2021 Apr 21]. In: StatPearls [Internet]. Treasure Island (FL): StatPearls Publishing; 2022 Jan-. Available at: https://www.ncbi.nlm.nih.gov/books/NBK538226/. Accessed: 23.3.2022

[50] Durnin, J. V. G. A. & Womersley, J. 1974. Body fat assessed from total body density and its estimation from skinfold thickness: measurements on 481 men and women aged from 16 to 72 years. British Journal of Nutrition 32 (1), 77–97. DOI: 10.1079/bjn19740060

[51] Stefanovska, A., Bracic, M., & Kvernmo, H. D. (1999). Wavelet analysis of oscillations in the peripheral blood circulation measured by laser Doppler technique. IEEE Transactions on Biomedical Engineering, 46(10), 1230-1239. DOI:10.1109/10.790500

[52] Julien, C. (2006). The enigma of Mayer waves: Facts and models. Cardiovascular Research, 70(1), 12–21, DOI: https://doi.org/10.1016/j.cardiores.2005.11.008